

# Fighting off field dependence in MSSM Higgs-mass corrections of order $\alpha_t \alpha_s$ and $\alpha_t^2$

Florian Domingo<sup>1\*</sup> and Sebastian Paßehr<sup>2†</sup>

<sup>1</sup>*Bethe Center for Theoretical Physics & Physikalisches Institut der Universität Bonn,  
 Nußallee 12, D-53115 Bonn, Germany*

<sup>2</sup>*Institute for Theoretical Particle Physics and Cosmology,  
 RWTH Aachen University, Sommerfeldstraße 16, 52074 Aachen, Germany.*

The connection between gauge and Higgs sectors makes supersymmetric extensions of the Standard Model predictive frameworks for the derivation of Higgs masses. In this paper, we study the contamination of such predictions by field-renormalization constants, in the MSSM with two-loop gaugeless corrections of  $\mathcal{O}(\alpha_{t,b} \alpha_s, \alpha_{t,b}^2)$  and full momentum dependence, and demonstrate how strict perturbative expansions allow to systematically neutralize the dependence on such unphysical objects. On the other hand, the popular procedure consisting in an iterative pole search remains explicitly dependent on field counterterms. We then analyze the magnitude of the intrinsic uncertainty that this feature implies for the iterative method, both in non-degenerate and near-degenerate regimes, and conclude that this strategy does not improve on the predictions of the more straightforward expansion. We also discuss several features related to the inclusion of the orders  $\alpha_{t,b} \alpha_s$  and  $\alpha_{t,b}^2$  in the so-called ‘fixed-order’ approach, such as the resummation of UV-logarithms for heavy supersymmetric spectra.

---

\* email: [florian.domingo@csic.es](mailto:florian.domingo@csic.es)

† email: [passehr@physik.rwth-aachen.de](mailto:passehr@physik.rwth-aachen.de)

# Contents

<b>1. Introduction</b>	<b>1</b>
<b>2. Inclusion of 2L corrections to the Higgs mass observables</b>	<b>3</b>
2.1. Invariance under field-renormalization . . . . .	3
2.2. Non-degenerate case . . . . .	4
2.3. Degenerate case . . . . .	6
<b>3. Field-dependence in the mass predictions for a non-degenerate scenario</b>	<b>9</b>
3.1. Preliminary considerations . . . . .	9
3.2. Corrections of $\mathcal{O}(\alpha_q \alpha_s)$ . . . . .	11
3.3. Corrections of $\mathcal{O}(\alpha_q^2)$ . . . . .	16
<b>4. Field-dependence in the mass predictions in near-degenerate scenarios</b>	<b>20</b>
4.1. $\mathcal{CP}$ -violating mixing between heavy states . . . . .	21
4.2. $\mathcal{CP}$ -conserving mixing with the SM-like Higgs . . . . .	23
4.3. Three-state mixing . . . . .	26
<b>5. Resummation of UV-logarithms of <math>\mathcal{O}(\alpha_q, \alpha_q \alpha_s, \alpha_q^2)</math> and field dependence</b>	<b>29</b>
<b>6. Conclusions</b>	<b>36</b>
<b>A. Scattering by scalar resonances and propagator matrix</b>	<b>37</b>
A.1. General considerations . . . . .	37
A.2. Propagator matrix in perturbative QFT at 2L order . . . . .	38
A.3. Vertex corrections in perturbative QFT at 1L order . . . . .	40
<b>References</b>	<b>41</b>

## 1. Introduction

The discovery of a Standard-Model (SM)-like Higgs boson at the LHC [1–3] and the growingly precise measurements of its characteristics [4–6] make the need for controlled theoretical predictions in the Higgs sector of models of new physics quite clear, if one wishes to exploit associated observables and constrain the parameter space of beyond-the-SM (BSM) theories. In many cases, such precision calculations are difficult to conduct in the full model, *e.g.* due to the non-perturbative nature of the theory, and can only be performed in an effective context, in the limit of decouplingly heavy new physics. While the absence of conclusive signs of BSM physics at the LHC seems to justify the relevance of this type of approach anyway, the case of supersymmetric (SUSY) extensions of the SM [7, 8] is still remarkable in that it provides a perturbative framework up to relatively high energies.

Discussions of radiative corrections in the SUSY Higgs sector have a long-lasting history, of which the reader can find a summary in the recent review [9]. In particular, the higher-order contributions have a sizable impact on the mass of the SM-like state—which is automatically constrained to take tree-level values of electroweak (EW) magnitude and acquires sensitivity to new-physics scales via ultraviolet (UV) logarithms. Recently, the KUTS initiative has stimulated substantial advances in various related directions, such as calculations at fixed order (FO) [10–31] or in the context of low-energy Effective Field Theories (EFTs) [32–45], hybrid approaches

combining FO and EFT results [46–51], or the development of public codes [52–58]. The two-loop (2L) corrections to the SM-like Higgs mass of the MSSM—where one-loop (1L) contributions are mostly of  $\mathcal{O}(\alpha_t)$ <sup>1</sup>—are dominated by the contributions of order  $\alpha_t \alpha_s$  [10–13, 59–62] and  $\alpha_t^2$  [14–17, 63–65]—this does not necessarily apply to the other Higgs states of the model however.

In Ref. [66], we argued that terms violating the EW symmetry in an uncontrolled fashion were introduced in the predictions of masses and decays at the 1L order unless one carefully expands and truncates the various contributions entering the amplitudes. In particular, momentum-dependent corrections can lead to an explicit dependence on field-renormalization constants, thus producing UV-logarithms that have no quantitative meaning. While such artificial effects are formally of a higher order compared to that of the explicitly included self-energies, it is important to assess their numerical impact in order to estimate the actual gain in predictivity when incorporating radiative corrections in a fashion that explicitly depends on the regularization procedure.<sup>2</sup> Alternatively, a strict expansion and truncation order-after-order can limit the dependence on the field and gauge-fixing regulators and provide results where spurious symmetry-violating effects are systematically neutralized. The purpose of the present paper is to explain how such a formalism can be extended to address 2L mass corrections. We focus on the orders  $\alpha_q \alpha_s$  and  $\alpha_q^2$ , since these are fully exploitable at 2L, while the generic EW corrections miss some contributions needed for a direct connection to observable quantities. We build upon the existing results of Refs. [13–16], but include full momentum dependence now, also making use of the relations derived in Ref. [31]. Below, we restrict ourselves to the simplest model where the considered orders matter, *i. e.* the Minimal Supersymmetric Standard Model (MSSM), although the method straightforwardly applies to extensions, *e. g.* the Next-to-MSSM (NMSSM)—yet more care is then needed in order to consistently account for the gaugeless limit and process the more motivated scenarios with large radiative Higgs mixing.

In parallel with the computations at FO, where self-energies are derived order after order in the full model considered in a given renormalization scheme, the mass-gap suggested by the absence of discovery of new-physics particles has encouraged the discussion of SUSY Higgs sectors in the context of EFTs, allowing for a resummation of the large UV-logarithms that develop between the SUSY and EW scales; see *e. g.* the recent work of Refs. [32–45] and a more complete list of references in the review [9]. While the effects that we discussed in Ref. [66] also formally apply in such EFTs, the weight of regulators in the definition of mass observables is less critical than in FO calculations. Indeed, the direct variation of the gauge-fixing parameters or the field counterterms in the EFT is necessarily reduced in such a formalism where large logarithms are forced to follow an  $SU(2) \times U(1)$ -conserving pattern. On the other hand, such a variation represents only a partial picture in testing the connection between observables in the EFT context, as the MSSM–EFT matching procedure then plays a determining part in establishing this relation. This connection between the predicted Higgs masses and observable input is however at the center of what we probe through variations of regulators in the FO approach. We will not attempt to address the question of this relation in EFTs here.

---

<sup>1</sup> By convention, we denote the considered classes of Feynman diagrams by the type of the involved couplings  $\alpha_f = Y_f^2/(4\pi)$ ,  $\alpha_s = g_s^2/(4\pi)$ , and  $\alpha = g_{\text{EW}}^2/(4\pi)$ , where  $Y_f$  is the Yukawa coupling of fermion  $f$ ,  $g_s$  is the strong gauge coupling, and  $g_{\text{EW}}$  is any of the electroweak gauge couplings. In addition, we introduce  $\alpha_q \equiv \alpha_{t,b}$  when considering corrections controlled by the Yukawa couplings of both heavy quarks.

<sup>2</sup> Here, we employ the term ‘regularization’ in reference to the procedure giving a meaning to ill-defined self-energies away from their mass shell, not in reference to the counting of UV-divergences in Feynman amplitudes. Field-renormalization constants are the usual regulators—and the only ones that we consider in this paper—allowing such an extrapolation, and the ambiguity rests with their arbitrary finite part, from which actual observables are supposedly independent.

In Sect. 2, we analyze how to avoid or minimize the dependence of 2L corrections to the Higgs masses on the choice of field renormalization, taking this criterion as our guideline for the inclusion of the 2L contributions of  $\mathcal{O}(\alpha_t \alpha_s)$  and  $\mathcal{O}(\alpha_t^2)$ . We then numerically compare the corresponding mass predictions with those obtained through an iterative pole search, both in non-degenerate and near-degenerate scenarios, checking how variations of the field counterterms affect each in view of the magnitude of the 2L effects. We also probe how the effective-potential approximation performs for SM and non-SM Higgs states. This forms the content of Sect. 3 and Sect. 4. In Sect. 5, we perform a resummation of UV-logarithms of  $\mathcal{O}(\alpha_q, \alpha_q \alpha_s, \alpha_q^2)$  in the FO context, as the increasing weight of these effects for large SUSY scales otherwise limits the applicability of the FO approach. A brief summary is provided in Sect. 6.

## 2. Inclusion of 2L corrections to the Higgs mass observables

In this section, we present a brief description of the computation of Higgs masses at higher order, with reference to more detailed derivations in the appendix. We explicitly extract the dependence of the radiative contributions on Higgs-field counterterms and analyze the conditions for its cancellation at the level of Higgs-mass predictions at the 2L order.

### 2.1. Invariance under field-renormalization

As usual in Quantum Field Theory, the mass observables are calculated from the two-point truncated and connected correlators of the model. The complex zeroes of the characteristic polynomial in the Higgs sector should indeed correspond to the poles describing the Higgs resonances in particle scattering: a derivation is proposed in Appx. A. The defining equation for these poles  $\mathcal{M}_k^2$  thus reads:

$$\det \left[ \mathcal{M}_k^2 \mathbb{1} - M_{\text{tree}}^2 + \hat{\Sigma}(\mathcal{M}_k^2) \right] = 0. \quad (1)$$

where  $M_{\text{tree}}^2 = \text{diag}[m_i^2]$  represents the tree-level mass matrix and  $\hat{\Sigma}(p^2)$  is the renormalized self-energy matrix for external momentum  $p$ .

A problematic feature in Eq. (1) is that the renormalized self-energies  $\hat{\Sigma}_{ij}(p^2)$  are not well-defined away from their mass-shell at  $p^2 = (m_i^2 + m_j^2)/2$ . Indeed, absorption of the UV-divergences in such objects requires the introduction of field-renormalization constants,

$$\phi_i \rightarrow \left( \sqrt{Z} \right)_{ij} \phi_j \equiv \left( \sqrt{\mathbb{1} + \delta Z^{(1)} + \delta Z^{(2)} + \dots} \right)_{ij} \phi_j, \quad (2)$$

where the upper indices in parentheses refer to the loop order of the renormalization constant. However, since quantum fields are not measurable as such, these field counterterms should be strict bookkeeping quantities, which drop out at the level of observables. An iterative resolution of Eq. (1), as often advocated in the literature [17–19, 56, 57, 67–73], leads to an explicit dependence of the predicted masses on the field counterterms. This dependence should ideally become negligibly small when sufficiently high orders are included in the calculation and, in the meanwhile, the variation of the field counterterms could be seen as setting a lower bound on the higher-order uncertainty, by weighing such terms of higher order that are introduced in the pole search.

In Ref. [66], we argued against this iterative approach, in particular because it generates symmetry-violating terms that are not controlled by the vacuum-expectation values (v.e.v.-s) of the Higgs fields, but appear as pure artifacts of the formalism. Consequently, these partial higher-order, gauge-dependent terms introduced by the pole search do not represent a genuine estimate of higher-order corrections but amount to an intrinsic error of the procedure. Instead, we preferred to employ an explicit expansion and truncation where the dependence on field counterterms and gauge-fixing parameters vanishes or is minimized order-by-order. At 1L, this procedure leads us to systematically use diagonal self-energies evaluated on their mass-shell, while off-diagonal self-energies can be dismissed as contributions of higher order. Only in near-degenerate scenarios are the replacement  $\hat{\Sigma}_{ij}(p^2) \xrightarrow{p^2 \sim m_i^2} \hat{\Sigma}_{ij}((m_i^2 + m_j^2)/2)$  and the inclusion of off-diagonal self-energies justified by the counting  $m_i^2 - m_j^2 = \mathcal{O}(1L)$ .

Below, we discuss how to extend this procedure to include 2L mass corrections. As the considered orders do not involve EW gauge corrections, we must take solely independence from field-renormalization constants as our guiding criterion. This condition can be formulated in two different fashions:

1. the observables should be invariant under any choice of field counterterm;
2. the observables are UV-finite without need of considering field counterterms.

The second prescription proves to be a weaker requirement than the first one, in particular because the UV-divergent part of  $d\Sigma_{ij}/dp^2$  is symmetric under the exchange  $i \leftrightarrow j$ , so that amplitudes may in general depend on antisymmetric finite contributions to the field counterterms while these are not needed to achieve UV-finiteness. In practice, the first criterion is satisfied in the non-degenerate case, while we must content ourselves with the second one in the near-degenerate scenario—at least in the strategy presented in Ref. [66]. We will look upon the second condition as being roughly equivalent to an invariance under symmetric choices of the field counterterms—in fact a more constraining requirement.

## 2.2. Non-degenerate case

For a non-degenerate state with tree-level mass  $m_i$ , it is possible to extract the nearby pole  $\mathcal{M}_i^2$  in the propagator matrix by solving the recursive Eq. (1); at the 2L order this amounts to solving  $\mathcal{M}_i^2 \stackrel{!}{=} \widetilde{M}_i^2(\mathcal{M}_i^2)$ , where  $\widetilde{M}_i^2$  is the quantity defined in Eq. (40)—refer *e. g.* to the derivation in Appx. A.2. The right-hand side of this equation can be further expanded using the condition  $\mathcal{M}_i^2 = \bar{p}_{ii}^2 + \mathcal{O}(2L) = m_i^2 + \mathcal{O}(1L)$  in the argument of the renormalized self-energies ( $\hat{\Sigma}^{(k)}$  represents the renormalized self-energy of  $k$ -loop order):

$$\mathcal{M}_i^2 = m_i^2 - \hat{\Sigma}_{ii}^{(1)}(m_i^2) - \left[ \hat{\Sigma}_{ii}^{(2)}(m_i^2) + (\bar{p}_{ii}^2 - m_i^2) \frac{d\hat{\Sigma}_{ii}^{(1)}}{dp^2}(m_i^2) - \sum_{j \neq i} \frac{\hat{\Sigma}_{ij}^{(1)}(m_i^2) \hat{\Sigma}_{ji}^{(1)}(m_i^2)}{m_i^2 - m_j^2} \right] + \mathcal{O}(3L). \quad (3)$$

The leading correction  $\hat{\Sigma}_{ii}^{(1)}(\mathcal{M}_i^2)$  has been expanded so that it gives a contribution that is independent from field renormalization (and gauge-fixing) at strict  $\mathcal{O}(1L)$ .

Similarly, invariance under variations of the 2L field counterterm dictates the choice  $p^2 \stackrel{!}{=} m_i^2$  as the argument of  $\hat{\Sigma}_{ii}^{(2)}$  in Eq. (3). In addition, restriction to the orders  $\alpha_q \alpha_s$  and  $\alpha_q^2$  entails a specific distinction between corrections of Yukawa- and gauge-type since both are otherwise mixed by the EW symmetry-breaking. A clean separation is only possible in the gaugeless limit (*i. e.*  $g_{EW} \stackrel{!}{=} 0$ ), where the tree-level spectrum slightly differs from the original one: the mass ‘ $m_i$ ’

entering the self-energy of 2L order computed in the gaugeless limit and ensuring independence from the 2L field counterterm is not the original tree-level mass, but its gaugeless counterpart  $\check{m}_i$ . The difference with  $m_i$  corresponds to the order neglected in the gaugeless approximation. In the non-degenerate scenario, the identification of the ‘original’ Higgs state with its gaugeless counterpart is fortunately straightforward.

The choice of momenta in the 1L<sup>2</sup> terms of Eq. (3) should allow the cancellation of the dependence on the field counterterms of 1L order in the 2L contributions. While we already expanded the momenta in the off-diagonal terms of Eq. (3) and set them to  $m_i^2$ , any value  $\bar{p}_{ij}^2 = m_i^2 + \mathcal{O}(1\text{L})$  is *a priori* as legitimate as long as dependence on the field counterterms is not considered. Let us therefore analyze the dependence of  $\hat{\Sigma}_{ii}^{(2)}$  on the 1L field counterterms. It originates in two pieces: 1L diagrams with counterterm insertion (1L×CT) and tree-level graphs with counterterm squared insertion (CT<sup>2</sup>):<sup>3</sup>

$$\begin{aligned} \hat{\Sigma}_{ii}^{(2)}(p^2) \ni & \frac{1}{4} (p^2 - \check{m}_i^2) \delta Z_{ii}^2 + \delta Z_{ii} \left[ \check{\Sigma}_{ii}^{(1)}(p^2) - \delta \check{M}_{ii}^2 \right] \\ & + \sum_{j \neq i} \left\{ \frac{1}{4} (p^2 - \check{m}_j^2) \delta Z_{ji}^2 + \delta Z_{ji} \left[ \check{\Sigma}_{ij}^{(1)}(p^2) - \delta \check{M}_{ij}^2 \right] \right\}; \end{aligned} \quad (4)$$

the 1L×CT and CT<sup>2</sup> contributions to the tadpoles cancel one another. Here,  $\Sigma_{ij}$  (or  $\check{\Sigma}_{ij}$ ) stands for the unrenormalized self-energy;  $\delta M_{ij}^2$  (or  $\delta \check{M}_{ij}^2$ ) denote the mass and  $\delta Z_{ji}$  the field counterterms of 1L order. The  $\check{\phantom{x}}$  notation highlights that the corresponding quantities are obtained in the approximations applied in the 2L calculation (*e.g.* the gaugeless limit).

From the 1L<sup>2</sup> terms emerge the following contributions depending on field renormalization:

$$\begin{aligned} (\bar{p}_{ii}^2 - m_i^2) \frac{d\hat{\Sigma}_{ii}^{(1)}}{dp^2}(m_i^2) - \sum_{j \neq i} \frac{\hat{\Sigma}_{ij}^{(1)}(\bar{p}_{ij}^2) \hat{\Sigma}_{ji}^{(1)}(\bar{p}_{ij}^2)}{\bar{p}_{ij}^2 - m_j^2} \ni \\ (\bar{p}_{ii}^2 - m_i^2) \delta Z_{ii} - \sum_{j \neq i} \frac{1}{\bar{p}_{ij}^2 - m_j^2} \left\{ \frac{1}{4} [\delta Z_{ij} (\bar{p}_{ij}^2 - m_i^2) + \delta Z_{ji} (\bar{p}_{ij}^2 - m_j^2)]^2 \right. \\ \left. + [\delta Z_{ij} (\bar{p}_{ij}^2 - m_i^2) + \delta Z_{ji} (\bar{p}_{ij}^2 - m_j^2)] (\Sigma_{ij}^{(1)}(\bar{p}_{ij}^2) - \delta M_{ij}^2) \right\}. \end{aligned} \quad (5)$$

The requirement for cancellation of the field-renormalization dependence between Eq. (4) and Eq. (5) dictates the following conditions:

$$\bar{p}_{ii}^2 - m_i^2 \rightarrow - \left[ \check{\Sigma}_{ii}^{(1)}(\check{m}_i^2) - \delta \check{M}_{ii}^2 \right], \quad \Sigma_{ij}^{(1)}(\bar{p}_{ij}^2) - \delta M_{ij}^2 \rightarrow \check{\Sigma}_{ij}^{(1)}(\check{m}_i^2) - \delta \check{M}_{ij}^2, \quad \bar{p}_{ij}^2 \rightarrow \check{m}_i^2. \quad (6)$$

In other words, the self-energies employed in the 1L<sup>2</sup> terms should be calculated in the same approximation as in the 2L calculation in order to avoid the inclusion of arbitrary UV-logarithms in the calculation.

<sup>3</sup> In this analysis of the dependence on 1L field counterterms  $\delta Z_{ij}$  (for commodity we omit the superscript <sup>(1)</sup>), we do not display the 2L term  $(\delta Z_{ii}^{(2)} - \sum_k \frac{1}{4} \delta Z_{ik}^2) (p^2 - m_i^2)$  emerging simply from the expansion of Eq. (2), which separately cancels out for  $p^2 \stackrel{!}{=} m_i^2$ , as the vanishing condition for the dependence on the 2L field counterterm  $\delta Z_{ii}^{(2)}$ . This restores agreement between our expansion and the standard conventions for field counterterms—see Eq. (2).

### 2.3. Degenerate case

We assume the existence of a degenerate sector (denoted by ‘ $D$ ’). In this case, one should consider the effective mass matrix  $\widetilde{M}_D^2(s)$  of Eq. (44), evaluated at a pole

$$\mathcal{M}_I^2 = \bar{p}_{ij}^2 + \mathcal{O}(2L) = m_{ij}^2 + \mathcal{O}(1L) \quad (7)$$

of the propagator—refer to Appx. A.2 for a derivation. For two field directions  $i, j \in D$ , we define the notation  $m_{ij}^2 \equiv (m_i^2 + m_j^2)/2$ .

Then, there exists a unitary matrix  $\mathbf{U}^I$  such that

$$(\mathbf{U}^I)^* \cdot \left[ \mathcal{M}_I^2 \mathbf{1}_D - \widetilde{M}_D^2(\mathcal{M}_I^2) \right] \cdot (\mathbf{U}^I)^\dagger = \text{diag}[\mathcal{D}_J] \quad (8)$$

with  $\mathcal{D}_I \equiv 0$  ( $\mathcal{D}_J$ ,  $J \neq I$  has no particular relevance), hence

$$\sum_{j \in D} \left[ \widetilde{M}_D^2(\mathcal{M}_I^2) \right]_{ij} (U_{Ij}^I)^* = \mathcal{M}_I^2 (U_{Ii}^I)^*, \quad \sum_{i, j \in D} (U_{Ii}^I)^* (U_{Ij}^I)^* \left[ \mathcal{M}_I^2 \delta_{ij} - \left[ \widetilde{M}_D^2(\mathcal{M}_I^2) \right]_{ij} \right] = 0. \quad (9)$$

Thus,  $\mathcal{M}_I^2$  is an eigenvalue of  $\widetilde{M}_D^2(\mathcal{M}_I^2)$  and its eigenvector  $(U_{Ij}^I)^*$  generates the kernel of  $\left[ \mathcal{M}_I^2 \mathbf{1}_D - \widetilde{M}_D^2(\mathcal{M}_I^2) \right]^\dagger \cdot \left[ \mathcal{M}_I^2 \mathbf{1}_D - \widetilde{M}_D^2(\mathcal{M}_I^2) \right]$ . These are the defining properties that we are going to exploit below after expanding  $\widetilde{M}_D^2(\mathcal{M}_I^2)$ .

As explained in Ref. [66], it is possible, at the 1L order, to expand  $\widetilde{M}_D^2(\mathcal{M}_I^2)$  in a fashion that is invariant under field renormalization (in the ‘weak’ sense discussed in Sect. 2.1):

$$\widetilde{M}_D^2(\mathcal{M}_I^2) = \widetilde{M}_D^{2(1)} + \mathcal{O}(2L) \quad \text{with} \quad (\widetilde{M}_D^{2(1)})_{ij} \equiv m_i^2 \delta_{ij} - \hat{\Sigma}_{ij}^{(1)}(m_{ij}^2) \quad (10)$$

(which now has lost its dependence on the value of the pole). We denote the associated poles and eigenvectors of 1L order as  $\mathcal{M}_I^{2(1)}$  and  $S_{Ij} \equiv (U_{Ij}^{I(1)})^*$ : the poles are simply given by the eigenvalues of  $\widetilde{M}_D^{2(1)}$  while the matrix  $\mathbf{U}^{I(1)}$  is obtained from the diagonalization of  $\left[ \mathcal{M}_I^{2(1)} \mathbf{1}_D - \widetilde{M}_D^{2(1)} \right]^\dagger \cdot \left[ \mathcal{M}_I^{2(1)} \mathbf{1}_D - \widetilde{M}_D^{2(1)} \right]$ . There is a subtle difference in the definition of the eigenvectors with respect to the procedure presented in Ref. [66]: we ensure the exact cancellation of off-diagonal terms in  $(\mathbf{U}^{I(1)})^* \cdot \left[ \mathcal{M}_I^{2(1)} \mathbf{1}_D - \widetilde{M}_D^{2(1)} \right] \cdot (\mathbf{U}^{I(1)})^\dagger$  now, while they could still amount to  $\mathcal{O}(2L)$  in Ref. [66]; the reason is that we now also want to put 2L effects under control.

Let us now consider the 2L order:

$$\begin{aligned} \widetilde{M}_D^2(\mathcal{M}_I^2) = & \left[ (\widetilde{M}_D^{2(1)})_{ij} - \hat{\Sigma}_{ij}^{(2)}(m_{ij}^2) - (\bar{p}_{ij}^2 - m_{ij}^2) \frac{d\hat{\Sigma}_{ij}^{(1)}}{dp^2}(m_{ij}^2) \right. \\ & \left. + \sum_{l \notin D} \frac{(m_{ij}^2 - m_l^2) \hat{\Sigma}_{il}^{(1)}(\bar{p}_{ijl}^2) \hat{\Sigma}_{jl}^{(1)}(\bar{p}_{jil}^2)}{(m_i^2 - m_l^2)(m_j^2 - m_l^2)} \right]_{i, j \in D} + \mathcal{O}(3L) \end{aligned} \quad (11)$$

Once again, the dependence on field-renormalization constants of 2L order is neutralized by setting  $p^2 \stackrel{!}{=} \check{m}_{ij}^2 = \mathcal{M}_I^2 + \mathcal{O}(1L)$  in the argument of  $\hat{\Sigma}_{ij}^{(2)}$ . We still need to determine the momenta  $\bar{p}_{ij}^2 = \mathcal{M}_I^2 + \mathcal{O}(2L)$  and  $\bar{p}_{ijl}^2 = \mathcal{M}_I^2 + \mathcal{O}(1L)$ . To this end, we consider the dependence on  $1L^2$  field counterterms, directly restricting ourselves to the symmetric case  $\delta Z_{ji} = \delta Z_{ij}$ . Then, instead of the diagonal matrix element of Eq. (4) one has to take the full self-energy matrix for the

degenerate sector into account, depending on 1L field counterterms as follows:

$$\hat{\Sigma}_{ij}^{(2)}(p^2) \ni \sum_k \left\{ \frac{1}{4} (p^2 - \check{m}_k^2) \delta Z_{ki} \delta Z_{kj} + \frac{1}{2} \left( \delta Z_{ki} \left[ \check{\Sigma}_{kj}^{(1)}(p^2) - \delta \check{M}_{kj}^2 \right] + \delta Z_{kj} \left[ \check{\Sigma}_{ki}^{(1)}(p^2) - \delta \check{M}_{ki}^2 \right] \right) \right\}. \quad (12)$$

With the choice  $\bar{p}_{ij}^2 \equiv m_{ij}^2 \equiv \bar{p}_{ji}^2$  one has

$$\sum_{l \notin D} \frac{(m_{ij}^2 - m_l^2) \hat{\Sigma}_{il}^{(1)}(m_{ij}^2) \hat{\Sigma}_{jl}^{(1)}(m_{ij}^2)}{(m_i^2 - m_l^2) (m_j^2 - m_l^2)} \ni \sum_{l \notin D} \left\{ \frac{1}{4} (m_{ij}^2 - m_l^2) \delta Z_{li} \delta Z_{lj} + \frac{1}{2} \delta Z_{li} \left[ \Sigma_{lj}^{(1)}(m_{ij}^2) - \delta M_{lj}^2 \right] \left[ 1 + \frac{1}{2} \frac{m_j^2 - m_i^2}{m_i^2 - m_l^2} \right] + \frac{1}{2} \delta Z_{lj} \left[ \Sigma_{li}^{(1)}(m_{ij}^2) - \delta M_{li}^2 \right] \left[ 1 + \frac{1}{2} \frac{m_i^2 - m_j^2}{m_i^2 - m_l^2} \right] \right\}. \quad (13)$$

Then, the dependence on field-renormalization constants  $\delta Z_{li}$  with  $i \in D$ ,  $l \notin D$ , cancels out against the one of Eq. (12), provided  $\Sigma^{(1)} - \delta M^2 \rightarrow \check{\Sigma}^{(1)} - \delta \check{M}^2$  and up to terms of 3L order involving an additional mass suppression.

If we assume that the degeneracy is lifted at the 1L order, *i. e.*  $|\mathcal{M}_I^2 - \mathcal{M}_J^2| > \mathcal{O}(2L)$  for  $I \neq J$ , then the off-diagonal elements of  $(\mathbf{U}^{I(1)})^* \cdot [\mathcal{M}_I^2 \mathbf{1}_D - \widetilde{M}_D^2(\mathcal{M}_I^2)] \cdot (\mathbf{U}^{I(1)})^\dagger$  are negligible, since of 2L order when the diagonal splitting is of 1L order. We can thus focus on the diagonal element

$$\widetilde{\mathcal{D}}_I \equiv \sum_{i,j \in D} S_{Ii} S_{Ij} \left\{ \left( \mathcal{M}_I^2 - \mathcal{M}_I^{2(1)} \right) \delta_{ij} + \hat{\Sigma}_{ij}^{(2)}(m_{ij}^2) + (\bar{p}_{ij}^2 - m_{ij}^2) \frac{d\hat{\Sigma}_{ij}^{(1)}}{dp^2}(m_{ij}^2) - \sum_{l \notin D} \frac{(m_{ij}^2 - m_l^2) \hat{\Sigma}_{il}^{(1)}(m_{ij}^2) \hat{\Sigma}_{jl}^{(1)}(m_{ij}^2)}{(m_i^2 - m_l^2) (m_j^2 - m_l^2)} \right\}. \quad (14)$$

We define  $\bar{p}_{ij}^2 \equiv (\bar{p}_{ij}^{2(i)} + \bar{p}_{ij}^{2(j)})/2$  and, from the 1L eigenstate equation (adding a convenient 2L term):

$$\bar{p}_{ij}^{2(i)} \equiv m_i^2 - S_{Ii}^{-1} \sum_{k \in D} S_{Ik} \left[ \hat{\Sigma}_{ik}^{(1)}(m_{jk}^2) + \frac{m_{ik}^2 - m_j^2}{2} \frac{d\hat{\Sigma}_{ik}^{(1)}}{dp^2}(m_{ik}^2) \right] = \mathcal{M}_I^2 + \mathcal{O}(2L). \quad (15)$$

Then, we obtain  $\widetilde{\mathcal{D}}_I = \sum_{i,j \in D} S_{Ii} S_{Ij} \left[ (\mathcal{M}_I^2 - \mathcal{M}_I^{2(1)}) \delta_{ij} + \mathcal{W}_{ij} \right]$  with

$$\mathcal{W}_{ij} \equiv \hat{\Sigma}_{ij}^{(2)}(m_{ij}^2) - \frac{1}{2} \sum_{k \in D} \left\{ \left[ \hat{\Sigma}_{ik}^{(1)}(m_{ij}^2) + \frac{m_{ij}^2 - m_k^2}{2} \frac{d\hat{\Sigma}_{ik}^{(1)}}{dp^2}(m_{ik}^2) \right] \frac{d\hat{\Sigma}_{jk}^{(1)}}{dp^2}(m_{jk}^2) + (i \leftrightarrow j) \right\} - \sum_{l \notin D} \frac{(m_{ij}^2 - m_l^2) \hat{\Sigma}_{il}^{(1)}(m_{ij}^2) \hat{\Sigma}_{jl}^{(1)}(m_{ij}^2)}{(m_i^2 - m_l^2) (m_j^2 - m_l^2)}. \quad (16)$$



The dependence of  $\mathcal{W}_{ij}$  on  $\delta Z_{ij}$  with  $i, j \in D$  almost cancels (provided all 1L<sup>2</sup> quantities are calculated in the same approximations as the self-energies of 2L order, *e.g.* in the gaugeless limit), up to a remainder of 3L order:

$$\frac{m_i^2 - m_j^2}{8} \left[ \delta Z_{ki} \frac{d\Sigma_{jk}}{dp^2}(m_{jk}^2) - \delta Z_{kj} \frac{d\Sigma_{ik}}{dp^2}(m_{ik}^2) \right]. \quad (17)$$

We find no obvious method to absorb this piece by adding a finite term of 3L order to  $\mathcal{W}_{ij}$ ; thus, after applying the condition  $\tilde{\mathcal{D}}_I \stackrel{!}{=} \mathcal{O}(3L)$ , a subleading field-renormalization dependence remains in the determination of the pole of 2L order by

$$\mathcal{M}_I^{2(2)} \equiv \mathcal{M}_I^{2(1)} - \sum_{i,j \in D} S_{Ii} S_{Ij} \mathcal{W}_{ij} \bigg/ \sum_{k \in D} S_{Ik}^2. \quad (18)$$

This persisting dependence on field-renormalization constants in the degenerate case is intimately related to the form of the dependence of the off-diagonal self-energy of 2L order on 1L field counterterms—see Eq. (12). In the non-degenerate case, this object only intervenes in the mass corrections of 3L order, so that we can expect the field-renormalization dependence to be tackled by the inclusion of the diagonal  $\hat{\Sigma}_{ii}^{(3)}$  (which, however, goes far beyond our purpose and our current means). The 2L terms of Eq. (15) (contributing at 3L order) have been chosen so as to avoid a quadratic dependence on the field counterterms. Other choices are of course possible. While the full cancellation of the dependence on field counterterms thus fails in the degenerate scenario, we still expect an improvement in the expansion method, as compared to the iterative pole search, due to the careful pairing of 2L and 1L<sup>2</sup> effects.

In case the degeneracy is not lifted at 1L order, we can still define  $\mathcal{M}_I^{2(2)}$  as an eigenvalue of the effective mass matrix

$$\tilde{\mathcal{M}}_{\text{eff}}^{2(2)} \equiv \left[ m_i^2 \delta_{ij} - \hat{\Sigma}_{ij}^{(1)}(m_{ij}^2) - \mathcal{W}_{ij} \right], \quad i, j \in D. \quad (19)$$

Indeed, similarly to the 1L piece in Eq. (10), the 2L corrections  $\mathcal{W}_{ij}$  of Eq. (16) are independent from the chosen pole, the selection being ensured by the projection via the eigenvectors  $\mathbf{U}^I$ . It is then convenient to directly consider these eigenvectors, albeit slightly dependent on the choice of field renormalization, as determining the mixing matrix  $\mathbf{S}$  in the degenerate subspace at 2L order. In addition, the normalization  $\sum_{k \in D} S_{Ik}^2 \stackrel{!}{=} 1$  simplifies the application of this object, as can be read from Eq. (18) or the derivation of the Higgs-decay amplitudes in Appx. A.3.

Finally, we stress that it is necessary to compute all the 1L<sup>2</sup> pieces in the approximation of the 2L calculation, *i.e.* all self-energies, mass counterterms and tree-level masses in  $\mathcal{W}$  are replaced by  $\check{\Sigma}^{(1)}$ ,  $\delta\check{\mathcal{M}}$  and  $\check{m}$ . An apparent difficulty accompanies the observation that the identification of ‘original’ and ‘gaugeless’ states is no longer trivial in the degenerate scenario. Yet, as the full 2L + 1L<sup>2</sup> mass contribution is collected within the block  $\mathcal{W}$ , it is possible to compute the latter in the gaugeless base and then rotate it to the ‘original’ base using the gauge eigenbase as reference. This *ad-hoc* procedure is however a sign that the combination of gaugeless 2L effects with a full 1L calculation is not defined in a completely consistent fashion in the near-degenerate case.

### 3. Field-dependence in the mass predictions for a non-degenerate scenario

We first investigate the numerical significance of radiative corrections to the masses of MSSM Higgs bosons in the clearly defined configuration where all states are non-degenerate, and assess the weight of the dependence on field counterterms in various methods of evaluation. The required Feynman diagrams are computed with the help of `FeynArts` [74], `FormCalc` [75, 76], `TwoCalc` [77] and `TLDR` [31]. The 1L integrals are implemented analytically, while the 2L integrals are numerically evaluated with the assistance of `TSIL` [78].

#### 3.1. Preliminary considerations

We focus on a ‘typical’ MSSM scenario with squarks of third generation ( $\tilde{Q}_3$ ) and gluinos ( $\tilde{g}$ ) at the edge of the mass region probed by the LHC ( $m_{\tilde{Q}_3} \sim 1.5$  TeV and  $M_3 \sim 2$  TeV;  $A_t = 2.3$  TeV,  $A_b = 1$  TeV). EW-only-interacting SUSY particles are given a sub-TeV mass. The ratio of the doublet Higgs v.e.v.-s,  $t_\beta$ , is set to 10 and we vary the charged-Higgs mass between 0.5 TeV and 4 TeV. In these conditions, the neutral SM-like Higgs ( $h$ ), with mass at the EW scale, and the heavy-doublet states ( $H$ ,  $A$ ), with masses comparable to that of the charged Higgs ( $H^\pm$ ), are clearly non-degenerate. The  $\mathcal{CP}$ -even ( $H$ ) and  $\mathcal{CP}$ -odd ( $A$ ) heavy states do not mix in the absence of  $\mathcal{CP}$ -violation, which we assume in this section. One can thus safely employ the formalism corresponding to the non-degenerate scenario. The lagrangian parameters in the Higgs sector are renormalized in the same scheme as employed in Refs. [66, 79], *i. e.* with cancellation of the tadpoles, on-shell conditions for the EW gauge-boson, SM-fermion and charged-Higgs masses, while  $t_\beta$  is defined in the  $\overline{\text{DR}}$  scheme.

It is instructive to first consider the corrections of 1L order to the tree-level masses  $m_{h_i}$  of the neutral Higgs bosons  $h_i \in \{h, H, A\}$ . In Fig. 1, we show the corresponding shifts in mass squared,  $\Delta^{(1)}M_{h_i}^2 \equiv M_{h_i}^{2(1)} - m_{h_i}^2 = -\Re \left[ \hat{\Sigma}_{h_i h_i}^{(1)}(m_{h_i}^2) \right]$ .<sup>4</sup> The orange curves correspond to the gaugeless limit, while the full 1L shift is shown in blue. The situation of the SM-like Higgs is straightforward: the radiative corrections of Yukawa type  $\mathcal{O}(\alpha_{t,(b)})$ , captured in the gaugeless approach, indeed dominate the 1L shift. Contributions of EW type, beyond the gaugeless description, amount to only  $\sim 15\%$ . The gaugeless limit can thus be seen as predictive for this state.<sup>5</sup>

Nevertheless, the impact of the various contributions follows a different pattern in the case of the heavy-doublet states. A first identifiable feature corresponds to the ‘spikes’ in the vicinity of  $M_{H^\pm} = 3$  TeV: these are associated with threshold effects in the loop integrals of the self-energies, when  $M_{H,A} \sim m_X + m_Y$  for  $X$  and  $Y$  two particle species entering the loop diagram ( $m_X$  and  $m_Y$ , their masses). At  $M_{H^\pm} \sim 3$  TeV, these internal ‘on-shell’ lines are squarks of the third generation, contributing at  $\mathcal{O}(\alpha_q)$ . The sharp variation in the mass shift is consequently a physical effect, although it is not quantitatively described in the ‘free-particle’ expansion—we will make no attempt at addressing the threshold behavior by accounting for squark interactions in this paper: see *e. g.* Ref. [80]. Comparable features also appear close to  $M_{H^\pm} \approx 1$  TeV for the blue curve (full 1L corrections) and correspond to electroweakino loops: these do not show in the gaugeless limit as EW interactions are turned off.

<sup>4</sup>In the case of the heavy-doublet states, one could more properly consider the radiative corrections to the mass-splitting between neutral and charged states (otherwise, the squared tree-level mass  $m_{h_i}^2$  is not straightforwardly related to observable quantities): as the charged Higgs is renormalized on-shell in our scheme, this definition is equivalent.

<sup>5</sup>However, contributions of  $\mathcal{O}(\alpha_t)$  are reduced by large QCD effects—which could be in part absorbed in the tree-level Yukawa couplings in a convenient scheme. This ultimately increases the impact of EW contributions lost in the gaugeless approximation.

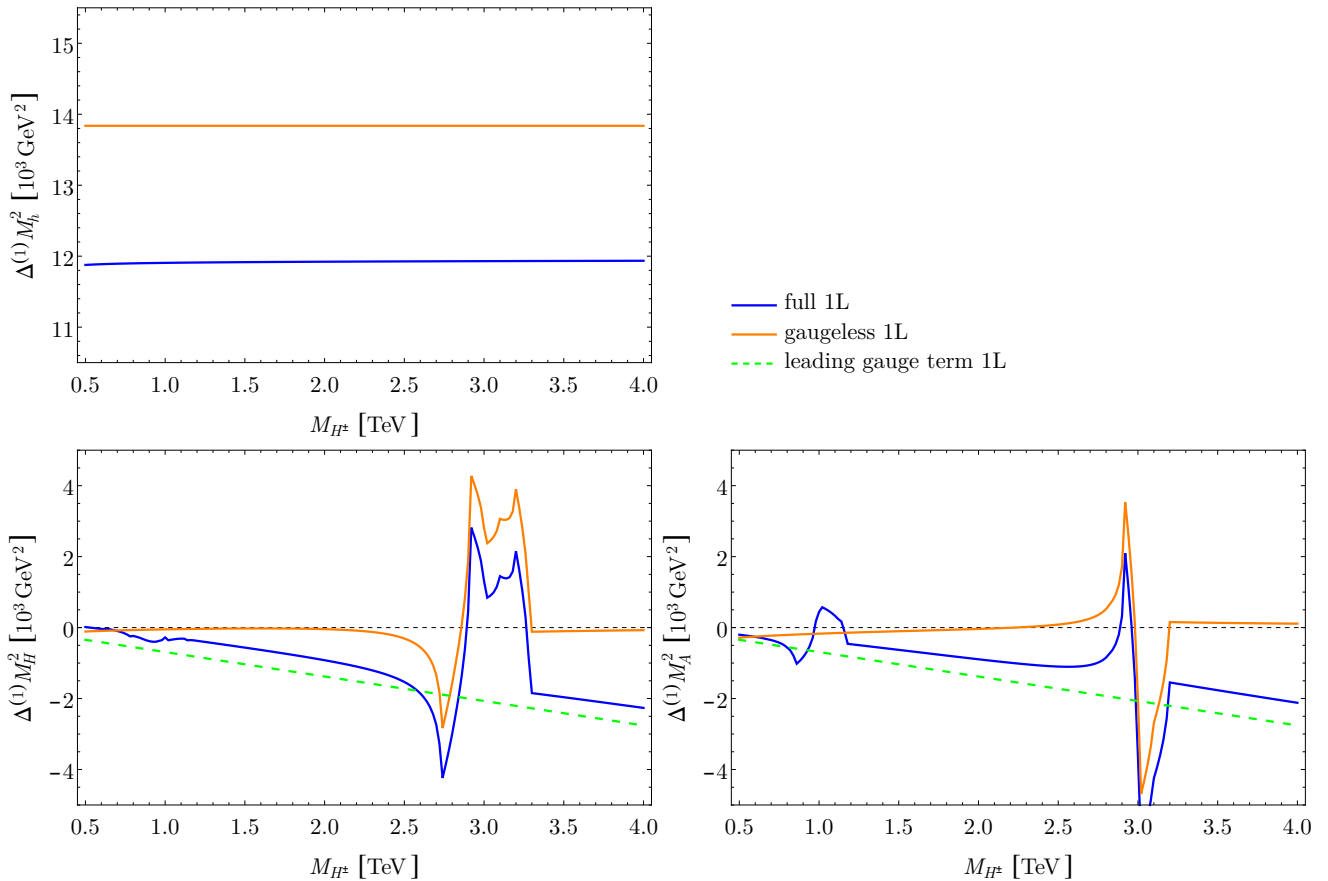


**Figure 1.:** Mass shifts at 1L for the neutral Higgs states. The full 1L effect is shown in blue and the corresponding result in the gaugeless limit in orange. For the heavy states (lower row), the leading contribution from gauge loops, scaling linearly with the Higgs mass, is presented in dashed green.

Beyond this threshold behavior, the pattern of 1L corrections is essentially flat in the gaugeless limit while a slope is definitely identifiable in the presence of gauge effects. As explained in Sect. 3.2 of Ref. [66], the radiative contributions of gauge type to the squared mass-splitting between heavy-doublet states generate a term scaling linearly with the Higgs mass. This leading effect is shown as a dashed green line in Fig. 1 and indeed captures the slope of the full 1L result. The shift between the green and blue curves is due to corrections scaling like  $M_{\text{EW}}^2 \ln^k M_{H^\pm}^2 / M_{\text{EW}}^2$ , where  $k \in \{0, 1\}$  and  $M_{\text{EW}}^2 \sim M_Z^2$  denotes the EW scale. Therefore, radiative corrections of Yukawa type do not capture the bulk of the contribution to the mass-splitting between heavy states and corrections of orders  $\alpha_q \alpha_s$  or  $\alpha_q^2$  are not expected to dominate the 2L corrections either. While these orders are fully under control, their inclusion does not improve the numerical precision of the mass predictions to the heavy states as long as dominant corrections of EW gauge-type are not considered. The latter are known as far as scalar self-energies are concerned [31], but are currently not exploitable as 2L contributions to the vector self-energies that are needed for renormalization and the connection to observable input are still missing. Consequently, when we discuss the known  $\mathcal{O}(\alpha_q \alpha_s, \alpha_q^2)$  at the level of the heavy-doublet states below, it is purely for the sake of testing the formalism described in Sect. 2 on controlled orders: the theoretical prediction is actually not improved as compared to the strict 1L result.

### 3.2. Corrections of $\mathcal{O}(\alpha_q \alpha_s)$

The (S)QCD corrections have a specific status in the contributions of 2L order to the Higgs masses, because no corresponding 1L<sup>2</sup> effects are associated. Thus, this order does not entail the inclusion of any off-diagonal self-energies—unless these are already needed at 1L, *i. e.* in the near-degenerate case. Given the large impact of QCD corrections to effects of Yukawa-type, they are particularly relevant for an accurate determination of the mass of the SM-like state.

In Fig. 2, we plot the shifts of the squared masses obtained at the considered order, *i. e.*

$$\Delta^{(2,\alpha_q\alpha_s)} M_{h_i}^2 \equiv M_{h_i}^{2(2,\alpha_q\alpha_s)} - M_{h_i}^{2(1)} = -\Re \left[ \hat{\Sigma}_{h_i h_i}^{(2,\alpha_q\alpha_s)}(m_{h_i}^{2(\text{gl})}) \right], \quad (20)$$

with corrections obtained in the gaugeless (gl) limit. The solid orange curves have momentum evaluated at the tree-level (gaugeless) mass of the Higgs states. The cyan dashed lines are derived in the effective-potential approximation, *i. e.* with momentum set to 0. This approximation is ‘exact’ in the case of the SM-like Higgs, because the corresponding tree-level mass in the gaugeless limit is indeed equal to 0 (this is not necessarily true in extensions of the MSSM), so that the orange and cyan curves overlap. For the heavy-doublet states, threshold effects originating in squark loops are again prominent (when considering momentum dependence). Even far from the threshold region, the effective-potential approximation does not appear as a particularly useful approach for the heavy states, as its predictions for the order  $\alpha_q \alpha_s$  are  $\mathcal{O}(100\%)$  away from the actual momentum-dependent contributions. This is not surprising for Higgs states with mass differing significantly from 0, even in the gaugeless limit. In this context, the self-energies of order  $\alpha_q \alpha_s$  with vanishing momentum can at best provide an estimate of the corresponding order in an assessment of the uncertainties, but are not predictive.

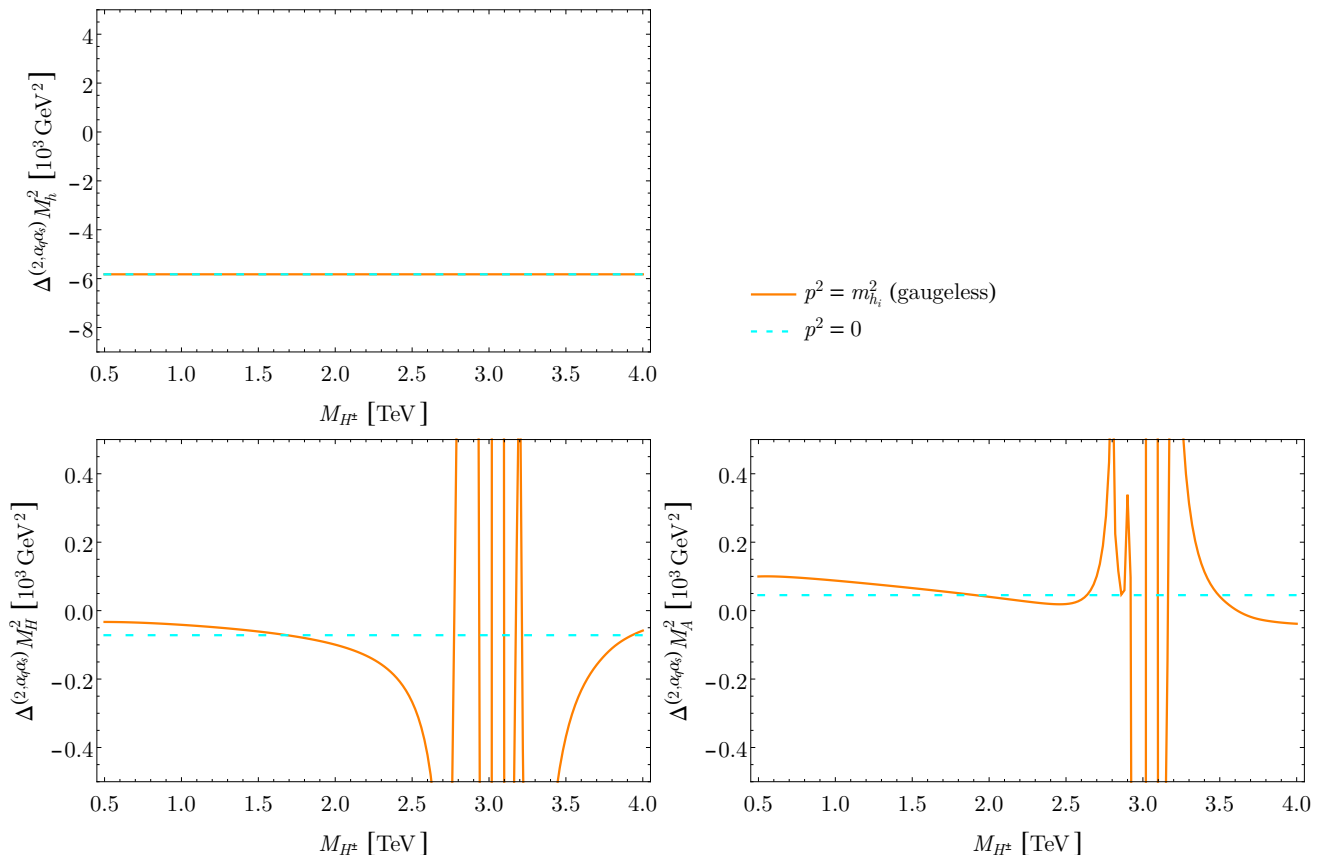


**Figure 2.:** Mass shifts at  $\mathcal{O}(\alpha_q \alpha_s)$  for the neutral Higgs states. The result in the gaugeless limit is shown in orange with momentum set to the (gaugeless) tree-level mass. The dashed cyan curve corresponds to the effective-potential approximation.

In conformity with the discussion of Sect. 2, the mass shifts of  $\mathcal{O}(\alpha_q \alpha_s)$  presented in orange in Fig. 2 (or those of 1L order in Fig. 1) are independent from the field counterterms, because the self-energies have been expanded for momenta in the vicinity of the tree-level masses, and truncated at the strict desired order—meaning in practice that the self-energies are evaluated at the tree-level Higgs mass. For definiteness, we remind here the formal expression defining the pole mass in this expansion-and-truncation approach for a non-degenerate state  $h_i$ :

$$M_{h_i}^{2(2,\alpha_q\alpha_s)} = m_{h_i}^2 - \Re \left[ \hat{\Sigma}_{h_i h_i}^{(1)}(m_{h_i}^2) + \hat{\Sigma}_{h_i h_i}^{(2,\alpha_q\alpha_s)}(m_{h_i}^{2(\text{gl})}) \right]. \quad (21)$$

In competition with such an expansion, a popular approach consists in iteratively replacing the momenta in the self-energies by the value derived in the pole-mass determination. As off-diagonal effects do not matter at  $\mathcal{O}(\alpha_q \alpha_s)$  in a non-degenerate scenario,<sup>6</sup> we define such a pole search of order  $\alpha_q \alpha_s$  by simply considering the shift of the diagonal element of the effective mass matrix. In other words, the equation that we solve iteratively in this subsection reads

$$\mathfrak{M}_{h_i}^{2(2,\alpha_q\alpha_s)} = m_{h_i}^2 - \hat{\Sigma}_{h_i h_i}^{(1)} \left( \mathfrak{M}_{h_i}^{2(2,\alpha_q\alpha_s)} \right) - \hat{\Sigma}_{h_i h_i}^{(2,\alpha_q\alpha_s)} \left( \mathfrak{M}_{h_i}^{2(2,\alpha_q\alpha_s)} \right) \quad (22)$$

with  $\mathfrak{M}_{h_i}^{2(2,\alpha_q\alpha_s)}$  denoting the (complex) pole mass—by an abuse of language, we will employ the same notation for its real part in the discussion below. In order to achieve UV-finite results for the renormalized self-energies of Eq. (22) away from  $p^2 = m_{h_i}^2$ , the definition of these objects requires the introduction of field counterterms, thereby generating a dependence of higher order on field regulators in  $\mathfrak{M}_{h_i}^{2(2,\alpha_q\alpha_s)}$ .

To understand the differences between the expansion and iteration procedures, we investigate the mass shift between both through an expansion, where we only keep leading terms:

$$\begin{aligned} \mathfrak{M}_{h_i}^2 - M_{h_i}^2 &\approx - \left( \mathfrak{M}_{h_i}^2 - m_{h_i}^2 \right) \hat{\Sigma}_{h_i h_i}^{(1)'} - \left( \mathfrak{M}_{h_i}^2 - m_{h_i}^{2(\text{gl})} \right) \hat{\Sigma}_{h_i h_i}^{(2,\text{gl})'} - \hat{\Sigma}_{h_i h_i}^{(1,\text{gl})} \hat{\Sigma}_{h_i h_i}^{(1,\text{gl})'} \\ &\approx \hat{\Sigma}_{h_i h_i}^{(2,\text{gl})} \hat{\Sigma}_{h_i h_i}^{(1,\text{gl})'} + \left[ m_{h_i}^{2(\text{gl})} - m_{h_i}^2 + \hat{\Sigma}_{h_i h_i}^{(1,\text{gl})} + \hat{\Sigma}_{h_i h_i}^{(2,\text{gl})} \right] \hat{\Sigma}_{h_i h_i}^{(2,\text{gl})'} \\ &\quad + \hat{\Sigma}_{h_i h_i}^{(1,\text{EW})'} \left[ \hat{\Sigma}_{h_i h_i}^{(1,\text{gl})} + \hat{\Sigma}_{h_i h_i}^{(2,\text{gl})} \right] + \hat{\Sigma}_{h_i h_i}^{(1,\text{EW})} \left[ \hat{\Sigma}_{h_i h_i}^{(1,\text{gl})'} + \hat{\Sigma}_{h_i h_i}^{(2,\text{gl})'} \right] + \hat{\Sigma}_{h_i h_i}^{(1,\text{EW})'} \hat{\Sigma}_{h_i h_i}^{(1,\text{EW})} \end{aligned} \quad (23)$$

with all self-energies evaluated at the (gaugeless) tree-level mass, ' indicating differentiation with respect to the external momentum squared, 'gl' and 'EW' referring to the gaugeless and electroweak contributions respectively. We assumed  $\hat{\Sigma}_{h_i h_i}^{(1)} \approx \hat{\Sigma}_{h_i h_i}^{(1,\text{EW})} + \hat{\Sigma}_{h_i h_i}^{(1,\text{gl})}$  (which may be seen as a definition of the EW piece). The systematic appearance of derivative self-energies makes evident the dependence on field counterterms.

Below, we study the stability of Higgs-mass predictions of  $\mathcal{O}(\alpha_q \alpha_s)$  under variations of the field-renormalization constants. For simplicity, we restrict ourselves to a 'minimal' form of the field counterterms, considering on-shell (OS) or  $\overline{\text{DR}}$  field-renormalization constants. In the  $\overline{\text{DR}}$  approach, the only loose parameter is the renormalization scale  $\mu_{\text{UV}}$ ; its variation between the physical scales of the model, *i. e.* the EW and the SUSY scales, offers a measurement of the arbitrariness introduced in the definition and UV-regularization of physical observables, hence a lower bound on the associated 'error'.<sup>7</sup> Yet, this very specific pattern where distinct counterterms

<sup>6</sup> Off-diagonal contributions actually produce EW-violating pieces of higher order, but numerically dominant in the decoupling limit, see Ref. [66].

<sup>7</sup> It indeed corresponds to an 'error' introduced by the formalism rather than an 'uncertainty', because the partial higher orders contained in the field counterterms typically violate the properties that are expected from actual higher-order corrections; a genuine uncertainty estimate would have to quantitatively assess the impact of higher orders (*e. g.* by estimating genuine higher-order logarithms).

are correlated by a common regulator may underestimate the actual theoretical uncertainty. In this picture, the MSSM Higgs-field counterterms can be written as

$$\delta Z_{ij}^{\overline{\text{DR}}} = (X_{id}^R X_{jd}^R + X_{id}^I X_{jd}^I) \delta Z_{H_d} + (X_{iu}^R X_{ju}^R + X_{iu}^I X_{ju}^I) \delta Z_{H_u} \quad (24)$$

where  $X_{if}^{R,I}$  encodes the decomposition of the tree-level neutral Higgs state  $h_i$  on the gauge-eigenbase:  $h_i = X_{id}^R h_d^0 + X_{iu}^R h_u^0 + X_{id}^I a_d^0 + X_{iu}^I a_u^0$ . At the 1L order one has<sup>8</sup>

$$\delta Z_{H_d}^{(1)} = -\frac{3\alpha_b + \alpha_\tau}{4\pi} \left[ \overline{\Delta}_{\text{UV}}^{-1} + \ln \frac{\mu_{\text{ren}}^2}{\mu_{\text{UV}}^2} \right], \quad \delta Z_{H_u}^{(1)} = -\frac{3\alpha_t}{4\pi} \left[ \overline{\Delta}_{\text{UV}}^{-1} + \ln \frac{\mu_{\text{ren}}^2}{\mu_{\text{UV}}^2} \right]. \quad (25)$$

Here, we neglect the Yukawa couplings of the first and second generation. The symbol  $\overline{\Delta}_{\text{UV}}^{-1}$  represents the UV-divergence (including universal finite pieces). The finite piece can be viewed as resetting the renormalization scale of the fields from  $\mu_{\text{ren}}$  to  $\mu_{\text{UV}}$ . Similarly, the 2L field-renormalization constants of order  $\alpha_q \alpha_s$  read

$$\delta Z_{H_d}^{(2,\alpha_q\alpha_s)} = \frac{\alpha_b \alpha_s}{2\pi^2} \left[ \left( \overline{\Delta}_{\text{UV}}^{-1} + \frac{\mu_{\text{ren}}^2}{\mu_{\text{UV}}^2} \right)^2 - \left( \overline{\Delta}_{\text{UV}}^{-1} + \frac{\mu_{\text{ren}}^2}{\mu_{\text{UV}}^2} \right) \right], \quad (26a)$$

$$\delta Z_{H_u}^{(2,\alpha_q\alpha_s)} = \frac{\alpha_t \alpha_s}{2\pi^2} \left[ \left( \overline{\Delta}_{\text{UV}}^{-1} + \frac{\mu_{\text{ren}}^2}{\mu_{\text{UV}}^2} \right)^2 - \left( \overline{\Delta}_{\text{UV}}^{-1} + \frac{\mu_{\text{ren}}^2}{\mu_{\text{UV}}^2} \right) \right]. \quad (26b)$$

Only Yukawa and the QCD-gauge couplings appear in these expressions of the  $\overline{\text{DR}}$  field counterterms. Since the EW corrections (gauge, gauginos) generate a vanishing UV-divergence at 1L, the corresponding pieces are insensitive to scale variations in the field counterterms. Accordingly, the variations of  $\mu_{\text{UV}}$  that we consider below probe all terms except for the last of Eq. (23). Thus, this type of scale variation is meaningful as long as Yukawa effects dominate and the gaugeless approximation holds. On the other hand, if corrections of EW type are large, the partial higher order appearing in the last term of Eq. (23) is not tested and the uncertainty from scale variation is only partial.

The approach with OS-renormalized fields allows to take into account the impact of EW corrections to a certain extent, but it does not allow for variations. In this case, we simply express the field counterterms as cancelling the differentiated self-energies at the corresponding tree-level (OS) mass:

$$\delta Z_{ij}^{\text{OS}} \equiv -\frac{d\Sigma_{ij}}{dp^2} (p^2 = m_{ij}^2), \quad (27)$$

which is a symmetric, but (for off-diagonal field counterterms) not fully conventional choice. We could define this object in the gaugeless limit, in which case EW corrections would still be overlooked. In practice, one then recovers results within the scope of the  $\overline{\text{DR}}$  scale variation. Therefore we dismiss this choice. More usefully, we can define the 1L field counterterms in the full model, *i. e.* including EW effects. We can then compare the differences between this procedure and the  $\overline{\text{DR}}$  evaluations. However, we do not attempt to express the 2L field counterterms in this scheme, keeping them  $\overline{\text{DR}}$  with  $\mu_{\text{UV}} = m_t$ , first, because the 2L contributions are explicitly calculated in the gaugeless limit, secondly because the evaluation of the differentiated 2L functions is technically involved.

<sup>8</sup> We refer the reader to Refs. [81, 82] and references therein for calculations of the anomalous dimension of the Higgs fields. We recover the same results at the one- and two-loop order by explicitly computing derivatives of the Higgs self-energies and assessing their UV-divergence.

In Fig. 3, we compare the Higgs-mass predictions of 1L order and  $\alpha_q \alpha_s$  obtained via an expansion—using Eq. (21)—or an iterative pole search—using Eq. (22)—for  $M_{H^\pm} = 1$  TeV. At the level of the SM-like state (upper row), the mass shift between the 1L and  $\mathcal{O}(\alpha_q \alpha_s)$  predictions is sizable (in our renormalization scheme), and much larger than the dispersion between the expansion and iteration methods. The dependence of the iteration method on the field-renormalization constants induces a variation with the regulator  $\mu_{UV}$ , when evaluating the latter between the EW and SUSY scales, which (in the considered scenario) amounts to about 5 GeV at 1L (long-dashed magenta curve) and about 3 GeV at  $\mathcal{O}(\alpha_q \alpha_s)$  (solid purple curve). This reduction of the scale dependence originates in the destructive interplay between the two orders, not in the completion of the partial order introduced by the pole search—which requires the terms of  $\mathcal{O}(\alpha_q^2)$  (see next subsection). Inclusion of the  $\mathcal{O}(\alpha_q \alpha_s)$  corrections in the effective-potential approximation (short-dashed pink curve) leads to very comparable results, confirming the adequacy of this approach for the SM-like state: the 2L effects are in fact introduced at their correct tree-level gaugeless mass value. The evaluation with OS field counterterms, represented by a cross in the column on the left of each plot, returns results very near that of the expansion.

In the second and third rows of Fig. 3, we consider the shifts in squared mass for the heavy neutral states as compared to the charged one. The plots on the left show the dispersion of the mass predictions depending on the chosen order. Once again, the mass shift associated with the inclusion of  $\mathcal{O}(\alpha_q \alpha_s)$  corrections is larger than that induced by the choice of method (expansion vs. iteration). However, contrarily to the case of the SM-like state, the effective-potential approximation ostensibly falls far away from the actual momentum-dependent result, implying that this approach is not predictive for the heavy-doublet states. Here, we should comment on the definition of this approach, since it is not completely straightforward. Indeed, beyond the zero-momentum assumption in the neutral Higgs self-energy of  $\mathcal{O}(\alpha_q \alpha_s)$ , we also set the momentum equal to 0 in the corresponding charged-Higgs counterterm.<sup>9</sup> However, the charged Higgs self-energy at vanishing momentum requires the introduction of charged-Higgs field counterterms as well in order to obtain UV-finite results. Given that observables are supposed to be independent from field counterterms, the latter could be chosen *a priori* without connection to the neutral field counterterms: this is the choice governing the short-dashed pink curves, where  $\overline{\text{DR}}$  conditions at the scale  $m_t$  are employed. Alternatively, one can correlate the charged and neutral counterterms in the  $\overline{\text{DR}}$  scheme, *i. e.* employ a common scale  $\mu_{UV}$ : this is shown in dotted pink, with much reduced variations along  $\mu_{UV}$  due to  $SU(2)$ -cancellations between neutral and charged counterterms—though in no way suggestive of an improved reliability of the effective-potential method (the results for full momentum-dependent  $\mathcal{O}(\alpha_q \alpha_s)$  are significantly away).<sup>10</sup> We do not consider the OS field counterterms for the charged Higgs in the effective-potential approach, since these are infrared-divergent, which explains that only one pink cross appears in each plot. The relative failure of the effective-potential approximation to capture the  $\mathcal{O}(\alpha_q \alpha_s)$  corrections is not really surprising, as the corresponding Higgs masses are far from  $p^2 = 0$ , even in the gaugeless limit. Similarly, the large scale dependence in the dashed pink line proceeds from the necessary inclusion of a large correction proportional to the field counterterm to absorb the UV-divergences of the self-energies at  $p^2 = 0$ .

<sup>9</sup> One could also evaluate the charged Higgs counterterm at  $p^2 = M_{H^\pm}^2$ , in which case one obtains a mass prediction very close to the dashed pink line. However, if one employs the effective-potential approximation in order to avoid the lengthy evaluation of 2L momentum-dependent integrals, it appears more natural to use the condition  $p^2 = 0$  in all 2L self-energies.

<sup>10</sup> The charged-Higgs mass counterterm appears neither in the diagonal nor off-diagonal self-energies contributing to the mass of the lightest Higgs (in the gaugeless limit); therefore, the distinction in the renormalization of the charged-Higgs propagator is invisible in the first row of Fig. 3.

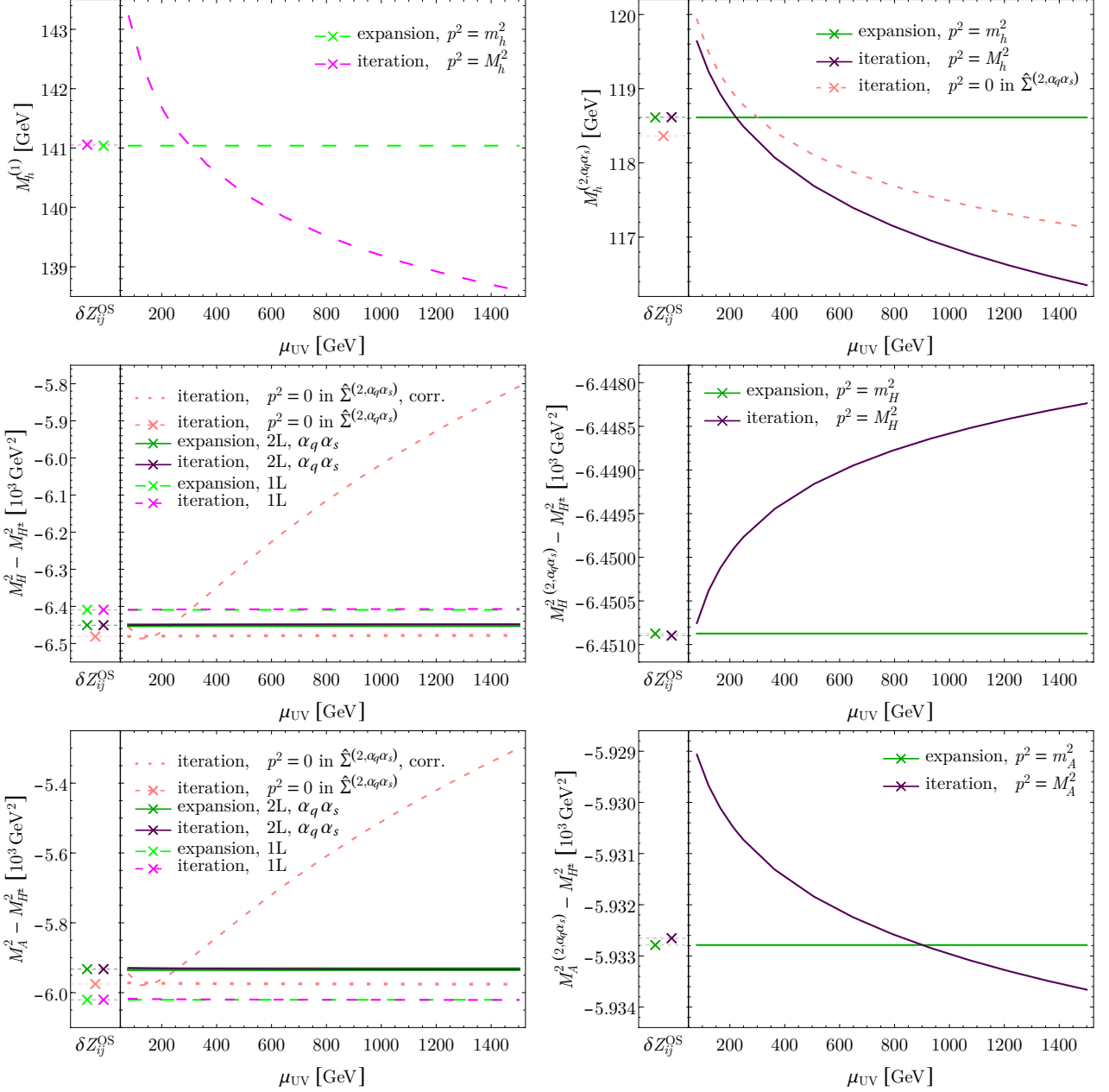


**Figure 3.:** Dependence on the field counterterms at 1L order and  $\mathcal{O}(\alpha_q \alpha_s)$  for  $M_{H^\pm} = 1$  TeV. The off-diagonal effects are neglected in the iteration of the momenta injected in the self-energies. The long-dashed curves correspond to 1L evaluations (green: expansion; magenta: iterative pole search). In the short-dashed and dotted pink curves, the  $\mathcal{O}(\alpha_q \alpha_s)$  are included in the effective-potential approximation, but an iteration on the momentum of the 1L self-energy is included. In the short-dashed curves, the counterterms of the charged-Higgs fields are set to fixed values; in the dotted curves, they are correlated with those of the neutral fields. The solid lines represent calculations of  $\mathcal{O}(\alpha_q \alpha_s)$  with full momentum dependence: the masses are derived via an expansion (dark green), or an iterative pole search (purple). The crosses in the columns on the left of the plots correspond to the evaluations with OS field counterterms.

*Up:* Mass of the light SM-like state at 1L (left plot; long-dashed curves) and at order  $\alpha_q \alpha_s$  (right).

*Middle and Bottom:* Squared mass-splitting between the  $\mathcal{CP}$ -even (Middle) or  $\mathcal{CP}$ -odd (Bottom) heavy-doublet state and the charged Higgs; general perspective (left) and details of the 2L predictions (right).



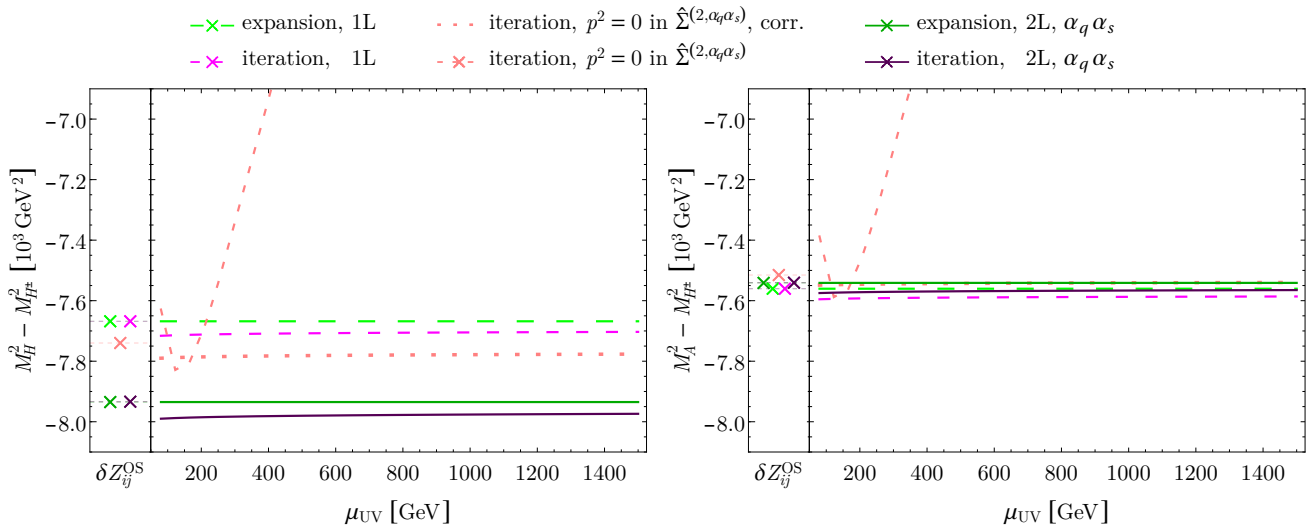


**Figure 4.:** Dependence on the field counterterms at 1L order and  $\mathcal{O}(\alpha_q \alpha_s)$  for  $M_{H^\pm} = 2.5 \text{ TeV}$ . The conventions are similar to those of Fig. 3.

The plots on the right compare the momentum-dependent mass predictions of  $\mathcal{O}(\alpha_q \alpha_s)$  in the expansion (green) and iteration (purple) methods. We observe that the scale variations are not necessarily sufficient to allow both predictions to overlap—though the size of this dispersion remains compatible with the amplitude of the variations with  $\mu_{UV}$ . The origin of this separation between the expansion and iteration method is associated with the relevance of EW corrections at 1L for the heavy-doublet states. The last term of Eq. (23) indeed becomes sizable but, as we explained above, the scale variation does not probe the incompleteness of this order. As it is, these partial  $\mathcal{O}(\alpha^2)$  effects are most certainly misleading and should not be interpreted as meaningful contributions of the iterative pole search. In fact, the evaluation with OS field counterterms typically pulls the iterative pole search in the direction of the expansion.

We complete this discussion about the mass prediction at  $\mathcal{O}(\alpha_q \alpha_s)$  for the heavy-doublet states with another example in Fig. 4:  $M_{H^\pm} = 2.5 \text{ TeV}$ , so that effects beyond the gaugeless approximation, both threshold and EW, are more relevant. The main difference with respect to the previous case is that the choice of procedure (expansion vs. iteration) leads to clearly separated predictions, not connected by the scale variation. As explained above, this shift originates in the last term of Eq. (23), which is not probed by the scale variation, though it is of partial higher order, hence not predictive. Considering the case of OS field counterterms—a setup that is sensitive to this term—extends the range of variation of the iterative pole search to engulf the prediction of the expansion. Once again, the effective-potential approximation provides no actual gain in precision with respect to the strict 1L calculation.

### 3.3. Corrections of $\mathcal{O}(\alpha_q^2)$

The inclusion of order  $\alpha_q^2$  brings about the interplay between 2L and  $1L^2$  effects that we discussed in Sect. 2. Off-diagonal self-energies indeed become meaningful in the mass calculation even in the non-degenerate case—while they led to non-decoupling  $SU(2)$ -violating effects of higher order in a 1L calculation [66]. As explained in this reference, it is crucial, in the case of the heavy-doublet states, to properly include  $1L^2$  off-diagonal contributions to the charged-Higgs mass in the 2L counterterms.

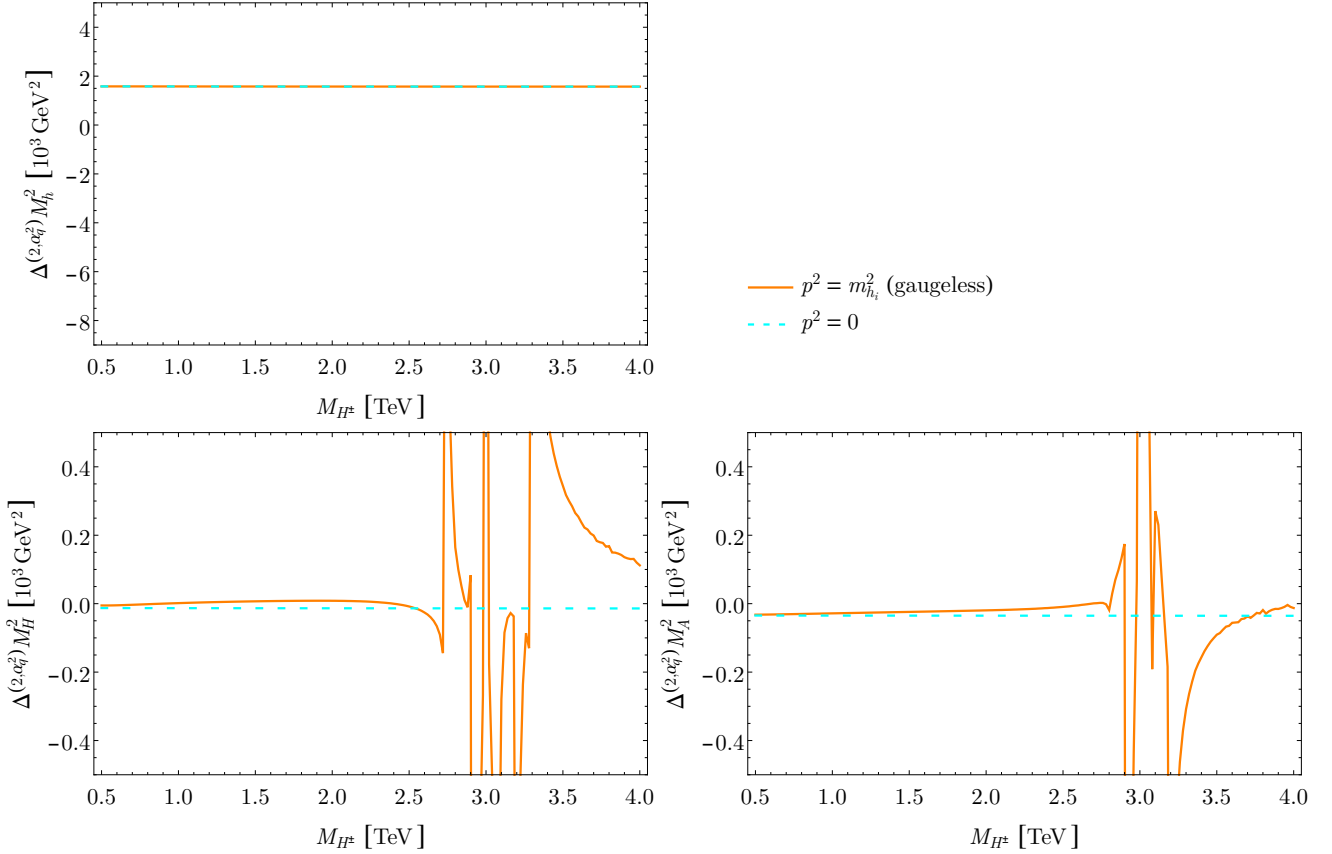


**Figure 5.:** Mass shifts at  $\mathcal{O}(\alpha_q^2)$  for the neutral Higgs states. The color-code follows the conventions of Fig. 2. The wiggly lines at  $M_{H^\pm}^2 \gtrsim 3.5$  TeV reveal numerical instabilities in the evaluation of 2L integrals containing the tiny ratios of  $m_b^2/M_{H^\pm}^2$ .

Once again, we first investigate the mass shifts generated at this order, in Fig. 5. Here, with all objects defined in the gaugeless limit, one has

$$\begin{aligned} \Delta^{(2, \alpha_q^2)} M_{h_i}^2 &\equiv M_{h_i}^{2(2, \alpha_q^2)} - M_{h_i}^{2(2, \alpha_q \alpha_s)} \\ &= -\Re \left[ \hat{\Sigma}_{h_i h_i}^{(2, \alpha_q^2)}(m_{h_i}^2) - \hat{\Sigma}_{h_i h_i}^{(1)}(m_{h_i}^2) \frac{d\hat{\Sigma}_{h_i h_i}^{(1)}(m_{h_i}^2)}{dp^2} - \sum_{j \neq i} \frac{\hat{\Sigma}_{h_i h_j}^{(1)}(m_{h_i}^2) \hat{\Sigma}_{h_j h_i}^{(1)}(m_{h_i}^2)}{m_{h_i}^2 - m_{h_j}^2} \right]. \end{aligned} \quad (28)$$

As before, the effective-potential approximation is only meaningful for the SM-like state, though it seems to work somewhat better for heavy states at low values of  $M_{H^\pm}$  than at  $\mathcal{O}(\alpha_q \alpha_s)$ . Threshold effects again appear in association with squark loops for  $M_{H^\pm} \approx 3$  TeV, when the momentum dependence is accounted for. The background far from threshold contributions is essentially flat, as radiative corrections of  $\mathcal{O}(\alpha_q^2)$  typically scale like  $M_{\text{EW}}^2 \ln^k M_{H^\pm}^2 / M_{\text{EW}}^2$ ,  $k \in \{0, 1, 2\}$ , at large  $M_{H^\pm}$  (provided the charged-Higgs mass is renormalized on-shell).

The Higgs masses  $M_{h_i}^{2(2, \alpha_q^2)}$  defined via the expansion in Eq. (28) are by construction independent from field renormalization. Alternatively, one can numerically solve Eq. (1) with the momentum-dependent self-energy matrix including contributions up to  $\mathcal{O}(\alpha_q^2)$ , defining the poles  $\mathfrak{M}_{h_i}^{2(2, \alpha_q^2)}$ . As self-energies are evaluated away from their mass-shell, it is once again necessary to call upon field renormalization to neutralize UV-divergences and give a meaning to corresponding objects. In addition to the 1L field counterterms of Eq. (25), one should consider

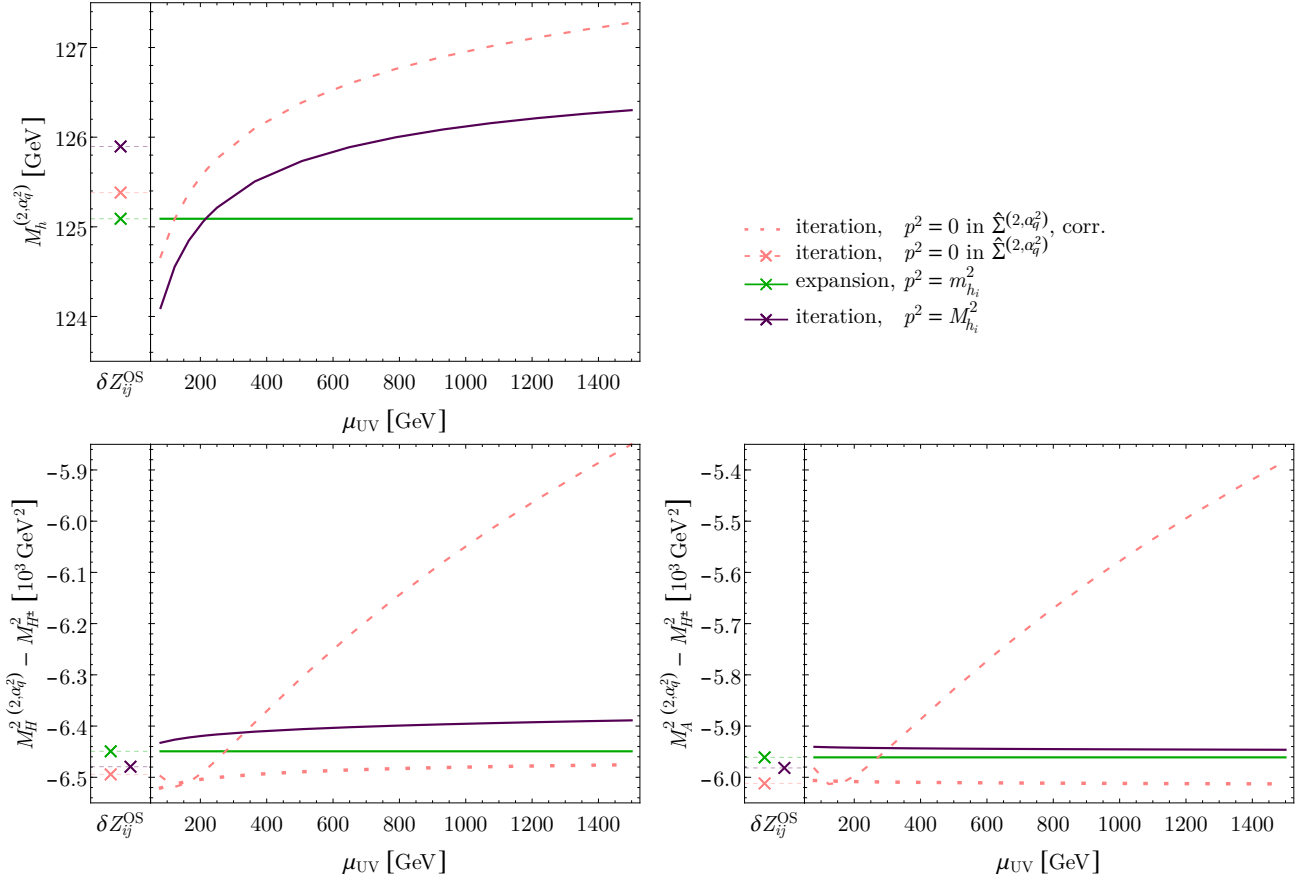


**Figure 6.:** Dependence on the field-counterterms in mass predictions of order  $\alpha_q^2$ . The solid green line is derived with the expansion at strict order, the purple one, with an iterative pole search. The 2L self-energies are included in the effective potential approximation for the dashed pink curve.

the 2L field counterterms of order  $\alpha_q^2$ , reading (in the  $\overline{\text{DR}}$  scheme)

$$\delta Z_{H_d}^{(2, \alpha_q^2)} = -\frac{3\alpha_b(3\alpha_b + \alpha_t)}{32\pi^2} \left\{ \left[ \overline{\Delta}_{\text{UV}}^{-1} + \frac{\mu_{\text{ren}}^2}{\mu_{\text{UV}}^2} \right]^2 - \left[ \overline{\Delta}_{\text{UV}}^{-1} + \frac{\mu_{\text{ren}}^2}{\mu_{\text{UV}}^2} \right] \right\}, \quad (29a)$$

$$\delta Z_{H_u}^{(2, \alpha_q^2)} = -\frac{3\alpha_t(\alpha_b + 3\alpha_t)}{32\pi^2} \left\{ \left[ \overline{\Delta}_{\text{UV}}^{-1} + \frac{\mu_{\text{ren}}^2}{\mu_{\text{UV}}^2} \right]^2 - \left[ \overline{\Delta}_{\text{UV}}^{-1} + \frac{\mu_{\text{ren}}^2}{\mu_{\text{UV}}^2} \right] \right\}. \quad (29b)$$

In addition to these 2L field counterterms, the self-energies of order  $\alpha_q^2$  depend on the 1L field counterterms of Eq. (25) according to Eq. (12)—even when the momentum is set to the tree-level Higgs mass. As explained in Sect. 2, this dependence on field-renormalization constants is mirrored by that of the  $1L^2$  terms resulting in a cancellation for the full order. It is also worth noticing that the dependence on the charged-Higgs field already vanishes separately within the  $2L + 1L^2$  terms forming the charged-Higgs mass counterterm of  $\mathcal{O}(\alpha_q^2)$ .

In Fig. 6, we show the field-counterterm dependence of the mass prediction at  $\mathcal{O}(\alpha_q^2)$  for  $M_{H^\pm} = 1 \text{ TeV}$ . Once again, we compare the strict expansion—Eq. (28)—in solid green, with the iterative pole search, in solid purple. In this last case, the full  $\mathcal{CP}$ -even mass matrix of  $\mathcal{O}(\alpha_q^2)$  is included in the pole search—with gaugeless approximation for the 2L pieces. For the  $\mathcal{CP}$ -odd state, instead of considering the full matrix, we directly add the off-diagonal mixing contribution with the Goldstone boson  $[\hat{\Sigma}_{A^0 G^0}^{(1, \text{gl})}(p^2)]^2/m_A^2$  to the diagonal element—omission of this term would otherwise induce an artificial  $SU(2)$ -breaking among the heavy-doublet states, see Ref. [66].

Finally, the dashed and the dotted pink curves include the 2L corrections of  $\mathcal{O}(\alpha_q \alpha_s, \alpha_q^2)$  in the effective-potential approximation before performing the pole search. There, we use two slightly different procedures for the  $\mathcal{CP}$ -even and  $\mathcal{CP}$ -odd sectors, as we add a  $[\hat{\Sigma}_{A^0 G^0}^{(1, \text{gl})}(0)]^2/m_A^2$  term in the latter case, instead of keeping a full momentum-dependent 1L self-energy matrix. As before, the charged-Higgs field counterterms are either set to a fixed value (dashed curves) or correlated with the neutral sector (dotted).

At the level of the SM-like state, the corrections of  $\mathcal{O}(\alpha_q^2)$  are sufficiently significant to make them necessary in any attempt at precision predictions for the mass. Surprisingly, the variations with the field-renormalization scale are barely reduced as compared to the order  $\alpha_q \alpha_s$ —see Fig. 3—for the iterative approach. This situation originates in the inexact cancellation of the 1L<sup>2</sup> field counterterms that are generated in the variation of the 1L self-energy via the pole search, with those produced in the 2L corrections and assuming the gaugeless limit. A simple estimate actually suffices to recover the order of magnitude of these scale variations. The leading contribution from the pole search is a term  $-(\mathfrak{M}_h^{2(2, \alpha_q^2)} - m_h^2) \hat{\Sigma}'_{hh}(m_h^2)$ , generating a field-renormalization dependence  $\sim \delta Z_{hh} \hat{\Sigma}_{hh}^{(1, \alpha_q \alpha_s, \alpha_q^2)}(m_h^2)$  because all orders are involved in the mass shift. On the side of 2L self-energies, the dependence on field counterterms is dominated by the corresponding term  $-\delta Z_{hh} \hat{\Sigma}_{hh}^{(1, \text{gl})}(m_h^2)$ —see Eq. (4). The mismatch  $\hat{\Sigma}_{hh}^{(1, \alpha_q \alpha_s, \alpha_q^2)}(m_h^2) - \hat{\Sigma}_{hh}^{(1, \text{gl})}(m_h^2)$  is large—of the order of 100% of the magnitude of radiative corrections to the mass of the SM-like Higgs—while, dominated by  $\alpha_t$ ,  $\delta Z_{hh} \approx 0.1$  for a variation between the EW and SUSY scales. In the aftermath, an effect of  $\sim 2\%$  is assessed on the field dependence at the level of the mass. Curiously enough, we can expect a comparable uncertainty from missing EW orders due to the gaugeless approximation. Indeed, as we observed in Fig. 1, the gaugeless approximation works at  $\sim 15\%$  at 1L for the SM-like state while the squared-mass shift of  $\mathcal{O}(\alpha_q^2)$  is of order  $2 \cdot 10^3 \text{ GeV}^2$ ; combining the two numbers, we arrive at a FO uncertainty of percent level from uncontrolled 2L orders at the level of a  $\sim 125 \text{ GeV}$  Higgs mass—corresponding to the squared logarithms of  $\mathcal{O}(\alpha_t \alpha)$ . However, this coincidence does not establish the variation of field counterterms as a realistic uncertainty estimate for higher orders, as it strictly measures partial higher-order effects associated with the regularization of the pole-search procedure. We stress that the large dependence on field counterterms is intimately related to the size of the radiative corrections in the considered approach, *i. e.* to the FO procedure: in an EFT, contributions from the hierarchical spectrum would be absorbed within the tree-level couplings. Similar behaviours had been observed in Ref. [29]: see *e. g.* Fig. 3 of this reference. In addition, the mismatch between the total mass shift ( $\hat{\Sigma}_{hh}^{(1, \alpha_q \alpha_s, \alpha_q^2)}(m_h^2)$ ) and the gaugeless 1L self-energy could certainly be minimized via an adequate choice of renormalization conditions for the Yukawa couplings, absorbing the impact of higher orders.

Concerning the heavy-doublet states, the field dependence induced by the pole search is in fact increased in the  $\mathcal{CP}$ -even case with respect to  $\mathcal{O}(\alpha_q \alpha_s)$ —see Fig. 3. In contrast, the dependence on  $\overline{\text{DR}}$  field-renormalization constants remains mild in the  $\mathcal{CP}$ -odd case, which is a consequence of our adding the off-diagonal self-energies in the gaugeless limit, hence satisfying the cancellation of the field counterterms from off-diagonal terms with the diagonal 2L contributions. Moreover, we observe that even the enlarged field-scale variations of the  $\mathcal{CP}$ -even mass predictions do not capture the full magnitude of the dispersion between the expansion and iteration methods. Off-diagonal elements in the pole search indeed add further EW terms insensitive to the scale variation beyond that of the last term of Eq. (23); they correspond to partial higher-order  $\alpha \alpha_q$  and  $\alpha^2$  terms and cannot be interpreted as a genuine physical effect, because the completion of the order  $\alpha^2$  is likely to sizably affect them. Comparing the  $\overline{\text{DR}}$  regularization with that of OS field counterterms further extends the magnitude of the variations associated with the

iterative approach, making it sensitive to EW effects and filling the gap with the expansion procedure. Finally, for 2L self-energies derived in the effective-potential approximation (dashed pink curves), the scale dependence caused by the approximation  $p^2 = 0$  in the 2L self-energies reaches a magnitude much larger than the mass-squared shift induced by the inclusion of these contributions with respect to the strict 1L order. The predicted masses in the case of correlated field counterterms for the neutral- and charged-Higgs sectors (dotted lines) also fall significantly far away from the actual momentum-dependent 2L prediction—as compared to the shift from predictions of 1L order. This approach is thus meaningless for the heavy states.

To summarize, the inclusion of 2L corrections of orders  $\alpha_q \alpha_s$  and  $\alpha_q^2$  is essential in a precise prediction of the mass of the SM-like Higgs state and the effective-potential approximation is reasonably predictive at this level. However we have observed that these orders are of little consequence for the heavy-doublet states in a non-degenerate scenario, since one expects them to be superseded by EW corrections. In addition, the effective-potential approximation works poorly for such states, as the obtained mass shift does not quantitatively improve the predictions as compared to  $\mathcal{O}(1\text{L})$ . We also noted that the dependence on the field counterterm at the level of the SM-like state remains large in an iterative pole search including terms of  $\mathcal{O}(\alpha_q^2)$  due to the mismatch between the  $1\text{L}^2$  terms induced by the pole search and the corresponding 2L terms derived in the gaugeless limit: it thus appears that the iterative pole search at FO  $\alpha_q^2$  contains an intrinsic uncertainty of  $\sim \text{GeV}$ -size (depending on the hierarchy between the EW and SUSY scales). Concerning the heavy-doublet states, the dependence on  $\overline{\text{DR}}$  field counterterms appears comparatively reduced for a full calculation of  $\mathcal{O}(\alpha_q^2)$ . However, this simply indicates that EW effects, not Yukawa, dominate the corrections to the corresponding masses: the  $\overline{\text{DR}}$  renormalization is insensitive to these contributions, but the comparison with an OS regularization (as defined in Eq. (27)) allows to probe them and proves that the apparent gap between predictions from the expansion and the iterative pole search is strictly artificial. We thus conclude that there exists no advantage in employing the more costly iterative pole search in a non-degenerate scenario, as compared to the more straightforward expansion-and-truncation method. On the contrary, the partial higher orders introduced in the pole search may be unphysical and, in any case, they generate an ‘uncertainty’ intrinsic to the procedure and hardly representative of ‘genuine’ higher-order effects. Moreover, as the orders  $\alpha_q \alpha_s$  and  $\alpha_q^2$  are the leading 2L corrections only for the SM-like Higgs, there is little significance—as long as 2L EW orders are not under control—in maintaining them for the mass determination of heavy-doublet states; in particular the inclusion in the effective-potential approximation induces uncertainties that are larger than the genuine mass shift.

## 4. Field-dependence in the mass predictions in near-degenerate scenarios

Higgs mixing in the near-degenerate scenario makes the situation more subtle for the mass determination, and we study its practical implementation in this section. As it is, the complications originate less in the general formalism described in Sect. 2.3 than in the features of the gaugeless approximation and its matching to the full model.

## 4.1. $\mathcal{CP}$ -violating mixing between heavy states

In the MSSM, the phenomenologically most relevant scenario with mass degeneracy involves  $\mathcal{CP}$ -violating mixing between the neutral components of the heavy doublet. With the gaugeless description of  $\mathcal{O}(\alpha_q^2)$ , it is actually not possible, even for small mixing, to define loop-corrected masses according to the strict expansion of Eq. (3) since the  $\mathcal{CP}$ -even and  $\mathcal{CP}$ -odd components are exactly degenerate at tree level in the gaugeless limit.<sup>11</sup> However, as the mass-splitting between the two neutral components is of EW order, it can be regarded—consistently with the gaugeless counting—as numerically comparable to 1L effects and the near-degenerate formalism of Sect. 2.3 applies.

We turn to a scenario where  $\mathcal{CP}$ -violation is induced at the loop-level—the tree-level MSSM Higgs sector is always  $\mathcal{CP}$ -conserving—by the phase of the trilinear soft SUSY-breaking coupling in the stop sector,  $\phi_{A_t}$ . In practice, generating a sizable mixing (always scaling with an  $SU(2)$ -breaking v.e.v.) in this fashion requires a rather large trilinear coupling  $|A_t|$  as compared to the diagonal soft SUSY-breaking stop masses  $m_{\tilde{Q}_3, \tilde{T}}$ , which could potentially produce charge- and color-breaking minima—see *e.g.* Ref. [83] for a recent reference. As our discussion is meant to be strictly illustrative of the mass calculation, we disregard this problem below, and take  $m_{\tilde{Q}_3, \tilde{T}} \approx 1$  TeV,  $|A_t| = 3$  TeV,  $M_{H^\pm} = 0.5$  TeV,  $t_\beta = 10$ .

In the upper left-hand quadrant of Fig. 7, we compare the mixing entry of the effective mass matrix at 1L (solid cyan),  $\mathcal{O}(\alpha_q \alpha_s)$  (solid green),  $\mathcal{O}(\alpha_q^2)$  (solid magenta) with the diagonal mass-splitting at tree level (dashed black), 1L (dashed blue),  $\mathcal{O}(\alpha_q \alpha_s)$  (dashed green),  $\mathcal{O}(\alpha_q^2)$  (dashed purple), for varying  $\phi_{A_t}$ . We see that the diagonal mass-splitting at the radiative level vanishes for  $\phi_{A_t} \approx \frac{\pi}{4}$  while the off-diagonal mass entry is comparatively large: we thus expect a sizable mass-mixing in this region. The plot in the upper right-hand corner shows the squared mass-splitting between neutral and charged states at order  $\alpha_q^2$  in the expansion formalism for degenerate states. The blue and cyan dashed lines correspond to the diagonal entries of the effective mass matrix of Eq. (19), crossing at  $\phi_{A_t} \approx \frac{\pi}{4}$ . The other curves correspond to various evaluations of the masses corrected with the  $\mathcal{CP}$ -violating mixing: eigenvalues of the effective mass matrix in solid lines, diagonal elements after rotation by the mixing matrix defined at order  $\alpha_q \alpha_s$  in dashed lines and diagonal elements after rotation by the mixing matrix defined at 1L order in dotted lines. We see that these various definitions give very close results, even though the maximal mixing is clearly shifted in phase at 1L. In the lower left-hand quadrant, we plot the squared mass-splitting between neutral states at 1L (green),  $\mathcal{O}(\alpha_q \alpha_s)$  (blue) and  $\mathcal{O}(\alpha_q^2)$  (purple, orange and red, depending on the definition through eigenvalues or rotation of the effective mass matrix) in the expansion formalism. The diagonal splitting is shown in dashed lines. Once again, we observe the good agreement among definitions at order  $\alpha_q^2$ .

Finally, in the lower right-hand panel of Fig. 7, we consider the dependence on field counterterms for  $\phi_{A_t} = \frac{\pi}{4}$  in masses defined with the expansion formalism (red), in an iterative pole search with full momentum-dependence (blue) and in the effective-potential approximation for 2L self-energies, with correlated charged-Higgs  $\overline{\text{DR}}$  field counterterms (dotted green) or independent charged-Higgs field counterterms (dashed brown). In fact, the masses obtained with the expansion method are fully independent from the field counterterms, because the remainder of Eq. (17) exactly vanishes due to the exact degeneracy of the two tree-level masses in the gaugeless approximation. For the iterative pole searches, the situation is largely comparable to what we discussed in the non-degenerate case. The predicted masses for the mixed (heavy) states show only a mild dependence on field-scale variations: we should stress here that the  $\mathcal{CP}$ -violating self-energy is UV-finite without need of regularization by a field counterterm, so that the mixing

<sup>11</sup> For the SM-like Higgs, the mixing with the Goldstone boson always vanishes, so that this issue does not appear.

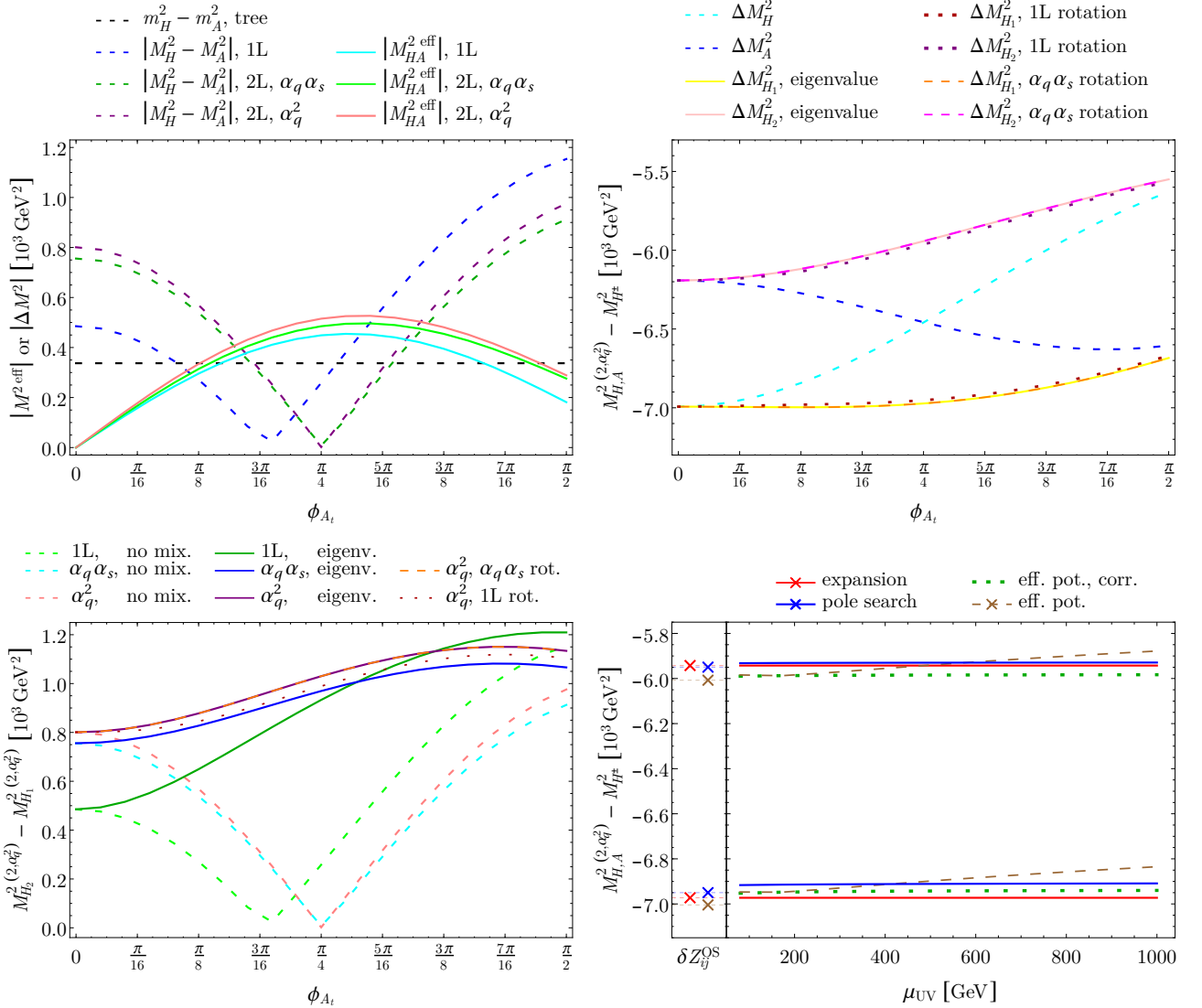


**Figure 7.:** Mass predictions in the  $\mathcal{CP}$ -violating scenario at  $\mathcal{O}(\alpha_q^2)$ .

*Up Left:* The size of the elements of the effective matrix elements is plotted against  $\phi_{A_t}$ ; more precisely, the mass-splitting between diagonal elements (dashed curves) is compared to the off-diagonal entry (solid curves) at various orders.

*Up Right:* Predicted mass-splitting between neutral and charged states at  $\mathcal{O}(\alpha_q^2)$ , without accounting for the mixing (blue/cyan dashed), or in various evaluations of the 2L mixing.

*Down Left:* Predicted mass-splitting between neutral states at various orders, without accounting for the mixing or including it.

*Down Right:* Field dependence of the predicted masses at  $\mathcal{O}(\alpha_q^2)$  for  $\phi_{A_t} = \frac{\pi}{4}$ , in the expansion formalism (red), with an iterative pole search retaining full momentum dependence (blue), or in the effective-potential description with correlated (green) or uncorrelated (brown) charged field counterterms. The crosses on the left correspond to the predictions with OS counterterms, while the scale variation employs a DR regularization of the self-energies.

entry in the mass matrix is itself completely blind to the  $\overline{\text{DR}}$  regularization of the fields—adding to the already noted insensitivity to EW effects. On the other hand, the OS field counterterms from Eq. (27) probe both effects: the corresponding mass predictions, indicated by crosses in the column at the left end of the plot, show a more significant deviation respective to those using a scale variation in the  $\overline{\text{DR}}$  renormalization, which closes the apparent gap with the masses of the expansion formalism. Once again, this difference appears as a strictly artificial effect originating in the iterative method. Lastly, the effective-potential approximation performs somewhat better than in the non-degenerate scenario, which should be put in perspective with the small value of  $M_{H^\pm}$ . The dependence on field counterterms of this description is made evident by the steeper variation with the scale (when keeping the charged-field counterterms uncorrelated).

## 4.2. $\mathcal{CP}$ -conserving mixing with the SM-like Higgs

As explained in the previous subsection, the  $\mathcal{CP}$ -violating mixing between heavy-doublet states always falls in the degenerate limit, even for small mixing, as long as 2L effects are considered in the gaugeless approximation. Therefore, in order to study the transition between degenerate and non-degenerate regimes, we consider the scenario of degenerate  $\mathcal{CP}$ -even states, *i. e.*  $M_{H^\pm} = \mathcal{O}(M_Z)$ , even though it is now only marginally relevant from a phenomenological perspective due to tight experimental limits—refer *e. g.* to the related work in Ref. [84]. As the latter rather motivate weak- than strong-mixing scenarios, we do not bother and try to accommodate a Higgs boson with a mass of 125 GeV. This type of mixing also differs from the  $\mathcal{CP}$ -violating mixing between heavy-doublet states in that the remainder of Eq. (17) no longer uniformly vanishes, meaning that the expansion formalism retains some amount of dependence on field counterterms, which we aim to quantify below.

In fact, the gaugeless approximation for 2L effects forbids an actual ‘mass-crossing’ in the off-diagonal  $1L^2$  term processed in the non-degenerate expansion formalism of Eq. (3), because the SM-like state takes a zero-mass in this limit. Therefore, this equation then returns a well-behaved mass-prediction, independent from field counterterms. On the other hand, this approach meets a first issue with the identification of gaugeless and ‘actual’ Higgs states, since the gaugeless state with mass equal to 0 is always SM-like, while the  $SU(2)$ -partner of the Goldstone bosons in the model with non-vanishing gauge couplings is distributed between both tree-level states, according to an angle  $\alpha - \beta$  ( $\alpha$  denoting the  $\mathcal{CP}$ -even tree-level mixing angle with respect to gauge eigenstates): as  $M_{H^\pm}$  narrows  $M_Z$ ,  $\alpha$  departs from  $\beta - \pi/2$  (for  $\beta > \frac{\pi}{4}$ ; while  $\alpha$  is fixed to this value in the gaugeless limit), underlining the irrelevance of a naive identification. However, performing a rotation of  $\alpha - \beta$  of the total 2L effects obtained in the gaugeless limit (including  $1L^2$  contributions for controlled dependence on field counterterms) is ill-defined outside of the degenerate regime. In addition, the recourse to the near-degenerate formalism is originally motivated by the need to consistently process off-diagonal contributions to the Higgs masses intervening at 1L order, due to the near-degeneracy of diagonal terms. On the other hand, it is misleading to maintain this mixing-matrix description when the non-degenerate regime applies, since it generates  $SU(2)_L$ -violating pieces that are not controlled by the EW-symmetry breaking, see Ref. [66]. It is thus legitimate to worry about defining the transition between both regimes.

In Fig. 8, we consider the same region in parameter space as in Sect. 3, but in the range  $M_{H^\pm} \in [100, 500]$  GeV. The first row of plots shows the general perspective of mixing in the  $\mathcal{CP}$ -even sector. In the plot on the left, we compare the off-diagonal mass-squared entry—we use  $\overline{\text{DR}}$  counterterms with  $\mu_{\text{UV}} = m_t$ —in the effective mass matrix of Eq. (19) (solid blue curve) to the diagonal splitting (dashed orange curve): in the range  $M_{H^\pm} \approx 120\text{--}150$  GeV, the mass-squared splitting is smaller than the off-diagonal self-energy, highlighting the need for a near-degenerate formalism. We stress that we include the block of 2L corrections obtained in the gaugeless



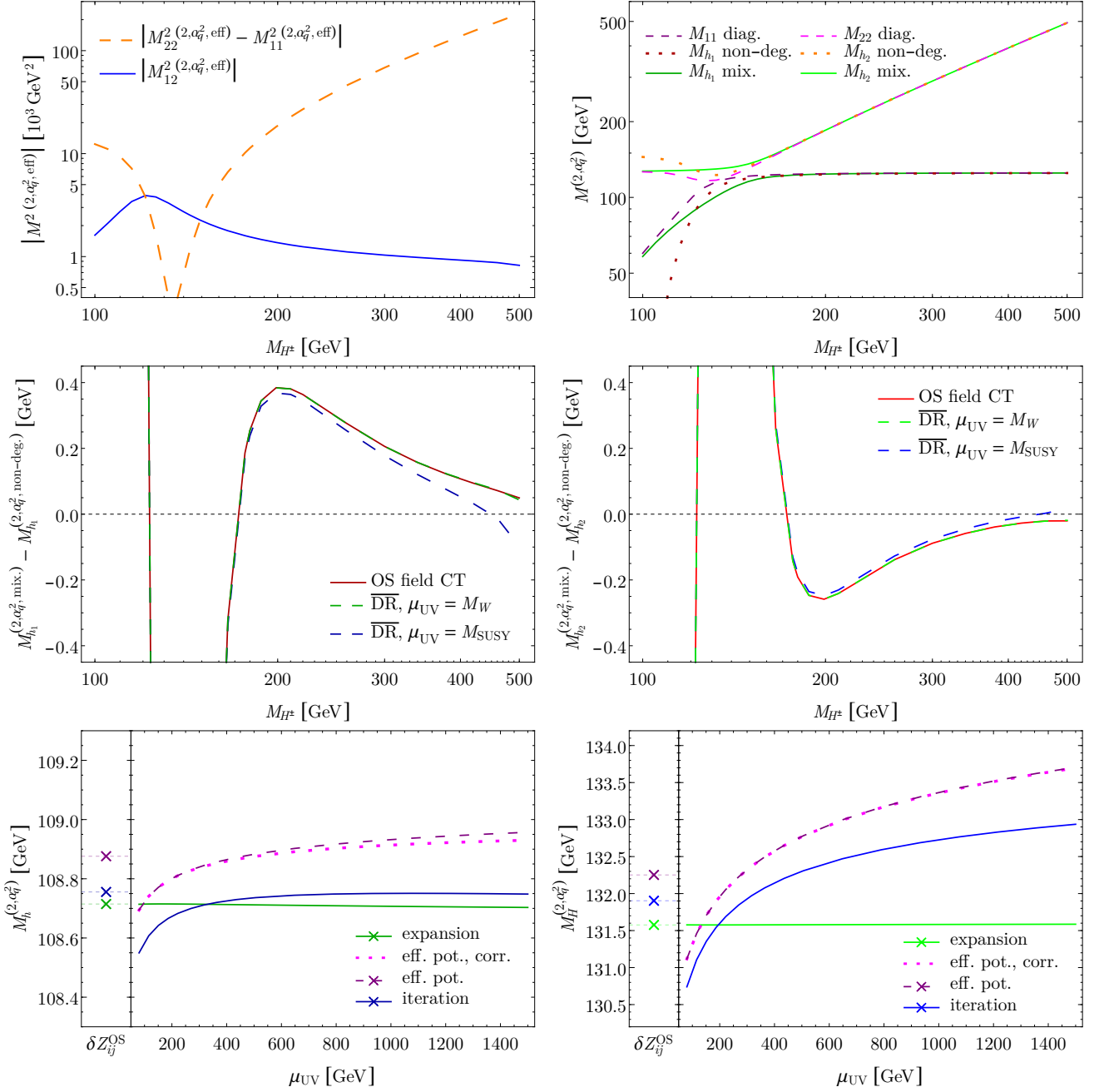


**Figure 8.:** Mass predictions at  $\mathcal{O}(\alpha_q^2)$  in the scenario with  $\mathcal{CP}$ -conserving mixing.

*Up Left:* Magnitude of the elements of the effective mass matrix (with  $\overline{\text{DR}}$  renormalization of the Higgs fields and  $\mu_{\text{UV}} = m_t$ ) of  $\mathcal{O}(\alpha_q^2)$ , diagonal mass-splitting (dashed orange) vs. off-diagonal entry (solid blue).

*Up Right:* Mass predictions (obtained with the expansion formalism) for the  $\mathcal{CP}$ -even states at  $\mathcal{O}(\alpha_q^2)$ , in the non-degenerate description (dotted lines), from the diagonal elements of the effective mass matrix (dashed) and from its eigenvalues (solid) (with  $\overline{\text{DR}}$  renormalization of the Higgs fields and  $\mu_{\text{UV}} = m_t$ ).

*Middle:* Difference between the mass predictions (obtained with the expansion formalism) in the near-degenerate and non-degenerate descriptions for the lightest (left) and heaviest (right)  $\mathcal{CP}$ -even states. Several regularizations of the self-energies with the Higgs field counterterms are considered: OS (solid red),  $\overline{\text{DR}}$  (dashed) with  $\mu_{\text{UV}} = M_W$  (green) and  $\mu_{\text{UV}} = M_{\text{SUSY}}$  (blue).

*Down:* Dependence of the mass predictions at  $M_{H^\pm} = 140$  GeV on the field regularization for the expansion formalism with degeneracy (green), in an effective-potential description (magenta and purple, depending on whether charged-Higgs field counterterms are correlated with the neutral ones) and in an iterative pole search retaining full momentum dependence (blue). The plot on the left (resp. right) corresponds to the lightest (resp. heaviest)  $\mathcal{CP}$ -even state. The crosses on the left-hand side of the plots correspond to the OS renormalization of the fields, and the curves to the  $\overline{\text{DR}}$  renormalization with varying scale.

limit after identification of the gauge eigenbasis, *i. e.* after rotation by an angle  $\alpha - \beta$ . On the right, we plot the masses of the  $\mathcal{CP}$ -even states obtained in various versions of the expansion formalism. The dashed purple and magenta lines correspond to the diagonal entries of the effective mass matrix of Eq. (19), crossing at  $M_{H^\pm} \approx 130$  GeV. The dotted orange and dark-red curves represent the masses obtained in the non-degenerate formalism, *i. e.* according to Eq. (3). These noticeably depart from the diagonal entries of the mixing formalism at low  $M_{H^\pm}$ , mainly due to the absence of corrections accounting for the tree-level mixing (*i. e.* no  $\alpha - \beta$  rotation), which are not straightforward to include in a meaningful way in the non-degenerate scenario. Finally, the eigenvalues of the effective mass matrix are plotted with solid green lines. Obviously, the predictions from the mixing formalism barely differ from those of the non-degenerate one above  $M_{H^\pm} \sim 160$  GeV.

In the second row of plots in Fig. 8, we study the difference between the degenerate and non-degenerate formalisms in the higher range of  $M_{H^\pm}$ . The latter is obviously small—a few 100 MeV for  $M_{H^\pm} \gtrsim 160$  GeV. In addition, the dependence of the effective mass matrix on the field counterterms is made obvious by the dispersion among the various choices ( $\overline{\text{DR}}$  with  $\mu_{\text{UV}} = M_W$ ,  $\overline{\text{DR}}$  with  $\mu_{\text{UV}} = M_{\text{SUSY}}$ , OS). However, this dispersion remains within  $\mathcal{O}(10 \text{ MeV})$ , although it tends to increase as  $M_{H^\pm}$  reaches 500 GeV, then outstretching somewhat the regime of validity of the near-degenerate method. Given the good agreement between the predictions obtained with Eq. (3) and Eq. (19) in the range  $M_{H^\pm} \approx 200\text{--}400$  GeV (corresponding to a 10%–1% mixing), there is no difficulty to extrapolate between the two. However, the combined results will still receive an uncertainty of order  $\mathcal{O}(100 \text{ MeV})$  from this extrapolation (in addition to other sources of theoretical uncertainties). It is actually unclear whether the non-degenerate regime should not be altogether preferred in this intermediate regime. The difficulty here consists in estimating the uncertainty from neglected off-diagonal EW effects: the corresponding mixing entry in the effective mass matrix indeed generates partial effects of EW 2L order, which are not quantitatively reliable—in particular because they do not necessarily satisfy the symmetries of the system, see Ref. [66].

In the last row of Fig. 8, we compare the dependence on the field-renormalization scale in the expansion, effective-potential and iterative strategies for a point with near-maximal mixing ( $M_{H^\pm} = 140$  GeV). Expectedly, the field dependence in the expansion approach, of the order of  $\sim 10$  MeV, is much smaller than that obtained with the other approaches, of GeV order. As announced in Sect. 2, this is related to the careful pairing of 2L and 1L<sup>2</sup> terms in the expansion, which limits the contamination of the mass prediction by partial higher-order effects.

Finally, we explained in Sect. 3 that the 2L corrections of  $\mathcal{O}(\alpha_q \alpha_s, \alpha_q^2)$  are not really quantitatively meaningful for heavy-doublet states, since one then expects larger EW 2L effects. On the other hand, these orders are known to be dominant for the SM-like state. Therefore, with  $M_{H^\pm} \sim M_Z$ , it appears necessary to keep these  $\mathcal{O}(\alpha_q \alpha_s, \alpha_q^2)$  corrections for the full effective mixing matrix. In Fig. 9, we compare the masses  $M^{(\alpha_q^2)}$  obtained with full  $\mathcal{O}(\alpha_q \alpha_s, \alpha_q^2)$  corrections (as we always considered them till now) and those obtained in the approximation where these corrections of order  $\alpha_q \alpha_s$  and  $\alpha_q^2$  are only applied in the SM-like direction, denoted as  $M^{(\alpha_q^2, \text{SM})}$ . The solid green lines correspond to the masses derived in the degenerate formalism, the dashed red and orange ones to those derived in the non-degenerate formalism. Obviously, the introduction of  $\mathcal{O}(\alpha_q \alpha_s, \alpha_q^2)$  for the non-SM states and mixings has little impact for all states in the parameter space above  $M_{H^\pm} \sim 300$  GeV, and may as well be neglected since these orders are not quantitatively predictive. On the other hand, they contribute significantly in the mixing regime, justifying a complete inclusion at low  $M_{H^\pm}$ .

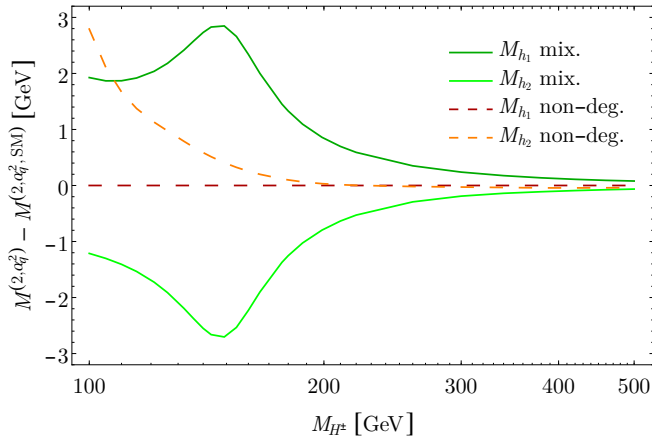


**Figure 9.:** Difference between the predicted masses (in the expansion formalism with  $\overline{\text{DR}}$  field counterterms at  $\mu_{\text{UV}} = m_t$ ) including the  $\mathcal{O}(\alpha_q \alpha_s, \alpha_q^2)$  gaugeless corrections for all states ( $M^{(\alpha_q^2)}$ ), and those obtained with 2L corrections only applied to the SM-like direction ( $M^{(\alpha_q^2, \text{SM})}$ ).

### 4.3. Three-state mixing

For completeness, we study a scenario involving three-state mixing, although of little phenomenological relevance in the MSSM due to strong experimental constraints on the properties of the observed Higgs state. Such a setup has been considered in particular in Refs. [85, 86], in view of studying interference effects close to degenerate scalar resonances, *e.g.* in the ‘toy’-scattering  $b\bar{b} \rightarrow h_i \rightarrow \tau^+\tau^-$ . The corresponding cross-section is then dominated by the  $S$ -channel exchange of Higgs bosons indeed. However, the formalism employed in these references fully disregards the dependence on field counterterms, both in the definition of the full propagator matrix and subsequent approximations, implying a sizable ‘uncertainty’ associated to regulators, as we show below. Instead, we prefer to describe such phenomena through the formalism derived in Appx. A, *i.e.* in a fashion minimizing the dependence on field counterterms (and linear gauge regulators).

For simplicity, we focus on the scattering  $b\bar{b} \rightarrow h_i \rightarrow \tau^+\tau^-$  via a trio of near-degenerate Higgs states  $h_i$ . A ‘naive’ Feynman-diagrammatic calculation would converge very slowly, due to the difference between the MSSM tree-level masses and the actual poles. It is thus useful to directly resum resonant effects. When performing this operation, one needs to extrapolate the form of the effective propagator away from tree-level Higgs masses. A direct resummation of self-energies as achieved in Ref. [85] then explicitly contaminates the pole values with gauge-dependent partial higher-order effects and field regulators. Instead, the identification of poles, residues and effective couplings via the expansion method, as proposed in Appx. A, minimizes the dependence on field counterterms and accordingly distributes the residues between pole and effective couplings, leading to an *a priori* more predictive result.

Below, we consider a scenario similar to that of Sect. 5.2 of Ref. [85] with  $M_{H^\pm} = 175$  GeV,  $\tan\beta = 50$ ,  $\phi_{A_t} = \pi/4$ . A first formal difficulty in such a setup with  $M_{H^\pm} \sim M_{\text{EW}}$  originates in the mixing of (charged and neutral) Higgs states with Goldstone and gauge bosons: in order to avoid problems of consistency with the gaugeless limit, we assume that this mixing can be processed in the perturbative (non-degenerate) description. The latter is justified in the gaugeless evaluation where *e.g.*  $|\hat{\Sigma}_{H^+G^-}^{(1,g^1)}(M_{H^\pm}^2/2)|/M_{H^\pm}^2 \approx 5 \cdot 10^{-4}$ , but also in the full model, with  $|\hat{\Sigma}_{H^+G^-}^{(1)}((M_{H^\pm}^2 + m_{G^\pm}^2)/2)|/M_{H^\pm}^2 \approx 1 \cdot 10^{-3}$ —gauge considerations justify the denominator  $M_{H^\pm}^2$  over  $M_{H^\pm}^2 - m_{G^\pm}^2$ . We may then focus on the three-state mixing in the neutral sector and consider the effective mass matrix of Eq. (19) or, alternatively, a mass derivation through

poles [GeV]	expansion			iteration		
	OS	$\overline{\text{DR}}$ EW	$\overline{\text{DR}}$ SUSY	OS	$\overline{\text{DR}}$ EW	$\overline{\text{DR}}$ SUSY
$\mathcal{M}_1$	$123.3 - 6.9 i$	$123.3 - 6.9 i$	$123.3 - 6.9 i$	$124.0 - 5.8 i$	$124.7 - 0.8 i$	$123.5 - 7.8 i$
$\mathcal{M}_2$	$123.8 - 7.6 i$	$123.8 - 7.6 i$	$123.8 - 7.6 i$	$124.6 - 6.6 i$	$125.0 - 6.9 i$	$124.3 - 8.4 i$
$\mathcal{M}_3$	$125.8 - 0.7 i$	$125.8 - 0.7 i$	$125.8 - 0.7 i$	$126.0 - 0.8 i$	$125.3 - 7.7 i$	$127.5 - 0.5 i$

**Table 1.:** Mass poles obtained in the scenario with three near-degenerate neutral states. In the left trio of columns, the masses are derived with the expansion method. In the righter one, the iterative method is employed. Three schemes are considered for the 1L Higgs fields: OS,  $\overline{\text{DR}}$  with  $\mu_{\text{UV}} = M_W$  ( $\overline{\text{DR}}$  EW) and  $\overline{\text{DR}}$  with  $\mu_{\text{UV}} = M_{\text{SUSY}} = 1 \text{ TeV}$  ( $\overline{\text{DR}}$  SUSY).

an iterative pole search. In fact, the mixing among neutral states is not numerically large in this scenario and the recourse to the degenerate formalism—although it is legitimized by the proximity in mass—is only forced upon us by the need to connect the gaugeless 2L corrections to the original Higgs states. The (square-roots of the) poles are provided in Tab. 1, considering both the expansion and the iterative methods, and employing three types of 1L field counterterms: OS,  $\overline{\text{DR}}$  with  $\mu_{\text{UV}} = M_{\text{EW}} = M_W$  and  $\overline{\text{DR}}$  with  $\mu_{\text{UV}} = M_{\text{SUSY}} = 1 \text{ TeV}$ . Similarly to the previous examples, the poles derived in the expansion formalism hardly depend on the choice of field renormalization (the variations are actually at the level of  $\sim 1 \cdot 10^{-5}$ ), while those obtained with an iterative pole search show fluctuations of GeV order (with varying hierarchies).

The effective couplings employed in the expansion approach are obtained at 1L from Eq. (53), which actually corresponds to a decay amplitude for the (loop-corrected) Higgs states. Such objects are independent on the choice of scheme for the fields. There exists no particular inconsistency—only added uncertainty—in working with different orders for the mass determination and the effective couplings, except possibly in the identification of the correspondence between poles and couplings. The latter offers no difficulty in the scenario with weak mixing considered here, and can always be made straightforward by using a mixing matrix defined at 2L order (at the cost of introducing a small dependence on field counterterms). QCD logarithms and  $t_\beta$ -enhanced corrections to the Higgs-bottom couplings are factorized out and resummed. Turning to the poles obtained in the iterative procedure, we adjoin to them effective couplings that are derived according to the recipe of Ref. [69] for decay amplitudes, objects that are then also explicitly dependent on the choice of field renormalization. We then combine these objects to define the cross-section  $\sigma[b\bar{b} \rightarrow H_{1,2,3} \rightarrow \tau^+\tau^-]$  in the Breit–Wigner description. These quantities are also gauge-dependent, see Ref. [66], but we only consider the 't Hooft–Feynman gauge here.

The results for the  $b\bar{b} \rightarrow \tau^+\tau^-$  scattering mediated by neutral Higgs states are shown in the left panel of Fig. 10. The cross-sections obtained with the expansion method, in green and cyan tones, are hardly distinguishable from one another, illustrating the weak dependence of this description on field renormalization. Conversely, the orange, red and magenta curves, obtained with different prescriptions for the field counterterms, demonstrate the strong dependence of the iterative method with off-shell momenta on these regulators: the predicted cross-sections then come with an in-built uncertainty of order 100%, strictly induced by the field dependence of the would-be (pseudo-)observables. Here, we note that this strong disparity among the cross-sections is mostly driven by the imaginary parts of the poles ( $\Gamma_{h_i}$ ): the amplitude of the resonances indeed scales like  $\Gamma_{h_i}^{-2}$ , so that moderate fluctuations of these quantities result in enhanced effects at the level of the scattering. The effective Higgs couplings to SM fermions,  $g_{\text{eff}}^{H_i f f}$  with  $f \in \{b, \tau\}$ , are shown in the right-hand panel of Fig. 10. With the expansion method (left-most column), the couplings of each Higgs resonance cluster at a definite point in the complex plane, irrespectively of the choice of scheme for the field renormalization. With the iteration method (right-most

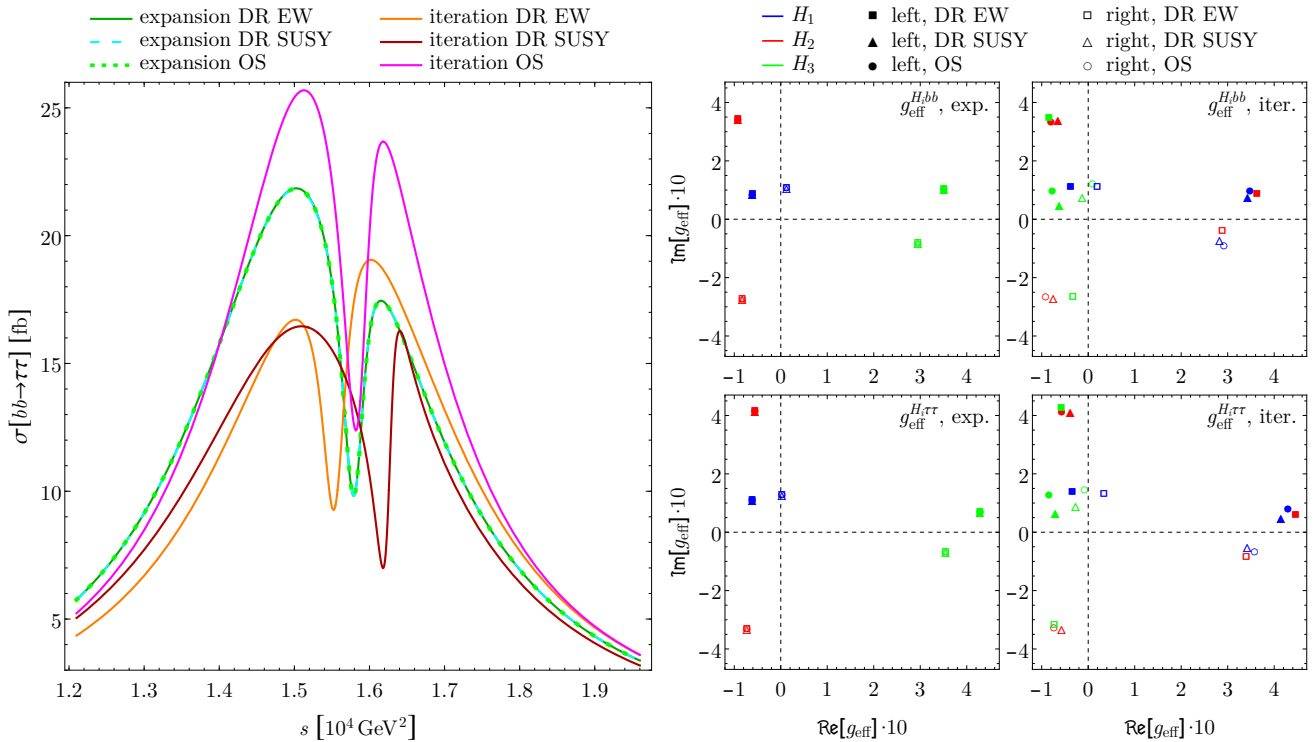


**Figure 10.:** Fermion scattering in the vicinity of three near-degenerate scalar resonances.

*Left:* Cross-section  $\sigma[bb \rightarrow \tau^+ \tau^-]$  obtained with poles and couplings in the expansion approach (dark-green, green and cyan, solid and dashed, depending on the scheme for field renormalization) and in the iterative method with off-shell momenta (solid orange, red and magenta in the  $\overline{\text{DR}}$  EW,  $\overline{\text{DR}}$  SUSY and OS schemes for fields, respectively).

*Right:* Effective Higgs couplings to bottom quarks (upper row) and  $\tau$  leptons (lower row) obtained in the expansion (left column) and in the iterative approaches (right column). Left- and right-handed couplings are depicted in the complex plane with filled and empty symbols respectively.

column), this clustering is still perceptible but looser, again highlighting the dependence on the choice of scheme. We note that the property  $(g_{\text{eff}}^{H_{iff}})_R = (g_{\text{eff}}^{H_{iff}})_L^*$  cannot be maintained with a complex mixing matrix, as derived at 2L order, which reveals the presence of partial 2L pieces in the couplings thus defined. However, at 1L order, it would also be possible to restore this property by employing a real mixing matrix, as in Ref. [66].

To summarize on these mass predictions in near degenerate scenarios, we have seen how, in many cases, this formalism was rather forced upon us by the gaugeless approximation for 2L effects, than by the actual size of the Higgs mixing. The exact degeneracy among the  $SU(2)_L$  partners of the charged Higgs at the tree level in the gaugeless limit thus forbids the description of  $1L^2$   $\mathcal{CP}$ -violating mixing terms in the formalism of Eq. (3). Similarly, the tree-level mixing angle  $\alpha - \beta$  of the full MSSM (including gauge terms), relevant for  $M_{H^\pm} \approx M_{\text{EW}}$ , can only be accounted for in an *ad-hoc* fashion in the gaugeless description, requiring a mixing-matrix formalism. This situation is not surprising as it naturally emerges from the neglected EW effects in the gaugeless description and can only be properly addressed by the inclusion of full EW 2L corrections. As it is, we observed that the expansion formalism for near-degenerate states, represented by the effective mass matrix of Eq. (19), provides predictive mass (pole) observables, showing little or no dependence on the choice of field renormalization, when the converse defect limits the usefulness of the iteration method.

## 5. Resummation of UV-logarithms of $\mathcal{O}(\alpha_q, \alpha_q \alpha_s, \alpha_q^2)$ and field dependence

In the previous sections, we have derived the Higgs masses and discussed the field dependence in a strict expansion at FO. Nevertheless, the large size of the radiative corrections of  $\mathcal{O}(2L)$  to the mass of the SM-like state in such an approach points at the slow convergence of the perturbative series in the presence of heavy (multi-TeV) SUSY particles. As is well-known, UV-logarithms of the type  $\ln^k M_{\text{SUSY}}^2/M_{\text{EW}}^2$ —with  $M_{\text{SUSY}}$  typically corresponding to the mass of the squarks of third generation—are responsible for these large effects and should be resummed for numerically meaningful predictions. One usually turns to the EFT framework—see *e.g.* Refs. [32–45]—in order to implement this resummation. However, for the corrections of  $\mathcal{O}(\alpha_q, \alpha_q \alpha_s, \alpha_q^2)$  that we discuss here, this operation can be performed directly in the FO context: all the relevant parameter input—strong gauge- and Yukawa couplings—is indeed accessible at low energy from SM observables, so that a matching at high scale is superfluous. Then, the (simple and squared) UV-logarithms contained in the FO expansion can be explicitly extracted and re-molded according to the flow of the Callan–Symanzik equations applying to the SM-like Higgs mass (or the mass-splitting between heavy states). While the method is thus formally distinct from that of an EFT, it is very similar at the technical level to the hybrid procedure described in Ref. [87], since both subtract UV-logarithms from the FO calculation to re-inject them in resummed form.

The relevant Renormalization-Group Equations (RGEs) are those obtained after screening-off the heavy fields—due to the large mass that cut these off in the emergence of UV-logarithms at the level of the loop functions: in other words, they match the field content of the SM, or of the Two-Higgs Doublet Model (THDM) for intermediate scales (if  $M_{H^\pm} \ll M_{\text{SUSY}}$ ). Further thresholds could be considered, depending on the relative scales of the gluino and the squarks of third generation, but we will not discuss them here. For the considered orders, the RGEs are entirely determined by the running of the quartic Higgs couplings, the EW v.e.v., the strong gauge- and Yukawa couplings. For definiteness, we collect the resummation formulae for the SM-like state in the gaugeless limit below:

$$\hat{\Sigma}_{hh}^{(\text{gl, resum})} = \int_{\ln M_{\text{EW}}^2}^{\ln M_{\text{SUSY}}^2} d \ln \mu^2 \left\{ -12 [\alpha_t^2(\mu) s_\beta^4 + \alpha_b^2(\mu) c_\beta^4] \left( 1 + \frac{16}{3} \frac{\alpha_s(\mu)}{4\pi} \right) + \beta_\lambda^{\alpha_q^2}(\mu) + \frac{6(\delta\lambda)^{(\alpha_q)}}{4\pi} [\alpha_t(\mu) s_\beta^2 + \alpha_b(\mu) c_\beta^2] \right\} v^2(\mu), \quad (30a)$$

$$\beta_\lambda^{\alpha_q^2}(\mu) \equiv \frac{12}{4\pi} \begin{cases} 5 [\alpha_t^3(\mu) s_\beta^4 + \alpha_b^3(\mu) c_\beta^4] + \alpha_t(\mu) \alpha_b(\mu) [\alpha_t(\mu) s_\beta^2 + \alpha_b(\mu) c_\beta^2], & \mu > M_{H^\pm}, \\ 5 [\alpha_t^3(\mu) s_\beta^6 + \alpha_b^3(\mu) c_\beta^6] - \alpha_t(\mu) s_\beta^2 \alpha_b(\mu) c_\beta^2 [\alpha_t(\mu) s_\beta^2 + \alpha_b(\mu) c_\beta^2], & \mu < M_{H^\pm}, \end{cases} \quad (30b)$$

$$\frac{d\alpha_s}{d \ln \mu^2} \equiv -7 \frac{\alpha_s^2}{4\pi} + \mathcal{O}(\alpha_s^3, \alpha_s^2 \alpha_q), \quad (30c)$$

$$\frac{d\alpha_t}{d \ln \mu^2} \equiv \begin{cases} \frac{1}{4\pi} \alpha_t \left[ \frac{9}{2} \alpha_t + \frac{1}{2} \alpha_b - 8 \alpha_s \right] + \mathcal{O}(\alpha_q \alpha, \alpha_s^2 \alpha_q, \alpha_s \alpha_q^2, \alpha_q^3), & \mu > M_{H^\pm}, \\ \frac{1}{4\pi} \alpha_t \left[ \frac{9}{2} \alpha_t s_\beta^2 + \frac{3}{2} \alpha_b c_\beta^2 - 8 \alpha_s \right] + \mathcal{O}(\alpha_q \alpha, \alpha_s^2 \alpha_q, \alpha_s \alpha_q^2, \alpha_q^3), & \mu < M_{H^\pm}, \end{cases} \quad (30d)$$

$$\frac{d\alpha_b}{d \ln \mu^2} \equiv \begin{cases} \frac{1}{4\pi} \alpha_b \left[ \frac{9}{2} \alpha_b + \frac{1}{2} \alpha_t - 8 \alpha_s \right] + \mathcal{O}(\alpha_q \alpha, \alpha_s^2 \alpha_q, \alpha_s \alpha_q^2, \alpha_q^3), & \mu > M_{H^\pm}, \\ \frac{1}{4\pi} \alpha_b \left[ \frac{9}{2} \alpha_b c_\beta^2 + \frac{3}{2} \alpha_t s_\beta^2 - 8 \alpha_s \right] + \mathcal{O}(\alpha_q \alpha, \alpha_s^2 \alpha_q, \alpha_s \alpha_q^2, \alpha_q^3), & \mu < M_{H^\pm}, \end{cases} \quad (30e)$$

$$\frac{d v^2}{d \ln \mu^2} \equiv -\frac{3 v^2}{4\pi} [\alpha_t s_\beta^2 + \alpha_b c_\beta^2] + \mathcal{O}(\alpha, \alpha_s \alpha_q, \alpha_q^2), \quad (30f)$$

$$(\delta\lambda)^{(\alpha_q)} \equiv [(\delta\lambda_2)^{(\alpha_q)} s_\beta^4 + (\delta\lambda_1)^{(\alpha_q)} c_\beta^4] \cdot [\alpha_t(\mu) s_\beta^2 + \alpha_b(\mu) c_\beta^2]^{-1}, \quad \mu > M_{H^\pm}, \quad (30g)$$

$$\frac{d(\delta\lambda_1)^{(\alpha_q)}}{d \ln \mu^2} \equiv -6 \alpha_b^2(\mu) + \mathcal{O}(\alpha_q^2 \alpha_s, \alpha_q^3), \quad \frac{d(\delta\lambda_2)^{(\alpha_q)}}{d \ln \mu^2} \equiv -6 \alpha_t^2(\mu) + \mathcal{O}(\alpha_q^2 \alpha_s, \alpha_q^3),$$

$$\frac{d(\delta\lambda)^{(\alpha_q)}}{d \ln \mu^2} \equiv -6 [\alpha_t^2(\mu) s_\beta^4 + \alpha_b^2(\mu) c_\beta^4] + \mathcal{O}(\alpha_q^2 \alpha_s, \alpha_q^3), \quad \mu < M_{H^\pm}. \quad (30h)$$

The resummation of gaugeless orders has little significance for the heavy-doublet masses, where EW corrections are dominant, and we thus omit the corresponding formulae. Contrarily to the EFT description where the EFT parameters are run down from a UV-matching scale to the Higgs (EW) scale, the RGEs of the FO description are run up from the SM (or THDM) input scale  $M_{\text{EW}}$ —set equal to  $m_t$  in practice—towards the scale corresponding to the heavy screened-off particles. The conversion of observable input (*e.g.* fermion and gauge pole masses) to running ( $\overline{\text{MS}}$ ) parameters generates further next-to-leading logarithms.

The RGEs summarized in Eq. (30) incorporate all the logarithmically-enhanced corrections that one can derive in the gaugeless limit at 2L order. We thus explicitly restrict ourselves to the leading order (LO) and next-to-LO (NLO) that are explicitly contained in the diagrammatic calculation of Higgs self-energies at 2L FO. However, RGEs of higher order could also be employed—in that case, without subtracting the higher-order logarithms in expanded form, since these have no equivalent in the diagrammatic calculation of  $\mathcal{O}(2L)$ . Furthermore, a few subtleties associated with the Higgs self-coupling parameter  $(\delta\lambda)^{(\alpha_q)}$  that are generated by loop effects of  $\mathcal{O}(\alpha_q)$  may be worth discussing. Indeed, the traditional (EFT) counting would associate to this object the boundary condition  $(\delta\lambda)^{(\alpha_q)}(M_{\text{SUSY}}) \stackrel{!}{=} 0$ , resulting in the low-energy boundary  $(\delta\lambda)^{(\alpha_q)}(M_{\text{EW}}) \approx 6 [\alpha_t^2 s_\beta^4 + \alpha_b^2 c_\beta^4] \ln M_{\text{SUSY}}^2/M_{\text{EW}}^2$ . This is also the choice that allows to reproduce the explicit logarithmic expansion of the FO calculation. Nevertheless, the choice  $(\delta\lambda)^{(\alpha_q)}(M_{\text{EW}}) \stackrel{!}{=} 0$  is also a perfectly legitimate condition due to the fundamental ambiguities in order counting— $\alpha_q \sim \alpha$  and  $\alpha_q \ln M_{\text{SUSY}}^2/M_{\text{EW}}^2 \sim 1$ —which allow the transmutation of the 2L quantity  $\alpha_q^2 \ln^2 M_{\text{SUSY}}^2/M_{\text{EW}}^2$  into the 1L object  $\alpha \ln M_{\text{SUSY}}^2/M_{\text{EW}}^2$ : instead of being resummed as logarithms of Yukawa type, the squared logarithms thus overlooked would be left as simple EW logarithms—and possibly resummed as such when absorbed within the quartic Higgs coupling  $\lambda(M_{\text{EW}})$ . As we do not perform this EW resummation here, however, the numerical difference between the two procedures can be sizable at large squark masses. To keep the comparisons simple, we therefore adopt the traditional counting by default, *i.e.* set

$$(\delta\lambda)^{(\alpha_q)}(M_{\text{EW}}) \stackrel{!}{=} \int_{\ln M_{\text{EW}}^2}^{\ln M_{\text{SUSY}}^2} d \ln \mu^2 6 [\alpha_t^2 s_\beta^4 + \alpha_b^2 c_\beta^4]. \quad (31)$$

With LO and NLO logarithms of  $\mathcal{O}(\alpha_q, \alpha_q \alpha_s, \alpha_q^2)$  properly resummed (up to another caveat that we discuss below), the higher-order uncertainty, controlled by terms  $\sim \alpha_q \alpha_s^2 \ln^3 M_{\text{SUSY}}^2/M_{\text{EW}}^2$  ( $\simeq 10$ – $30\%$ , at the level of the squared mass, for  $M_{\text{SUSY}} = 1.5$ – $10$  TeV) in the strict expansion, is now pushed back—as far as gaugeless orders are concerned—to  $\sim \alpha_q \alpha_s^2 \ln M_{\text{SUSY}}^2/M_{\text{EW}}^2$  ( $< 1\%$ ). In fact, the higher-order uncertainty is now controlled by EW 2L effects  $\sim \alpha_q \alpha \ln^2 M_{\text{SUSY}}^2/M_{\text{EW}}^2$  ( $\sim 0.2$ – $2\%$  for  $M_{\text{SUSY}} = 1.5$ – $10$  TeV). Furthermore, another term of gaugeless order appears in

the RGEs, originating in Higgs self-interactions:

$$\hat{\Sigma}_{hh}^{(gl, \alpha_q^3)} = \int_{\ln M_{EW}^2}^{\ln M_{SUSY}^2} d \ln \mu^2 \frac{12}{16 \pi^2} [(\delta\lambda)^{(\alpha_q)}(\mu)]^2 v(\mu)^2 = \mathcal{O}(\alpha_q^3 \ln^2 M_{SUSY}^2 / M_{EW}^2). \quad (32)$$

As this is a contribution of 3L order, it does not appear in the 2L calculation at FO. In order to resum all NLO logarithms of Yukawa-type, we add this term to our calculation nonetheless, instead of leaving it as a contribution of  $\mathcal{O}(\alpha)$ . Finally, it is fair to mention in this short uncertainty estimate that not only logarithmically-enhanced contributions may require the recourse to resummation techniques: see *e. g.* Ref. [88] for a resummation of squark-mixing terms.

EW logarithms of LO could also be resummed, as is routinely performed in the EFT description. Our method with input at the low-energy boundary continues to apply, without need of a matching at high scale. EW gauge couplings are indeed well-defined at the low-energy end. As to the quartic Higgs couplings, they can be obtained from the observables (Higgs masses and decays) that are predicted in the FO calculation, without or with partial UV-resummation. This is a straightforward recipe for a low-energy effective SM—only the (preliminary) mass prediction for the SM-like state is then needed—but accounting for a THDM threshold becomes more intricate as a larger basis of observables is then needed in order to identify the more numerous parameters of the Higgs potential; yet, the situation is no different at this level in an EFT approach, in principle. In fact, the somewhat less robust boundary condition for the Higgs self-interactions is the only drawback as compared to the EFT procedure: we anticipate it to amount to little at the numerical level, albeit a detailed comparison (beyond our current scope) would be needed in order to ascertain this claim. In this paper, we choose not to carry out the resummation of EW logarithms and go through the intricacies of a THDM threshold, first because this would exceed the bounds of gaugeless orders that we meant to discuss here, then because these effects remain comparatively small (and not necessarily related to the scale of the sole gluino and squarks of third generation), finally because the actual focus of the paper concerns the dependence on field counterterms and that the gaugeless orders are quite sufficient to measure its impact in a resummed mass prediction for the SM-like Higgs.

In the upper row of Fig. 11, we compare the explicit calculation of Higgs self-energies at FO in the gaugeless limit and the corresponding expansion in  $\ln^k M_{SUSY}^2 / M_{EW}^2$ . This latter expansion is obtained from the integration of the RGEs of Eq. (30) in a linear way, but—as mentioned above—additional logarithms of NLO intervene from the conversion of parameters in our scheme to  $\overline{MS}$  ones at the scale  $M_{EW}$ —*e. g.*  $m_t^{OS} = m_t^{\overline{MS}}(m_t) \left(1 + \frac{16}{3} \frac{\alpha_s}{4\pi} + \mathcal{O}(\alpha_q)\right)$ . The plots in the middle and lower rows show the impact of the resummation of the UV-logarithms for the prediction of the SM-like mass. Here, the UV-resummation is achieved by subtracting the identified UV-logarithms and substituting a resummed version where Eq. (30) is integrated numerically. The corresponding evaluations are shown in red and orange lines, while the blue and cyan lines correspond to the predictions without resummation. These calculations are conducted for both the expansion formalism (blue and red) and for the iterative pole search (cyan and orange) with  $\overline{DR}$  regularization of the Higgs fields ( $\mu_{UV} = M_W$  in solid and  $\mu_{UV} = M_{SUSY}$  in dashed lines). In the lower row, the orange and cyan curves correspond to the approximation  $p^2 = 0$  in the contributions of 2L order processed in an iterative fashion: their colors match those of the corresponding curves in the middle row, accounting for full momentum dependence.

On the left-hand side of Fig. 11, we consider an MSSM scenario with decoupling squarks and gluinos ( $m_{\tilde{Q}_{3,\tilde{T}}} \approx M_3 \stackrel{!}{=} M_{SUSY} \gg m_t$ ), keeping the mixing in the stop sector,  $X_t \equiv A_t - \mu/t_\beta$ , minimal, and setting  $M_{H^\pm} = 1 \text{ TeV}$ ,  $t_\beta = 10$  for the THDM sector. This is the ideal setup for



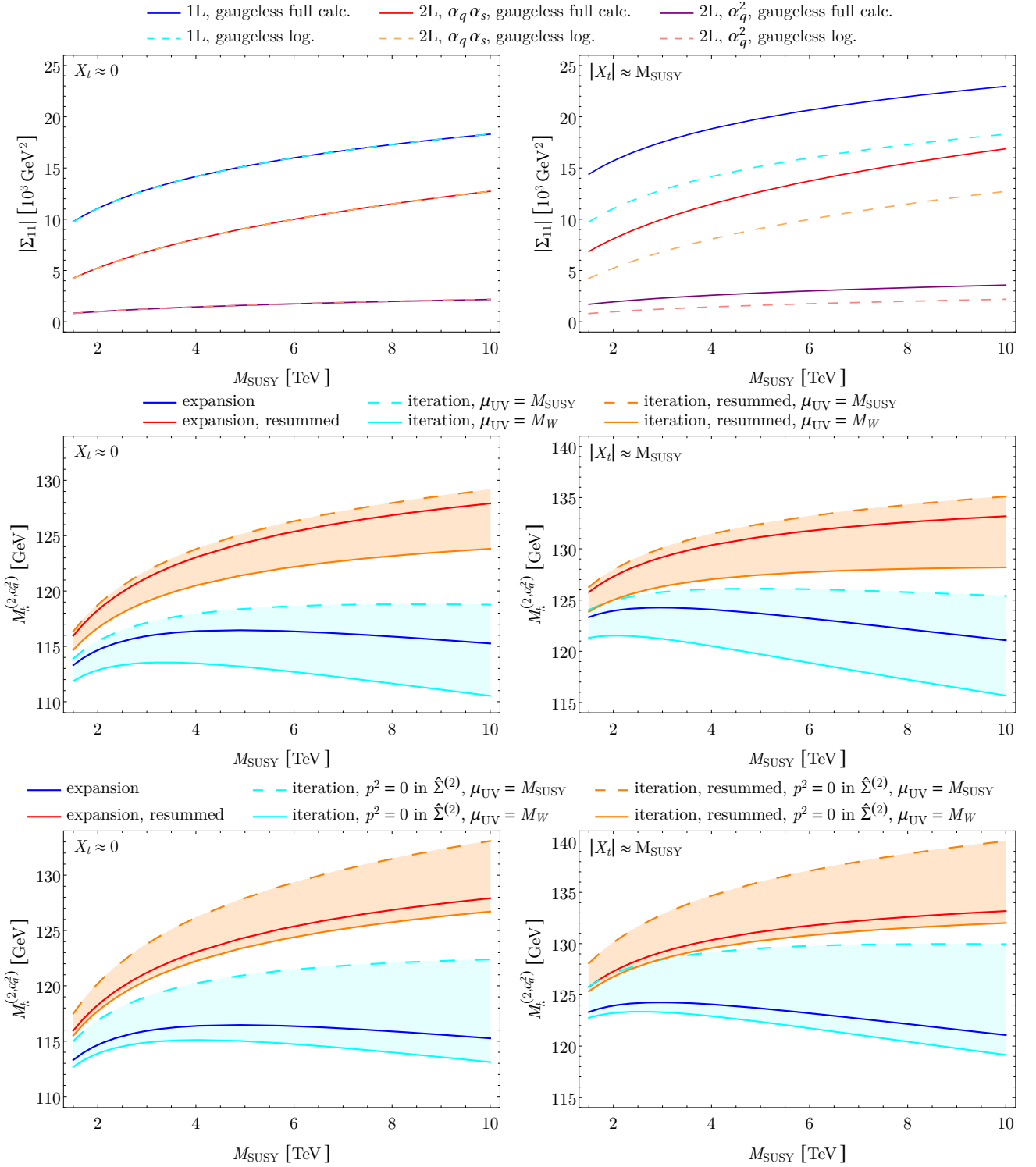


**Figure 11.:** Impact of the resummation of UV-logarithms of  $\mathcal{O}(\alpha_q, \alpha_q \alpha_s, \alpha_q^2)$  for the Higgs-mass prediction and the field dependence.

*Up:* Higgs self-energies in the gaugeless limit (solid curves) compared to the logarithmic expansion (dashed curves).

*Middle:* Mass predictions with resummed UV-logarithms (red and orange) compared to the strict FO expansion (blue and cyan). Both the expansion formalism (red and blue) and the iterative pole search with  $\overline{\text{DR}}$  field counterterms (orange and cyan; solid:  $\mu_{\text{UV}} = M_W$ ; dashed:  $\mu_{\text{UV}} = M_{\text{SUSY}}$ ) are considered.

*Down:* Same as in the middle row, but with two-loop self-energies evaluated at  $p^2 = 0$ .

*Left:* The stop mixing is set to negligible values.

*Right:* The stop mixing is kept at the SUSY scale.

checking the agreement between the logarithmic expansion and the FO calculations, as can be observed in the very narrow matching of the various self-energies. Turning to the mass predictions, the resummation of UV-logarithms accounts for a shift of already  $\sim 1.5$  GeV at  $M_{\text{SUSY}} \sim 1.5$  TeV and over 10 GeV at 10 TeV. As already noted in earlier works—see *e.g.* Ref. [9]—the resummation counteracts the tendency of mass predictions of  $\mathcal{O}(\alpha_q^2)$  to fall at large  $M_{\text{SUSY}}$ —due to large  $\ln^2 M_{\text{SUSY}}^2/M_{\text{EW}}^2$  added linearly in the strict FO expansion.

On the right-hand side of Fig. 11, we maintain the stop mixing at  $|X_t| \approx M_{\text{SUSY}}$ , which generates sizable shifts between the logarithmic expansion and the FO calculation (without endangering the relevance of the resummation of UV-logarithms). At least the leading orders from squark mixing are properly included within the non-logarithmic terms of the FO calculation.

As to the dependence of masses on field counterterms, in case an iterative pole search is employed, it is obvious that the resummation affects it only marginally, as the momenta evaluated in self-energies are still shifted with respect to the tree-level mass (the latter choice ensuring invariance in the expansion method). Correspondingly, the uncertainty associated with field variations steeply grows with increasing  $M_{\text{SUSY}}$  in the FO approach with iterative pole search, reaching  $\mathcal{O}(10\%)$  at  $M_{\text{SUSY}} \sim 10$  TeV—hence becoming larger than the actual higher-order uncertainty after resummation of the UV-logarithms. The approximation  $p^2 = 0$  in pieces of 2L order of the iterative pole search (lower row) tends to systematically over-estimate the mass as compared to the prediction with full momentum dependence, but does not reduce the magnitude of the dependence on field-renormalization constants. Given the similarity of the procedure employed in the hybrid calculation of Ref. [87], then refined in Refs. [29, 37, 41, 46–49], the corresponding predictions of the public code `FeynHiggs` [46, 47, 57, 60, 67, 87, 89, 90] are thus *a priori* subject to the large error associated with the field dependence. Yet, an *ad-hoc* choice of field counterterms, derived by comparison of the logarithms with those of an EFT (see Ref. [29]), then restores a more predictive behavior—largely compatible with that of the more straightforward expansion approach. We aim at a more detailed comparison in Fig. 12 for the same scenario as in the left-hand column of plots of Fig. 11 ( $X_t \approx 0$ ).

`FeynHiggs-2.18.0` delivers Higgs-mass predictions in the MSSM. The 2L corrections of order  $\alpha_q \alpha_s$  and  $\alpha_q^2$  are included in the effective-potential approximation, which is a relevant choice for the SM-like state, as already discussed. UV-logarithms can optionally be resummed and included in the hybrid approach described in Refs. [46–49, 87]. The default setup (labelled ‘vanilla `FeynHiggs`’ below) employs an iterative pole-search algorithm to find the loop-corrected Higgs masses. In order to neutralize the large unphysical scale dependence that is thus introduced by the field-renormalization constants, a special scheme has been devised in Ref. [29]; it includes all finite SUSY contributions in the field counterterms, thereby yielding the same logarithmic dependence as that of an EFT calculation. The predictions of ‘vanilla `FeynHiggs`’ are depicted as reference in all plots of Fig. 12 (blue and red short-dashed lines).

For consistency checks, `FeynHiggs` also provides some hidden flags that can be set through environment variables. Below, we make use of the following settings:

- `FHFOPOLEEQ=1` switches the determination of the loop-corrected masses to a partial perturbative expansion—only corrections for the diagonal self-energies are included; in the considered scenario with hierarchical Higgs sector, this is expected to agree relatively well with our calculation using the expansion formalism;
- with `FHFINFIELDDREN=0` the finite terms of the field-renormalization constants are set to zero, hence reverting the field counterterms to a simple  $\overline{\text{DR}}$  form;
- `FHTBSCALE=#` interprets the input value for  $\tan \beta$  at the scale # GeV, which can largely be seen as resetting the renormalization scale  $\mu_{\text{ren}}$  for this parameter.

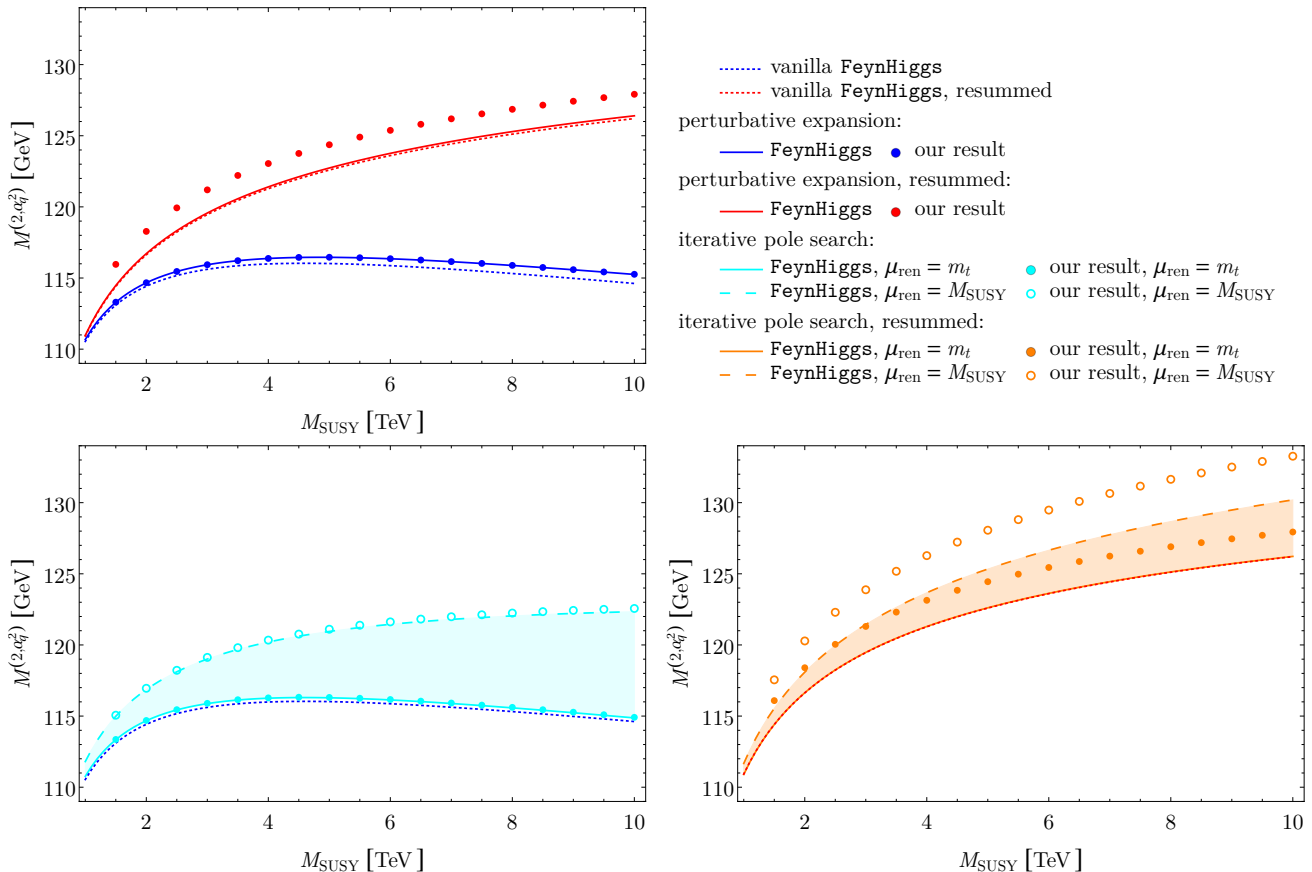


**Figure 12.:** Comparison of our results with those of `FeynHiggs`. Blue/cyan curves and symbols correspond to the mass predictions with strict FO expansion, while the red/orange ones include a resummation of UV-logarithms. Actual lines refer to masses determined with `FeynHiggs` whereas the disks and circles proceed from our own calculations. The default output of `FeynHiggs`, ‘vanilla `FeynHiggs`’, is plotted with short-dashed lines in all plots to serve as a reference. All other curves test different settings.

*Up Left:* The partial expansion available in `FeynHiggs` (solid lines) is compared with our own (disks).

*Bottom Left:* Results of the iterative pole search without resumming UV-logarithms. The calculations are performed with two different renormalization scales and the  $\overline{\text{DR}}$  input is correspondingly adjusted.

*Bottom Right:* Similar to bottom left, but now including the resummation of UV-logarithms.

In the upper-left plot of Fig. 12, we compare the mass predictions of the partial perturbative expansion available in `FeynHiggs` (solid curves) with the results using our own expansion formalism (disks). The plain FO determination is shown in blue, while a resummation of logarithms is included in the red curves. In the case of `FeynHiggs`, the setting `loglevel=2` is employed, which corresponds to the resummation of next-to-leading logarithms (NLL) for the case where all SUSY masses are large.<sup>12</sup> We observe an almost exact agreement of `FeynHiggs` and our formalism for this expansion approach; small differences at the level of predictions with resummed UV-logarithms are of the expected percent-order magnitude for unresummed EW logarithms (in our setup) and can thus be attributed to additional classes of logarithms that are included in the resummation of `FeynHiggs`. In addition, the resummation of EW logarithms may not be completely suited to our scenario where electroweakino and slepton masses are not varied with  $M_{\text{SUSY}}$ .

<sup>12</sup> A setting for higher precision is possible and performs a next-to-NLL resummation, but such effects are not considered in our calculation (though they could be added at a later stage), hence appear of limited use for the comparison that we conduct here and which focusses on field-dependence aspects.

In the lower row of Fig. 12, we compare our predictions (disks and circles) to the corresponding ones obtained with `FeynHiggs` (solid and dashed curves) when using an iterative pole-search algorithm with  $\overline{\text{DR}}$ -renormalized fields. In order to resemble the setup of `FeynHiggs`, our predictions include the 2L corrections in the effective-potential approximation. The plot on the left-hand side shows the FO results, while the curves on the right-hand side include resummed logarithms. In both plots we display predictions at the renormalization scales  $\mu_{\text{ren}} = m_t$  (solid curves or disks) and  $\mu_{\text{ren}} = M_{\text{SUSY}}$  (dashed curves or circles). The input value for the  $\overline{\text{DR}}$  parameter  $\tan\beta$  is interpreted at the scale  $m_t$  before being run to the chosen renormalization scale and fed as input: we thus make sure that we are comparing the same points in parameter space. The running of the additional  $\overline{\text{DR}}$  parameters  $m_b$  and  $A_b$  has a negligible impact in the chosen scenario. This whole procedure is meant to emulate the direct variation of finite field counterterms, as we considered it before, since an independent variation is not straightforwardly accessible in `FeynHiggs`. Again, we are able to recover the predictions of `FeynHiggs` at FO (left plot) to a good approximation, which confirms our observations as to the large inherent uncertainty associated with an iterative approach to the pole determination. A somewhat larger deviation is visible in the resummed prediction at the SUSY scale: we could not completely understand the origin of this discrepancy, but this may not matter much since the dependence on the choice of field renormalization in such a description spoils the logarithmic behavior anyway. In any case, it is obvious that the introduction of the UV-resummation does not neutralize the intrinsic uncertainty originating in the pole search. We note that the results obtained with  $\mu_{\text{UV}} = m_t$  are very close to the—in our opinion more reliable—predictions of the expansion procedure. This good performance is not completely mysterious in the considered scenario. Indeed, with the external momentum set to 0 in the 2L self-energies and a sizable hierarchy between  $M_{\text{EW}}$  and  $M_{H^\pm}$ , the difference between the iteration and expansion procedures for the determination of the mass of the SM-like Higgs can be estimated as  $-(\mathfrak{M}_h^2 - m_h^2) \hat{\Sigma}_{hh}^{(1)'}(m_h^2) + \hat{\Sigma}_{hh}^{(1,gl)}(0) \hat{\Sigma}_{hh}^{(1,gl)'}(0)$  (similarly to Eq. (23)). Then, in the gaugeless approximation,  $\hat{\Sigma}_{hh}^{(1,gl)'} \approx -\frac{3\alpha_t}{4\pi} s_\beta^2 \left[ \ln \mu_{\text{UV}}^2/m_t^2 - \frac{2}{3} + \mathcal{O}(X_t^2/M_{\text{SUSY}}^2) \right]$ , which vanishes for  $\mu_{\text{UV}} = \mathcal{O}(m_t)$  at small  $X_t$ . The inclusion of EW orders does not spoil this picture, as long as large logarithms do not develop from the electroweakino loops. Therefore, the apparent predictivity of the choice  $\mu_{\text{UV}} = m_t$  is very specific to this scenario and not reliable on fundamental grounds.

Finally, we turn to the predictions by ‘vanilla `FeynHiggs`’. These appear to be relatively close to our results obtained with the perturbative expansion (upper plot). Again, this comparative proximity is not really mysterious, as the injected counterterms in `FeynHiggs` have been designed such that one recovers the correct logarithmic behavior. Such a choice is comparable to our OS scheme for the field counterterms, for which we also observed comparative agreement with the expansion in similar setups: see the pink cross in the upper plot of Fig. 6. Therefore, although `FeynHiggs` employs an iterative pole search by default, it escapes the large uncertainty associated with this procedure through a judicious choice of field counterterms. Yet, a discrepancy reaching  $\mathcal{O}(1 \text{ GeV})$  at  $M_{\text{SUSY}} = 10 \text{ TeV}$  is visible in the strict FO approach—blue curves; both calculations are comparable in that they consider exactly the same orders. Unquestionably, this difference originates in the choice of procedure (expansion vs. iteration), since the simplified expansion available in `FeynHiggs` agrees with our method. This is therefore the magnitude of the error—again, we stress that this shift has no predictive value—contained in this choice for the mass determination, which should be included as an irreducible uncertainty to the predictions (beyond estimated higher-order effects). This contribution is somewhat reduced after inclusion of the UV-resummation (in this scenario), because  $\mathfrak{M}_h^2$  then comes closer to  $m_h^2 - \hat{\Sigma}_{hh}^{(1,gl)}(0)$  ( $\approx 162^2 \text{ GeV}^2$  at  $M_{\text{SUSY}} = 10 \text{ TeV}$ )—the difference between these two quantities controls the leading dependence on the field counterterm, proportional to  $\delta Z_{hh}$ .

In addition, the use of the technically more involved iteration method remains a choice of questionable efficiency since the predictivity of the FO calculation, directly accessible with the simple expansion procedure, is first wasted, then restored through the cross-reference of the logarithms with the EFT method. Finally, it is unlikely that this method can simultaneously produce predictive results at the level of the mass-splitting among heavy states. We therefore recommend the use of the more robust expansion and truncation procedure that we described in Sect. 2 after the principle of independence of observables from the choice of scheme for field renormalization.

## 6. Conclusions

In this paper, we investigated the dependence of MSSM Higgs masses on field counterterms in a FO approach at 2L. This dependence on regulators originates in the arbitrary regularization of Higgs self-energies away from their (tree-level) mass-shell, and is exacerbated when processing 2L and 1L<sup>2</sup> corrections in independent fashions. This situation is further complicated by the fact that—due to missing EW corrections in 2L vector self-energies—only effects of  $\mathcal{O}(\alpha_q \alpha_s, \alpha_q^2)$  are fully exploitable at 2L, rendering an evaluation in the gaugeless approximation necessary at the technical level. Masses derived in the strict expansion formalism evade these difficulties through a careful pairing of field-dependent pieces and the neutralization of field counterterms. On the other hand, the popular mass determination via an iterative pole search, computationally more costly, retains an explicit dependence on field regulators, which generates an irreducible uncertainty inherent to the method. In the case of the SM-like Higgs state, we have seen that this ‘error’ already amounts to a few GeV for a SUSY sector at the TeV scale. Concerning the heavy-doublet states, unlike the SM-like one, the known orders  $\alpha_q \alpha_s$  and  $\alpha_q^2$  are of limited relevance since EW corrections are expected to dominate. We still considered these contributions in order to test the impact of the regularization of Higgs self-energies away from their mass-shell. Then, a scale variation with  $\overline{\text{DR}}$  counterterms is insufficient to capture the full extent of the field dependence, which is driven by leading EW effects, and we also introduced an OS regularization for comparison. In all cases, variation of the field regulators demonstrated that the mass-shifts generated by the iterative pole search with respect to the expansion approach are purely artificial in nature, and we thus believe it justified to prefer the simpler—and field independent—method. This argument adds to the one of the symmetry considerations that we raised at 1L order in Ref. [66].

In the presence of mass degeneracies, the expansion formalism can be extended to account for mixing effects in a fashion keeping the dependence on field regulators to a minimum. We studied several scenarios involving large mixing effects as well as the transition with the non-degenerate regime. The inclusion of 2L effects in the gaugeless approximation has various consequences at this level, such as imposing the degeneracy of heavy Higgs states in the presence of CP-violating mixing or complicating the connection between the gaugeless and ‘full’ tree-level Higgs states. At a technical level, it would thus seem desirable to put full 2L EW corrections under control, which would allow to escape the constraints of the gaugeless approximation and limit the use of a near-degenerate formalism strictly to scenarios with large mixing. As far as the dependence on field counterterms is concerned, the situation is very similar, however, in the non-degenerate and near-degenerate scenarios.

In addition, we observed that the effective-potential approximation for 2L self-energies leads to quantitatively reliable results only when applied to the mass of the SM-like state. Considering the numerical cost of evaluating 2L integrals at non-vanishing momentum, as well as the irrelevance (in the absence of EW 2L corrections) of the orders  $\alpha_q \alpha_s$  and  $\alpha_q^2$  for heavy-doublet states, it makes limited sense, in the non-degenerate case, to consider 2L gaugeless self-energies for any other

external state than the SM-like one. Furthermore, the limited pertinence of this approximation for non-vanishing tree-level masses questions as to the applicability of corresponding calculations to extensions of the MSSM, away from an MSSM-like regime, since tree-level masses do not necessarily vanish then, even in the gaugeless limit.

Given that large UV-logarithms develop with increasingly heavy SUSY spectrum, the strict FO formalism suffers from a slow convergence of the perturbative series. This issue can be evaded through an explicit resummation of logarithmic effects. This resummation can be directly included in the context of the FO calculation, without resorting to a matching scale, simply by exploiting low-energy observables as input, and we explicitly performed this operation for the orders  $\alpha_q$ ,  $\alpha_q \alpha_s$  and  $\alpha_q^2$ . As this resummation does not modify the problem of the regularization of Higgs self-energies away from their mass-shell, it does not affect our conclusions concerning the dependence of mass predictions at FO on field counterterms. This situation contrasts with the concurrent computation method through EFTs, where artificial field-dependent terms cannot receive large logarithmic enhancement—due to the very structure of the EFT that embeds UV-logarithms within effective tree-level couplings—but not with *e.g.* the hybrid approach of Ref. [87]. Nevertheless, we have also shown how the judicious choice of field renormalization devised in Ref. [29] for the public code `FeynHiggs` largely shields the latter from excessive uncertainties associated with the iterative mass determination.

## Acknowledgments

We thank Henning Bahl for discussions about properties of `FeynHiggs`. S.P. acknowledges support by the BMBF Grant No.05H18PACC2. F.D. acknowledges support of the BMBF Verbund-Projekt 05H2018 and the DFG grant SFB CRC-110 *Symmetries and the Emergence of Structure in QCD*.

## A. Scattering by scalar resonances and propagator matrix

### A.1. General considerations

For definiteness, we consider the  $2 \rightarrow 2$  scattering process  $b\bar{b} \rightarrow \tau^+\tau^-$  mediated by scalar (neutral Higgs) resonances, with a center-of-mass energy  $\sqrt{s}$ . The amplitude can be formally written as

$$\mathcal{A}[b\bar{b} \rightarrow \tau^+\tau^-] = [\bar{v}_b(\bar{p}_b) \iota \check{V}_{Sbb}^\alpha u_b(p_b)] \iota \check{P}_{\alpha\beta}^S [\bar{v}_\tau(\bar{p}_\tau) \iota \check{V}_{S\tau\tau}^\beta u_\tau(p_\tau)]. \quad (33)$$

In this appendix, the  $\check{\circ}$  notation represents vectors and matrices in scalar space—corresponding to the Greek indices,  $\alpha, \beta$ , which are implicitly summed over. The symbols have the following meaning:

- The propagator  $\check{P}^S$  is a symmetric matrix in scalar space, depending on the external momentum squared  $s \equiv (p_b + \bar{p}_b)^2$ . As is customary in particle physics, we assume that this object can be decomposed into single poles and a continuum:

$$\check{P}^S(s) = \sum_H \frac{\check{R}_H}{s - \mathcal{M}_H^2} + \check{C}(s) \quad (34)$$

where  $\check{C}$  is a ‘smooth’ function of  $s$ .

Without loss of generality,

$$\check{R}_H = \sum_m r_{H_m} \check{E}_{H_m} \check{E}_{H_m}^T, \quad (35)$$

where  $\check{E}_{H_m}$  are vectors generating the subspace associated with the pole  $\mathcal{M}_H^2$ , while  $r_{H_m}$  is a normalization ('residue' if  $\check{E}_{H_m}$  is normalized).

- The vertex operator  $\check{V}_{Sff}$  is a 'column'-vector in scalar space and—since it corresponds to interactions with scalar resonances—can be decomposed as *e.g.*  $\check{V}_{Sff} = \check{V}_{Sff}^L P_L + \check{V}_{Sff}^R P_R$  in spinor space, where  $P_{L,R}$  represent the chiral projectors while  $\check{V}_{Sff}^{L,R}$  have no spinor indices left. *A priori*,  $\check{V}_{Sff}^{L,R}$  are functions of  $p_f$  and  $\bar{p}_f$ , which we can replace by  $m_f^2$  (kept implicit) and  $s = (p_f + \bar{p}_f)^2$  due to Lorentz invariance. By 'physical' hypothesis, these functions of  $s$  are 'smooth', so that, near a pole  $\mathcal{M}_H^2$  of the propagator,

$$\check{V}_{Sff}^{L,R}(s) \underset{s \sim \mathcal{M}_H^2}{=} \check{V}_{Sff}^{L,R}(\mathcal{M}_H^2) + (s - \mathcal{M}_H^2) \frac{d\check{V}_{Sff}^{L,R}}{ds}(\mathcal{M}_H^2) + \dots \quad (36)$$

We write the scalar product  $r_{H_m}^{1/2} (\check{E}_{H_m}^T \check{V}_{Sff}^{L,R}(\mathcal{M}_H^2))$  as  $g_{H_m ff}^{L,R}$ .

From the analysis above, the scattering amplitude may thus be written as follows:

$$\mathcal{A}[b\bar{b} \rightarrow \tau^+ \tau^-] = f(s) + \sum_{H,m} \left[ \bar{v}_b(\bar{p}_b) \imath \left( g_{H_m bb}^{L,R} P_{L,R} \right) u_b(p_b) \right] \frac{\imath}{s - \mathcal{M}_H^2} \left[ \bar{v}_\tau(\bar{p}_\tau) \imath \left( g_{H_m \tau\tau}^{L,R} P_{L,R} \right) u_\tau(p_\tau) \right] \quad (37)$$

where  $f$  is a smooth function. Perturbative QFT, assuming it is in its regime of validity, should offer a predictive framework for the calculation of the objects defined above, in particular the (complex) poles  $\mathcal{M}_H^2$  and the effective couplings  $g_{H_m ff}^{L,R}$ .

## A.2. Propagator matrix in perturbative QFT at 2L order

The propagator matrix is defined as the inverse of the two-point function in the scalar sector:  $\check{P}^S(s) = [s \check{\mathbb{1}} - \check{M}_S^2(s)]^{-1}$ , where  $\check{M}_S^2(s) = \check{M}_{\text{tree}}^2 - \hat{\Sigma}(s)$  with  $\check{M}_{\text{tree}}^2$  denoting the tree-level mass matrix and  $\hat{\Sigma}(s) = \hat{\Sigma}^{(1)}(s) + \hat{\Sigma}^{(2)}(s) + \mathcal{O}(3\text{L})$  denoting the renormalized self-energy matrix. We work in the basis of the tree-level mass eigenstates, *i.e.*  $\check{M}_{\text{tree}}^2 = \text{diag}[m_i^2]$ .

**Non-degenerate case:** Let us consider  $s = m_i^2 + \mathcal{O}(1\text{L})$ , with  $m_i^2$  representing a non-degenerate tree-level mass, and define the matrix  $\check{\Omega}^i(s)$  from its elements ( $j, k \neq i$ )

$$\check{\Omega}_{ii}^i(s) \equiv 1 - \frac{1}{2} \sum_{j \neq i} \left[ \frac{\hat{\Sigma}_{ij}^{(1)}(s)}{m_i^2 - m_j^2} \right]^2, \quad \check{\Omega}_{jk}^i(s) \equiv \delta_{jk} - \frac{\hat{\Sigma}_{ij}^{(1)}(s) \hat{\Sigma}_{ik}^{(1)}(s)}{2 (m_i^2 - m_j^2) (m_i^2 - m_k^2)}, \quad (38a)$$

$$\check{\Omega}_{ij}^i(s) = -\check{\Omega}_{ji}^i(s) \equiv -\frac{1}{m_i^2 - m_j^2} \left[ \hat{\Sigma}_{ij}^{(1)}(s) + \hat{\Sigma}_{ij}^{(2)}(s) + \frac{\hat{\Sigma}_{ii}^{(1)}(s) \hat{\Sigma}_{ij}^{(1)}(s)}{m_i^2 - m_j^2} - \sum_{k \neq i} \frac{\hat{\Sigma}_{ik}^{(1)}(s) \hat{\Sigma}_{jk}^{(1)}(s)}{m_i^2 - m_k^2} \right]. \quad (38b)$$

It satisfies  $\check{\mathbf{\Omega}}^i(s) \cdot \check{\mathbf{\Omega}}^{iT}(s) = \check{\mathbf{1}} + \mathcal{O}(3L)$  as well as

$$[s \check{\mathbf{1}} - \check{M}_S^2(s)]_{jk} = \left( s - \widetilde{M}_i^2(s) \right) \check{\Omega}_{ij}^i(s) \check{\Omega}_{ik}^i(s) + \sum_{m,n \neq i} \check{\Omega}_{mj}^i(s) \check{\Omega}_{nk}^i(s) \left( s \delta_{jk} - \widetilde{M}_{jk}^2(s) \right) + \mathcal{O}(3L), \quad (39)$$

*i. e.* the  $\check{\mathbf{\Omega}}^i(s)$  ‘rotation’ isolates the direction  $i$  up to terms of 3L order, with the diagonal element (‘eigenvalue’) reading

$$\widetilde{M}_i^2(s) = m_i^2 - \hat{\Sigma}_{ii}^{(1)}(s) - \hat{\Sigma}_{ii}^{(2)}(s) + \sum_{j \neq i} \frac{\hat{\Sigma}_{ij}^{(1)}(s)^2}{m_i^2 - m_j^2} + \mathcal{O}(3L). \quad (40)$$

Coming back to the propagator matrix, we then have

$$\check{P}_{jk}^S(s) = \frac{1}{s \sim m_i^2} \frac{1}{s - \widetilde{M}_i^2(s)} \check{\Omega}_{ij}^i(s) \check{\Omega}_{ik}^i(s) + \dots, \quad (41)$$

where the ellipses represent non-singular pieces in the vicinity of  $s \sim m_i^2$ . We thus obtain a pole  $\mathcal{M}_i^2$  defined by the recursive condition  $\mathcal{M}_i^2 = \widetilde{M}_i^2(\mathcal{M}_i^2)$ , together with a residue

$$r_i^{-1} = 1 + \frac{d\hat{\Sigma}_{ii}^{(1)}}{ds}(\mathcal{M}_i^2) + \mathcal{O}(2L) \quad (42)$$

and the associated ‘eigenvector’  $\check{\Omega}_{ij}^i(\mathcal{M}_i^2)$ . Further perturbative expansion of the argument in the self-energies,  $\mathcal{M}_i^2 = m_i^2 - \hat{\Sigma}_{ii}^{(1)}(m_i^2) + \mathcal{O}(2L)$ , leads to the expression of Eq. (3) with the residue  $r_i^{-1} = 1 + \frac{d\hat{\Sigma}_{ii}^{(1)}}{ds}(m_i^2) + \mathcal{O}(2L)$ —as we restrict ourselves to vertex corrections of 1L order below, we do not attempt to control the residue beyond 1L order.

**Near-degenerate case:** Now, let us consider a degenerate sector  $D$ . We can still isolate it via a ‘rotation’  $\check{\mathbf{\Omega}}^D(s)$  satisfying  $\check{\mathbf{\Omega}}^D(s) \cdot \check{\mathbf{\Omega}}^{DT}(s) = \check{\mathbf{1}} + \mathcal{O}(3L)$ . In this case, one may choose ( $i, j \in D, k, l \notin D$ )

$$\check{\Omega}_{ij}^D(s) \equiv \delta_{ij} - \sum_{k \notin D} \frac{\hat{\Sigma}_{ik}^{(1)}(s) \hat{\Sigma}_{jk}^{(1)}(s)}{2(m_i^2 - m_k^2)(m_j^2 - m_k^2)}, \quad \check{\Omega}_{kl}^D(s) \equiv \delta_{kl} - \sum_{i \in D} \frac{\hat{\Sigma}_{ik}^{(1)}(s) \hat{\Sigma}_{il}^{(1)}(s)}{2(m_i^2 - m_k^2)(m_i^2 - m_l^2)}, \quad (43a)$$

$$\check{\Omega}_{ik}^D(s) = -\Omega_{ki}^i(s) \equiv -\frac{1}{m_i^2 - m_k^2} \left[ \hat{\Sigma}_{ik}^{(1)}(s) + \hat{\Sigma}_{ik}^{(2)}(s) + \sum_{j \in D} \frac{\hat{\Sigma}_{ij}^{(1)}(s) \hat{\Sigma}_{jk}^{(1)}(s)}{m_j^2 - m_k^2} - \sum_{l \notin D} \frac{\hat{\Sigma}_{il}^{(1)}(s) \hat{\Sigma}_{kl}^{(1)}(s)}{m_i^2 - m_l^2} \right]. \quad (43b)$$

Then, the object  $\check{\mathcal{P}}^{-1}(s) \equiv \check{\mathbf{\Omega}}^D(s) \cdot [s \check{\mathbf{1}} - \check{M}^2(s)] \cdot \check{\mathbf{\Omega}}^{DT}(s)$  satisfies  $\check{\mathcal{P}}_{ik}^{-1}(s) = \mathcal{O}(3L) = \check{\mathcal{P}}_{ki}^{-1}(s)$ , for  $i \in D$  and  $k \notin D$ , while  $\check{\mathcal{P}}_{ij}^{-1}(s) = s \delta_{ij} - \widetilde{M}_{Dij}^2(s)$  for  $i, j \in D$ , with

$$\widetilde{M}_{Dij}^2(s) \equiv m_i^2 \delta_{ij} - \hat{\Sigma}_{ij}^{(1)}(s) - \hat{\Sigma}_{ij}^{(2)}(s) + \sum_{k \notin D} \frac{(m_i^2 + m_j^2 - 2m_k^2) \hat{\Sigma}_{ik}^{(1)}(s) \hat{\Sigma}_{jk}^{(1)}(s)}{2(m_i^2 - m_k^2)(m_j^2 - m_k^2)} + \mathcal{O}(3L). \quad (44)$$

$(\check{\mathcal{P}}_{ij}^{-1}(s))_{i,j \in D}$  is still a symmetric matrix, hence can be written as  $\check{\mathbf{U}}^{DT}(s) \cdot \check{\mathcal{D}}(s) \cdot \check{\mathbf{U}}^D(s)$ , with a diagonal matrix  $\check{\mathcal{D}}(s)$  and a unitary matrix  $\check{\mathbf{U}}^D(s)$ . The equation  $\det[\check{\mathcal{D}}(s)] \stackrel{!}{=} 0$ , defining the



zeroes of the inverse propagator matrix in the degenerate sector, implies  $\det[s \check{\mathbb{1}}_D - \widetilde{M}_D^2(s)] \stackrel{!}{=} 0$ , since  $\det[\check{\mathbb{U}}^D(s)] \neq 0$ . Thus, the zeroes  $\mathcal{M}_I^2$  in the subspace  $D$  still satisfy an implicit eigenvalue condition

$$\det \left[ \mathcal{M}_I^2 \check{\mathbb{1}}_D - \widetilde{M}_D^2(\mathcal{M}_I^2) \right] = 0. \quad (45)$$

At the 2L order, it is no longer sufficient to simply derive  $\check{\mathbb{U}}^D$  from the eigenvectors of  $\widetilde{M}_D^2$ , because the orthogonality property is not necessarily satisfied by the diagonalizing matrices in the complex case. Instead, one should determine  $\check{\mathbb{U}}^D(\mathcal{M}_I^2)$  through the diagonalization of  $[\mathcal{M}_I^2 \check{\mathbb{1}}_D - \widetilde{M}_D^2(\mathcal{M}_I^2)]^\dagger \cdot [\mathcal{M}_I^2 \check{\mathbb{1}}_D - \widetilde{M}_D^2(\mathcal{M}_I^2)]$ . Then, close to the pole, the propagator matrix looks like

$$\check{P}^S(s) \underset{s \sim \mathcal{M}_I^2}{=} \frac{r_I (S_{Ii} S_{Ij})_{i,j \in D}}{s - \mathcal{M}_I^2} + \dots, \quad S_{Ii} \equiv \sum_{j \in D} (\check{U}_{Ij}^D(\mathcal{M}_I^2))^* \check{\Omega}_{ji}^D(\mathcal{M}_I^2), \quad (46a)$$

$$r_I^{-1} \equiv \sum_{i,j \in D} (\check{U}_{Ii}^D(\mathcal{M}_I^2))^* (\check{U}_{Ij}^D(\mathcal{M}_I^2))^* \left[ \delta_{ij} + \frac{d\hat{\Sigma}_{ij}^{(1)}}{ds}(\mathcal{M}_I^2) \right] + \mathcal{O}(2L). \quad (46b)$$

We note that for  $i \in D$  and  $k \notin D$  one has

$$S_{Ii} = (\check{U}_{Ii}^D(\mathcal{M}_I^2))^* + \mathcal{O}(2L), \quad S_{Ik} = - \sum_{j \in D} (\check{U}_{Ij}^D(\mathcal{M}_I^2))^* \frac{\hat{\Sigma}_{jk}^{(1)}(\mathcal{M}_I^2)}{m_j^2 - m_k^2} + \mathcal{O}(2L). \quad (47)$$

In addition, from  $(\check{\mathbb{U}}^D(s))^* \cdot [s \check{\mathbb{1}}_D - \widetilde{M}_D^2(s)] \cdot (\check{\mathbb{U}}^D(s))^\dagger = \check{\mathcal{D}}(s)$  and  $\check{\mathcal{D}}_{IJ}(\mathcal{M}_I^2) = 0$ , we obtain

$$\sum_{j \in D} \left( \widetilde{M}_D^2(\mathcal{M}_I^2) \right)_{ij} (\check{U}_{Ij}^D(\mathcal{M}_I^2))^* = \mathcal{M}_I^2 (\check{U}_{Ii}^D(\mathcal{M}_I^2))^*, \quad (48)$$

*i. e.*  $(\check{U}_{Ii}^D(\mathcal{M}_I^2))^*$  is still an eigenvector of  $\widetilde{M}_D^2(\mathcal{M}_I^2)$  for the eigenvalue  $\mathcal{M}_I^2$ .

### A.3. Vertex corrections in perturbative QFT at 1L order

Having extracted the poles from the propagator matrix, we may now turn to the effective couplings in Eq. (37). We restrict ourselves to an analysis of strict 1L order.

**Non-degenerate case:** The effective couplings of a resonance associated with a pole  $\mathcal{M}_i^2$  are straightforwardly derived from their definition in Sect. A.1 and those of the residue and of the ‘rotation’ matrix from Sect. A.2:

$$\begin{aligned} g_{iff}^{L,R} &\equiv r_i^{1/2} \sum_j \check{\Omega}_{ij}^i(\mathcal{M}_i^2) \left( \check{\mathcal{V}}_{Sff}^{L,R}(\mathcal{M}_i^2) \right)_j \\ &= \left[ 1 - \frac{1}{2} \frac{d\hat{\Sigma}_{ii}^{(1)}}{ds}(m_i^2) \right] \left( \check{\mathcal{V}}_{Sff}^{L,R(\text{tree})} \right)_i - \sum_{j \neq i} \frac{\hat{\Sigma}_{ij}^{(1)}(m_i^2)}{m_i^2 - m_j^2} \left( \check{\mathcal{V}}_{Sff}^{L,R(\text{tree})} \right)_j + \left( \check{\mathcal{V}}_{Sff}^{L,R(1)}(m_i^2) \right)_i + \mathcal{O}(2L). \end{aligned} \quad (49)$$

The derivative term originates in the residue, the mixing term in the ‘rotation’ matrix, and the 1L vertex from the expansion of  $\check{\mathcal{V}}_{Sff}^{L,R} = \check{\mathcal{V}}_{Sff}^{L,R(\text{tree})} + \check{\mathcal{V}}_{Sff}^{L,R(1)}(s) + \mathcal{O}(2L)$ . We simply recover the LSZ reduction.

**Near-degenerate case:** For the pole  $\mathcal{M}_I^2$ , we can write (in terms of the mixing matrix  $\mathbf{S}$  of Sect. A.2 at 1L order):

$$g_{Iff}^{L,R} = r_I^{1/2} \sum_{j \in D} S_{Ij} \left\{ \left( \check{\mathcal{V}}_{Sff}^{L,R(\text{tree})} \right)_j - \sum_{k \notin D} \frac{\hat{\Sigma}_{jk}^{(1)}(m_j^2)}{m_j^2 - m_k^2} \left( \check{\mathcal{V}}_{Sff}^{L,R(\text{tree})} \right)_k + \left( \check{\mathcal{V}}_{Sff}^{L,R(1)}(m_j^2) \right)_j \right\} + \mathcal{O}(2L). \quad (50)$$

Instead of directly expanding the residue, it is convenient in this case to exploit the invariance of observables (and  $\mathbf{S}$ ) under field renormalization and then use the on-shell scheme as intermediary. The field counterterms are simply shifted according to  $(\delta Z)_{ij}^{\text{OS}} = -\frac{d\hat{\Sigma}_{ij}^{(1)}}{ds}(m_{ij}^2) + \mathcal{O}(2L)$ —the  $\hat{\circ}$  notation continues to denote renormalized quantities in the original scheme. Correspondingly,

$$\left( \check{\mathcal{V}}_{Sff}^{L,R(1)}(m_j^2) \right)_j^{\text{OS}} = \left( \check{\mathcal{V}}_{Sff}^{L,R(1)}(m_j^2) \right)_j - \frac{1}{2} \sum_{k \in D} \frac{d\hat{\Sigma}_{jk}^{(1)}}{ds}(m_{jk}^2) \left( \check{\mathcal{V}}_{Sff}^{L,R(\text{tree})} \right)_k, \quad r_I^{\text{OS}} = \frac{1}{\sum_{k \in D} S_{Ik}^2}. \quad (51)$$

We can define the normalized mixing matrix as  $\tilde{S}_{Ij} \equiv (r_I^{\text{OS}})^{1/2} S_{Ij}$ . Finally, we observe for  $j \neq k$ ,

$$\frac{1}{2} \frac{d\hat{\Sigma}_{jk}^{(1)}}{ds}(m_{jk}^2) = \frac{\hat{\Sigma}_{jk}^{(1)}(m_j^2) - \hat{\Sigma}_{jk}^{(1)}(m_k^2)}{m_j^2 - m_k^2} + \mathcal{O}(2L). \quad (52)$$

Putting everything together, one finds

$$g_{Iff}^{L,R} \stackrel{!}{=} g_{Iff}^{L,R\text{OS}} = \sum_{i \in D} \tilde{S}_{Ii} \left\{ - \sum_{j \in D} \frac{\hat{\Sigma}_{ij}^{(1)}(m_i^2) - \hat{\Sigma}_{ij}^{(1)}(m_{ij}^2)}{m_i^2 - m_j^2} \left( \check{\mathcal{V}}_{Sff}^{L,R(\text{tree})} \right)_j - \sum_{k \notin D} \frac{\hat{\Sigma}_{ik}^{(1)}(m_i^2)}{m_i^2 - m_k^2} \left( \check{\mathcal{V}}_{Sff}^{L,R(\text{tree})} \right)_k + \left[ 1 - \frac{1}{2} \frac{d\hat{\Sigma}_{ii}^{(1)}}{ds}(m_i^2) \right] \left( \check{\mathcal{V}}_{Sff}^{L,R(\text{tree})} \right)_i + \left( \check{\mathcal{V}}_{Sff}^{L,R(1)}(m_i^2) \right)_i \right\} + \mathcal{O}(2L). \quad (53)$$

This defines a generalized LSZ reduction for the near-degenerate case.

As shown in Ref. [66], these loop-corrected couplings are explicitly independent of the field renormalization and minimize the dependence on linear gauge-fixing parameters. The properties of the resonance can then be straightforwardly interpreted as that of a ‘genuine’ particle, allowing for the definition of masses and decay widths in terms of the scattering cross-sections.

## References

- [1] ATLAS Collaboration, *Phys. Lett.* **B716**, 1 (2012), arXiv:1207.7214. [p 1]
- [2] CMS Collaboration, *Phys. Lett.* **B716**, 30 (2012), arXiv:1207.7235. [p 1]
- [3] ATLAS Collaboration, CMS Collaboration, *Phys. Rev. Lett.* **114**, 191803 (2015), arXiv:1503.07589. [p 1]
- [4] ATLAS Collaboration, CMS Collaboration, *JHEP* **08**, 045 (2016), arXiv:1606.02266. [p 1]
- [5] CMS Collaboration, A. M. Sirunyan, *et al.*, *Eur. Phys. J.* **C79**, 421 (2019), arXiv:1809.10733. [p 1]
- [6] ATLAS, G. Aad, *et al.*, *Phys. Rev. D* **101**, 012002 (2020), arXiv:1909.02845. [p 1]
- [7] H. Nilles, *Phys. Rept.* **110**, 1 (1984). [p 1]
- [8] H. Haber, G. Kane, *Phys. Rept.* **117**, 75 (1985). [p 1]
- [9] P. Slavich, S. Heinemeyer (eds.), E. Bagnaschi, *et al.*, (2020), arXiv:2012.15629. [pp 1, 2, 33]
- [10] S. Borowka, T. Hahn, S. Heinemeyer, G. Heinrich, W. Hollik, *Eur. Phys. J.* **C74**, 2994 (2014), arXiv:1404.7074. [pp 1, 2]
- [11] G. Degrandi, S. Di Vita, P. Slavich, *Eur. Phys. J.* **C75**, 61 (2015), arXiv:1410.3432. [pp 1, 2]
- [12] S. Borowka, T. Hahn, S. Heinemeyer, G. Heinrich, W. Hollik, *Eur. Phys. J.* **C75**, 424 (2015), arXiv:1505.03133. [pp 1, 2]
- [13] S. Borowka, S. Paßehr, G. Weiglein, *Eur. Phys. J.* **C78**, 576 (2018), arXiv:1802.09886. [pp 1, 2]
- [14] W. Hollik, S. Paßehr, *Phys. Lett.* **B733**, 144 (2014), arXiv:1401.8275. [pp 1, 2]

- [15] W. Hollik, S. Paßehr, *JHEP* **10**, 171 (2014), arXiv:1409.1687. [pp 1, 2]
- [16] S. Paßehr, G. Weiglein, *Eur. Phys. J. C* **78**, 222 (2018), arXiv:1705.07909. [pp 1, 2]
- [17] M. D. Goodsell, F. Staub, *Eur. Phys. J. C* **77**, 46 (2017), arXiv:1604.05335. [pp 1, 2, 3]
- [18] M. Goodsell, K. Nickel, F. Staub, *Eur. Phys. J. C* **75**, 32 (2015), arXiv:1411.0675. [pp 1, 3]
- [19] P. Drechsel, L. Galeta, S. Heinemeyer, G. Weiglein, *Eur. Phys. J. C* **77**, 42 (2017), arXiv:1601.08100. [pp 1, 3]
- [20] M. Goodsell, K. Nickel, F. Staub, *Phys. Rev. D* **91**, 035021 (2015), arXiv:1411.4665. [p 1]
- [21] M. Mühlleitner, D. T. Nhung, H. Rzehak, K. Walz, *JHEP* **05**, 128 (2015), arXiv:1412.0918. [p 1]
- [22] M. Goodsell, K. Nickel, F. Staub, *Eur. Phys. J. C* **75**, 290 (2015), arXiv:1503.03098. [p 1]
- [23] M. D. Goodsell, K. Nickel, F. Staub, *Phys. Lett. B* **758**, 18 (2016), arXiv:1511.01904. [p 1]
- [24] J. Braathen, M. D. Goodsell, P. Slavich, *JHEP* **09**, 045 (2016), arXiv:1606.09213. [p 1]
- [25] J. Braathen, M. D. Goodsell, *JHEP* **12**, 056 (2016), arXiv:1609.06977. [p 1]
- [26] J. Braathen, M. D. Goodsell, F. Staub, *Eur. Phys. J. C* **77**, 757 (2017), arXiv:1706.05372. [p 1]
- [27] T. Biekötter, S. Heinemeyer, C. Muñoz, *Eur. Phys. J. C* **78**, 504 (2018), arXiv:1712.07475. [p 1]
- [28] D. Stöckinger, J. Unger, *Nucl. Phys. B* **935**, 1 (2018), arXiv:1804.05619. [p 1]
- [29] H. Bahl, *JHEP* **02**, 121 (2019), arXiv:1812.06452. [pp 1, 19, 33, 37]
- [30] T. N. Dao, R. Gröber, M. Krause, M. Mühlleitner, H. Rzehak, *JHEP* **08**, 114 (2019), arXiv:1903.11358. [p 1]
- [31] M. D. Goodsell, S. Paßehr, *Eur. Phys. J. C* **80**, 417 (2020), arXiv:1910.02094. [pp 1, 2, 9, 10]
- [32] E. Bagnaschi, G. F. Giudice, P. Slavich, A. Strumia, *JHEP* **09**, 092 (2014), arXiv:1407.4081. [pp 1, 2, 29]
- [33] G. Lee, C. E. Wagner, *Phys. Rev. D* **92**, 075032 (2015), arXiv:1508.00576. [pp 1, 2, 29]
- [34] J. Pardo Vega, G. Villadoro, *JHEP* **07**, 159 (2015), arXiv:1504.05200. [pp 1, 2, 29]
- [35] P. Athron, J.-h. Park, T. Steudtner, D. Stöckinger, A. Voigt, *JHEP* **01**, 079 (2017), arXiv:1609.00371. [pp 1, 2, 29]
- [36] E. Bagnaschi, J. Pardo Vega, P. Slavich, *Eur. Phys. J. C* **77**, 334 (2017), arXiv:1703.08166. [pp 1, 2, 29]
- [37] H. Bahl, W. Hollik, *JHEP* **07**, 182 (2018), arXiv:1805.00867. [pp 1, 2, 29, 33]
- [38] J. Braathen, M. D. Goodsell, P. Slavich, *Eur. Phys. J. C* **79**, 669 (2019), arXiv:1810.09388. [pp 1, 2, 29]
- [39] E. Bagnaschi, G. Degrassi, S. Paßehr, P. Slavich, *Eur. Phys. J. C* **79**, 910 (2019), arXiv:1908.01670. [pp 1, 2, 29]
- [40] N. Murphy, H. Rzehak, (2019), arXiv:1909.00726. [pp 1, 2, 29]
- [41] H. Bahl, N. Murphy, H. Rzehak, *Eur. Phys. J. C* **81**, 128 (2021), arXiv:2010.04711. [pp 1, 2, 29, 33]
- [42] H. Bahl, I. Sobolev, *JHEP* **03**, 286 (2021), arXiv:2010.01989. [pp 1, 2, 29]
- [43] F. Staub, W. Porod, *Eur. Phys. J. C* **77**, 338 (2017), arXiv:1703.03267. [pp 1, 2, 29]
- [44] R. Harlander, J. Klappert, A. Ochoa Franco, A. Voigt, *Eur. Phys. J. C* **78**, 874 (2018), arXiv:1807.03509. [pp 1, 2, 29]
- [45] H. Bahl, I. Sobolev, G. Weiglein, *Phys. Lett. B* **808**, 135644 (2020), arXiv:1912.10002. [pp 1, 2, 29]
- [46] H. Bahl, W. Hollik, *Eur. Phys. J. C* **76**, 499 (2016), arXiv:1608.01880. [pp 2, 33]
- [47] H. Bahl, S. Heinemeyer, W. Hollik, G. Weiglein, *Eur. Phys. J. C* **78**, 57 (2018), arXiv:1706.00346. [pp 2, 33]
- [48] H. Bahl, S. Heinemeyer, W. Hollik, G. Weiglein, *Eur. Phys. J. C* **80**, 497 (2020), arXiv:1912.04199. [pp 2, 33]
- [49] H. Bahl, I. Sobolev, G. Weiglein, *Eur. Phys. J. C* **80**, 1063 (2020), arXiv:2009.07572. [pp 2, 33]
- [50] R. V. Harlander, J. Klappert, A. Voigt, *Eur. Phys. J. C* **80**, 186 (2020), arXiv:1910.03595. [p 2]
- [51] T. Kwasnitza, D. Stöckinger, A. Voigt, *JHEP* **07**, 197 (2020), arXiv:2003.04639. [p 2]
- [52] F. Staub, P. Athron, U. Ellwanger, R. Gröber, M. Mühlleitner, P. Slavich, A. Voigt, *Comput. Phys. Commun.* **202**, 113 (2016), arXiv:1507.05093. [p 2]
- [53] T. Hahn, S. Paßehr, *Comput. Phys. Commun.* **214**, 91 (2017), arXiv:1508.00562. [p 2]
- [54] R. V. Harlander, J. Klappert, A. Voigt, *Eur. Phys. J. C* **77**, 814 (2017), arXiv:1708.05720. [p 2]
- [55] P. Drechsel, R. Gröber, S. Heinemeyer, M. Mühlleitner, H. Rzehak, G. Weiglein, *Eur. Phys. J. C* **77**, 366 (2017), arXiv:1612.07681. [p 2]
- [56] P. Athron, M. Bach, D. Harries, T. Kwasnitza, J.-h. Park, D. Stöckinger, A. Voigt, J. Ziebell, *Comput. Phys. Commun.* **230**, 145 (2018), arXiv:1710.03760. [pp 2, 3]
- [57] H. Bahl, T. Hahn, S. Heinemeyer, W. Hollik, S. Paßehr, H. Rzehak, G. Weiglein, *Comput. Phys. Commun.* **249**, 107099 (2020), arXiv:1811.09073. [pp 2, 3, 33]
- [58] M. Gabelmann, M. Mühlleitner, F. Staub, *Eur. Phys. J. C* **79**, 163 (2019), arXiv:1810.12326. [p 2]
- [59] S. Heinemeyer, W. Hollik, G. Weiglein, *Phys. Rev. D* **58**, 091701 (1998), arXiv:hep-ph/9803277. [p 2]
- [60] S. Heinemeyer, W. Hollik, G. Weiglein, *Eur. Phys. J. C* **9**, 343 (1999), arXiv:hep-ph/9812472. [pp 2, 33]
- [61] S. Heinemeyer, W. Hollik, G. Weiglein, *Phys. Lett. B* **455**, 179 (1999), arXiv:hep-ph/9903404. [p 2]
- [62] S. Heinemeyer, W. Hollik, H. Rzehak, G. Weiglein, *Phys. Lett. B* **652**, 300 (2007), arXiv:0705.0746. [p 2]
- [63] S. P. Martin, *Phys. Rev. D* **71**, 016012 (2005), arXiv:hep-ph/0405022. [p 2]
- [64] A. Brignole, G. Degrassi, P. Slavich, F. Zwirner, *Nucl. Phys. B* **631**, 195 (2002), arXiv:hep-ph/0112177. [p 2]
- [65] A. Dedes, G. Degrassi, P. Slavich, *Nucl. Phys. B* **672**, 144 (2003), arXiv:hep-ph/0305127. [p 2]
- [66] F. Domingo, S. Paßehr, *Eur. Phys. J. C* **80**, 1124 (2020), arXiv:2007.11010. [pp 2, 4, 6, 9, 10, 12, 16, 18, 23, 25, 27, 28, 36, 41]
- [67] M. Frank, T. Hahn, S. Heinemeyer, W. Hollik, H. Rzehak, G. Weiglein, *JHEP* **0702**, 047 (2007), arXiv:hep-ph/0611326. [pp 3, 33]
- [68] G. Degrassi, P. Slavich, *Nucl. Phys. B* **825**, 119 (2010), arXiv:0907.4682. [p 3]
- [69] K. Williams, H. Rzehak, G. Weiglein, *Eur. Phys. J. C* **71**, 1669 (2011), arXiv:1103.1335. [pp 3, 27]
- [70] T. Graf, R. Gröber, M. Mühlleitner, H. Rzehak, K. Walz, *JHEP* **10**, 122 (2012), arXiv:1206.6806. [p 3]
- [71] P. Athron, J.-h. Park, D. Stöckinger, A. Voigt, *Comput. Phys. Commun.* **190**, 139 (2015), arXiv:1406.2319. [p 3]
- [72] F. Domingo, P. Drechsel, S. Paßehr, *Eur. Phys. J. C* **77**, 562 (2017), arXiv:1706.00437. [p 3]

- [73] T. N. Dao, L. Fritz, M. Krause, M. Mühlleitner, S. Patel, [Eur. Phys. J. C \*\*80\*\*, 292 \(2020\)](#), [arXiv:1911.07197](#). [p 3]
- [74] J. Küblbeck, M. Böhm, A. Denner, [Comput. Phys. Commun. \*\*60\*\*, 165 \(1990\)](#). [p 9]
- [75] T. Hahn, [Comput. Phys. Commun. \*\*140\*\*, 418 \(2001\)](#), [arXiv:hep-ph/0012260](#). [p 9]
- [76] T. Hahn, M. Pérez-Victoria, [Comput. Phys. Commun. \*\*118\*\*, 153 \(1999\)](#), [arXiv:hep-ph/9807565](#). [p 9]
- [77] G. Weiglein, R. Scharf, M. Böhm, [Nucl. Phys. \*\*B416\*\*, 606 \(1994\)](#), [arXiv:hep-ph/9310358](#). [p 9]
- [78] S. P. Martin, D. G. Robertson, [Comput. Phys. Commun. \*\*174\*\*, 133 \(2006\)](#), [arXiv:hep-ph/0501132](#). [p 9]
- [79] F. Domingo, S. Heinemeyer, S. Paßehr, G. Weiglein, [Eur. Phys. J. \*\*C78\*\*, 942 \(2018\)](#), [arXiv:1807.06322](#). [p 9]
- [80] M. Drees, M. M. Nojiri, [Phys. Rev. D \*\*49\*\*, 4595 \(1994\)](#), [arXiv:hep-ph/9312213](#). [p 9]
- [81] M. Sperling, D. Stöckinger, A. Voigt, [JHEP \*\*07\*\*, 132 \(2013\)](#), [arXiv:1305.1548](#). [p 13]
- [82] M. Sperling, D. Stöckinger, A. Voigt, [JHEP \*\*01\*\*, 068 \(2014\)](#), [arXiv:1310.7629](#). [p 13]
- [83] W. G. Hollik, G. Weiglein, J. Wittbrodt, [JHEP \*\*03\*\*, 109 \(2019\)](#), [arXiv:1812.04644](#). [p 21]
- [84] E. Bagnaschi, *et al.*, [Eur. Phys. J. \*\*C79\*\*, 617 \(2019\)](#), [arXiv:1808.07542](#). [p 23]
- [85] E. Fuchs, G. Weiglein, [JHEP \*\*09\*\*, 079 \(2017\)](#), [arXiv:1610.06193](#). [p 26]
- [86] E. Fuchs, G. Weiglein, [Eur. Phys. J. C \*\*78\*\*, 87 \(2018\)](#), [arXiv:1705.05757](#). [p 26]
- [87] T. Hahn, S. Heinemeyer, W. Hollik, H. Rzehak, G. Weiglein, [Phys. Rev. Lett. \*\*112\*\*, 141801 \(2014\)](#), [arXiv:1312.4937](#). [pp 29, 33, 37]
- [88] T. Kwasnitza, D. Stöckinger, (2021), [arXiv:2103.08616](#). [p 31]
- [89] S. Heinemeyer, W. Hollik, G. Weiglein, [Comput. Phys. Commun. \*\*124\*\*, 76 \(2000\)](#), [arXiv:hep-ph/9812320](#). [p 33]
- [90] G. Degrandi, S. Heinemeyer, W. Hollik, P. Slavich, G. Weiglein, [Eur. Phys. J. \*\*C28\*\*, 133 \(2003\)](#), [arXiv:hep-ph/0212020](#). [p 33]